

BIOCHEMICALLY REALISTIC MD AND KINETIC MODELS OF  
THE *RHODOBACTER SPHAEROIDES* BC<sub>1</sub> COMPLEX

BY

STUART WALLACE ROSE

DISSERTATION

Submitted in partial fulfillment of the requirements  
for the degree of Doctor of Philosophy in Biophysics and Computational Biology  
in the Graduate College of the  
University of Illinois at Urbana-Champaign, 2017

Urbana, Illinois

Doctoral Committee:

Professor Antony Crofts, Chair  
Professor Robert Gennis  
Professor Martin Gruebele  
Assistant Professor Taras Pogorelov

# Abstract

This work seeks to duplicate a realistic membrane for a more natural model of the *Rb. sphaeroides*  $bc_1$  complex which in past studies has lacked several details in composition of the fatty acids and relative quantities of each lipid. Past studies have shown some distortion on MD relaxation relating to a large void volume in the protein structures. In this model we have set up the membrane with the complement of lipids reported for the chromatophore membrane, and have taken steps to ameliorate the structural distortions on relaxation of the protein by populating the void with a complement of lipids. The MD model is used to determine diffusion constants and motions of the system in preparation for calculating potentials of mean force for wild type and ISP tether mutants. The current kinetic model provides a kinetic and thermodynamic understanding of the rate-limiting reaction, and associated partial processes that lead to successive turnovers. Since both bacterial and mitochondrial complexes have essentially the same catalytic core, their mechanisms are essentially similar, and a better understanding of the bacterial system can be extrapolated to the context of mitochondrial function, and medically important roles in cellular physiology, cardiovascular disease, apoptosis, and diseases associated with aging.

# Dedication

Neil M. Rose (in memory of my father) and Patricia M. Rose (mother)

Kristi Buhr (girl friend)

# Acknowledgements

- Prof. Antony Crofts and his Laboratory
- Prof. Taras Pogorelov
- Prof. Bob Gennis
- Prof. Martin Gruebele
- Dr. Josh Vermaas – invaluable scripting help

This work used the Extreme Science and Engineering Discovery Environment (XSEDE), which is supported by National Science Foundation grant number ACI-1548562

# Table of Contents

Chapter 1 Biochemistry of the <i>bc<sub>1</sub></i> Complex .....	1
Overall Aims .....	1
Biological Background.....	4
Structure of the <i>bc<sub>1</sub></i> Complex and Modified Q-cycle Mechanism.....	4
Enzyme-substrate Complex of First Turn Over at Qo site .....	7
Crystallographic Void in the <i>bc<sub>1</sub></i> Complex and Chromatophore Membrane.....	11
Chapter 2 Methods and Materials .....	17
Kinetic Model.....	20
Chapter 3 Membrane.....	21
Chapter 4 Simulation Set Up and Configurations.....	30
Equilibration and Preparation.....	30
Chapter 5 Modified Q-cycle: ES complex Formation .....	36
Chapter 6 ISP Head Group Dynamics .....	43
Set Up of Pathway of Head Group Movement .....	44
ES-complex Separation: A Fortunate Accident .....	47
References.....	54
Appendixes .....	59
Appendix A. Membrane Lipid Topologies .....	59
File: < RbSph_C36_lipid.inp> .....	59
Appendix B. Ubiquinones (UQ10 – UQ, UQH2, and neutral semiquinone).....	122
File: <ubiquinone.inp> .....	122
Appendix C. Script for calculation of Diffusion for Membrane Lipids.....	131

# Chapter 1 Biochemistry of the $bc_1$ Complex<sup>1</sup>

## Overall Aims

Electron transfer is central to energy conversion in all biological systems, and a fundamental aim of biophysics is to understand the physical laws that describe it. One approach to the elucidation of principles of electron transfer is by constructing models, but, for a particular system, these can represent many different levels of complexity. In this study, I have constructed realistic models of the *Rhodobacter (Rb.) sphaeroides* cytochrome  $bc_1$  complex at structural and mechanistic levels. The structural model includes the protein in a membrane separating aqueous phases, and is based on crystallographic data for the protein and biochemical literature on the native composition of the lipid membrane, taking care to deal with problematic features from previous studies. Under an XSEDE preliminary grant, our molecular dynamics (MD) model has been equilibrated using energy relaxation and MD simulation, and will provide a platform for atomistic studies. Although the operation of the cytochrome  $bc_1$  complex has been extensively studied, many aspects are still controversial. Our current kinetic model is based on extensive physicochemical studies over the last 40 years. In its present form, it provides a kinetic and thermodynamic understanding of the rate-limiting reaction, and associated partial processes that lead to successive turnovers (the model is of the protein with antimycin bound, which inhibits oxidation of heme  $b_H$  via the  $Q_i$ -site). The aim is to integrate models at these two different levels of understanding so that they can be used to explore mechanism more deeply at the atomistic

---

<sup>1</sup> Some of the material presented in this chapter was previously published 5. A. R. Crofts, Lhee, S., Crofts, S.B., Cheng, J. and Rose, S., Proton pumping in the  $bc_1$  complex: A new gating mechanism that prevents short circuits. *Biochim. Biophys. Acta* **1757**, 1019-1034 (2006).

level. An important parameter in Marcus' theory is the reorganization energy,  $\lambda$ , associated with dielectric response of the protein and solvent. We will determine from MD simulation the changes in electrostatic contour within the protein on change of state of redox centers involved in catalysis, and how the protein/solvent dielectric responds. We will explore changes in local structure on *in silico* mutagenesis to understand changes in function introduced. We will use umbrella sampling to follow diffusional processes. We will explore coulombic interactions that might be important in control. In the longer term, since a global model can be refined iteratively, an improved model will reflect an increasing level of understanding that can be exploited in design of experiments. Since both bacterial and mitochondrial complexes have essentially the same catalytic core, their mechanisms are essentially similar, and a better understanding of the bacterial system can be extrapolated to the context of mitochondrial *bc*<sub>1</sub> complex function, and medically important roles in cellular physiology, cardiovascular disease, apoptosis, and diseases associated with aging.

As our theoretical understanding of electron transfer pushes further into the quantum realm, it becomes clear that, at least in complex systems, there are limits to what we can *measure* in the atomistic domain with current technology. Although the Q-cycle mechanism of the *bc*<sub>1</sub> complex can be represented in kinetic models by measured rate constants and thermodynamic constraints for the main reactions, many partial processes are inaccessible to direct experimental investigation because they cannot be observed. These limits reflect both instrumentation, and the scale of computational models and calculations. The proton-pumping activity of the *bc*<sub>1</sub> complex is driven by redox free energy, and involves proton coupled electron transfer. Coupling can involve transfer of proton and electron through a common pathway, or through separate pathways, with very different coulombic consequences, playing directly into involvement of dielectric response in protein and solvent, and hence the role of reorganization energy,  $\lambda$ . In

addition, the  $Q_o$ -site reaction involves at least two partial processes involving substantial molecular displacements. Best characterized is the rotational displacement of the extrinsic head domain of the Rieske iron-sulfur protein (ISP) through  $\sim 30$  Å to transfer an electron from  $QH_2$  to heme  $c_1$ . It also seems likely that the  $Q^*$  intermediate formed in that reaction diffuses in the  $Q_o$ -site to bring it closer to its electron acceptor, heme  $b_L$  to facilitate rapid electron transfer. In the present model, these are both modelled as diffusional processes. Processes like diffusion can occur over an extended period of time out of range of calculation or modeling, but they can be tested in molecular dynamics simulation by constrained energy sampling techniques. These can provide important constraints to realistic models, and simulation can recover important information about energies and reaction path. The purpose of the present study is to produce an improved model of the cytochrome  $bc_1$  complex of *Rb. sphaeroides* and then use it to calculate biophysical quantities related to the enzymatic and redox activity of the complex and its linkage to substrates, ubiquinone(Q) and ubiquinol( $QH_2$ ) and cytochrome  $c_2$ .

The kinetic model is currently under revision to extend the treatment of control and gating processes. These have been explored in recent work on longevity on mutation of the Rieske iron-sulfur protein (ISP) (strain *isp-1(qm150)*) in *C. elegans*, and suppressor strains in the same subunit. The work revealed that a spring-loaded mechanism, previously proposed on the basis of similar mutations in bacteria, could explain the data (6, 7). In the context of the forward chemistry, the spring-loaded control revealed subtler gating processes needed to minimize production of reactive oxygen species (ROS), but not yet incorporated in the model. In addition, we will incorporate information from the thesis work of Rodney Burton, which has shown a novel intermediate ISPH.SQ complex at the  $Q_o$ -site, generated under conditions in which the SQ can accumulate.



# Biological Background

Variants of the  $bc_1$  complex are redox driven proton pumps that operate in mitochondria, chloroplasts and many aerobic or photosynthetic bacteria as a central component of the main energy conversion processes of the biosphere. The mitochondrial  $bc_1$  complex, more formally ubiquinol: cytochrome c oxidoreductase, is of interest from a human perspective because, in addition to its primary functions in energy conversion, its short-circuit reactions generate ROS. Generation of ROS is linked to cellular damage, and hence linkage to the aging process, cardiac disease, stroke, etc., and to interest in the control and gating processes associated with amelioration of these conditions. The complement of subunits increases with increased cellular complexity, but always contains a catalytic core of three subunits that carry the redox centers involved in the Q-cycle function. The  $bc_1$  complex sits in the membrane and generates a proton gradient across the membrane coupled to the redox reaction. The resulting proton gradient provides an energy source for important energetic processes such as synthesis of ATP.

## Structure of the $bc_1$ Complex and Modified Q-cycle Mechanism

The complex in both mitochondria and bacteria is a homodimer, with a catalytic core of three subunits in each monomer, cytochrome (cyt)  $b$ , cyt  $c_1$ , and ISP. In some bacterial complexes, no other subunits are structurally defined, but in *Rhodobacter sphaeroides*, the complex has an additional subunit (SU IV) of uncertain function. Mitochondrial complexes have up to 8 additional subunits. For some the function is known, for many uncertain (8-11), but none are directly involved in catalysis.

The  $bc_1$  complex in both mitochondria and bacteria is a homodimer with two identical monomers. The monomers are related by two-fold symmetry having an axis extending through the membrane plane and normal to the surface. The dimeric complex has two catalytic cores,

and each core consists of three subunits cytochrome (cyt) *b*, cyt *c*<sub>1</sub>, and ISP. In bacteria, each monomer has the three protein subunits of the catalytic core, and sometimes (as in *Rb. sphaeroides*) an additional subunit IV, not yet seen in crystallographic structures.

The Q-cycle function of the *bc*<sub>1</sub> complex is illustrated in Fig. 1.1, left. The schematic drawing from the PROMISE site, right, outlines the electron transfer centers. The side of the membrane on top is the matrix space of the mitochondria or the outside of the chromatophore (N-phase), and the bottom side is the intermembrane space (P phase) or inside of the chromatophore. Here, N and P refer to positive and negative values for proton potential,  $\Delta p = \Delta\psi - Z\Delta pH$ , where  $Z = 2.303RT/F \approx 59$  mV at 25° C. The function described is for the operation of one monomer of the dimer in a modified Q-cycle.

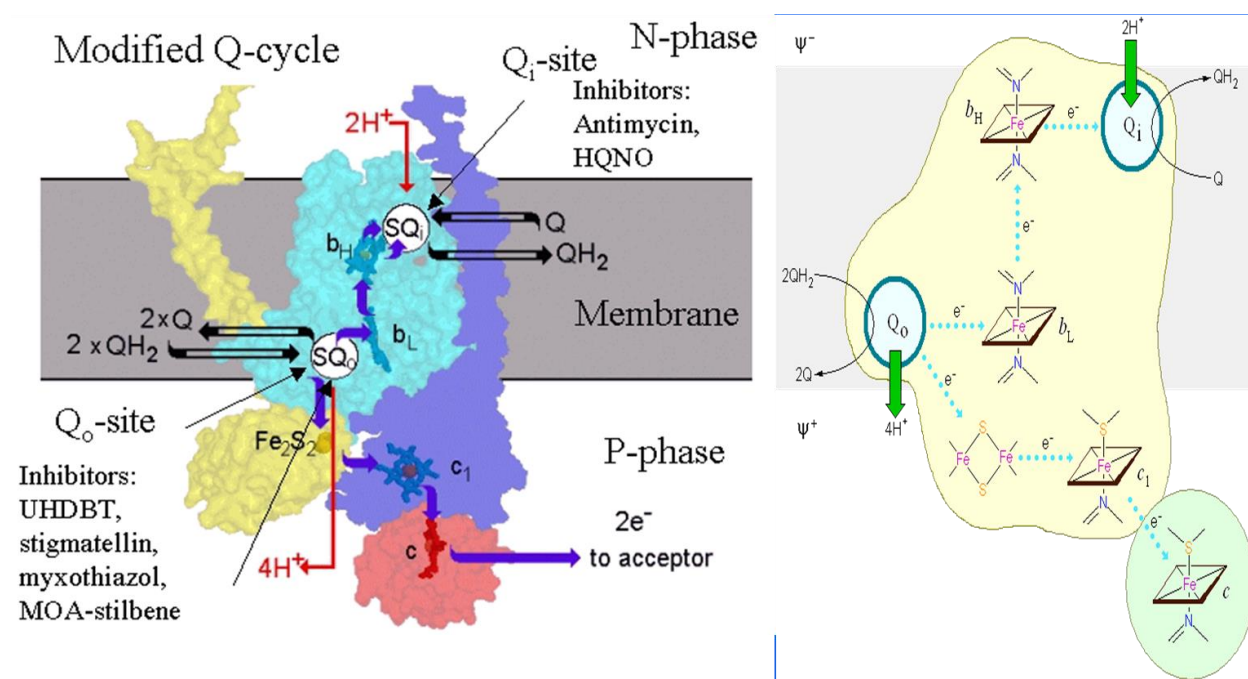
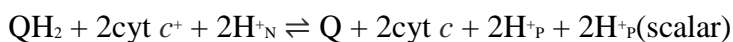


Figure 1.1 On the left is a sketch of the modified Q cycle superimposed on the structure of catalytic subunits of the bovine *bc*<sub>1</sub> complex. On the right is a schematic diagram of the redox centers involved.

In the Q-cycle mechanism, oxidation of quinol, QH<sub>2</sub>, and reduction quinone, Q, occur at physically separate sites in the *bc*<sub>1</sub> complex. This absurd and apparently futile reaction is redeemed by the topology and stoichiometry, to achieve the transfer of H<sup>+</sup> across the membrane.

At the Q<sub>o</sub>-site quinol is oxidized to quinone, with release of 2H<sup>+</sup> to the P-phase; and at the Q<sub>i</sub>-site (on the other side of the insulating phase), Q is reduced to QH<sub>2</sub>, with uptake of 2H<sup>+</sup> from the N-phase. At the Q<sub>o</sub>-site, quinol is oxidized first by the Fe<sub>2</sub>S<sub>2</sub> cluster in the extrinsic domain of the Rieske iron sulfur protein (ISP) which then moves away to transfer the electron to the heme of the cytochrome c<sub>1</sub> and release the proton. The bound heme c<sub>1</sub> then reduces the soluble cyt c. The initial product of this first electron transfer, the neutral semiquinone, QH<sup>•</sup>, at the Q<sub>o</sub>-site, is then oxidized by heme b<sub>L</sub> of cyt b, which passes the electron on to the Q<sub>i</sub>-site via heme b<sub>H</sub>. This bifurcation of electron transfer, with the first electron going down one path toward the cyt c and the second electron down the other path through cyt b<sub>L</sub>, known as the bifurcated reaction of the Q<sub>o</sub>-site, is the rate limiting process under conditions of substrate saturation. The key to understanding the process is that only one of the electrons from the two from a single quinol crosses the membrane. Since it takes two electrons to reduce Q to QH<sub>2</sub>, the Q<sub>o</sub>-site has to turnover twice in order for the Q<sub>i</sub>-site to complete the reduction. Although 2 protons are taken in at the Q<sub>i</sub>-site from the N-phase (outside of the chromatophore) on reduction of Q, and 4H<sup>+</sup> are released to the P-phase (inside the chromatophore) on oxidation of 2QH<sub>2</sub>, the charges are moved on the 2 electrons crossing the membrane in the b-heme chain, effectively from P- to N-sides. The chemistry at the two sites is electroneutral.

Proton pumping is achieved indirectly by movement of two negative charges across the membrane, carried by the electrons passing through the cyt b-heme chain from Q<sub>o</sub>-site to Q<sub>i</sub>-site, and by release or uptake of H<sup>+</sup>, respectively, on oxidation or reduction of quinone, to give an overall yield of 2H<sup>+</sup> pumped for each QH<sub>2</sub> oxidized:



In chromatophores, the electrogenic processes can be followed through the electrochromic carotenoid changes, which provide a “membrane voltmeter” function (12), and this convenience has allowed a detailed matching of electrogenic events to partial processes (13), (12), (14) and (15). By careful correction of absorbance changes in the cytochrome  $\alpha$ -band region for contributions from carotenoid changes (16), this approach was extended to measurement of driving forces from electron transfer during development of the proton gradient in the coupled steady-state (17), (18), and (19). Under static head conditions, the poise of the electron transfer chain was close to that expected from the modified Q-cycle in equilibrium with the proton gradient, indicating a tight control. These results were in line with results from mitochondrial studies (20) in which the proton gradient was varied through poisoning of the ATPase reaction. In the chromatophore experiments, the development of both electron transfer poise and proton gradient could be resolved kinetically.

### Enzyme-substrate Complex of First Turn Over at Q<sub>o</sub> site

The first electron transfer is the transfer of one electron from the Q<sub>o</sub> site substrate, quinol (QH<sub>2</sub>) to the ISP. Because the ISP extrinsic domain is mobile, it acts as a diffusible second substrate (albeit, a tethered one) in the reaction at the cyt *b*-interface, so that the binding of two substrates, ISP<sub>ox</sub> and QH<sub>2</sub>, is needed for formation of the enzyme substrate (ES-) complex. The ISP head group is docked to the Q<sub>o</sub> site against cyt *b* and seems to be held in place in part by hydrogen bonding to the Q<sub>o</sub> site occupant. The PDB file 1ntz has coordinates (with high B-factors) for a quinone occupant, but the experimental basis for these has not been discussed by the authors (21). None of the other structures currently available shows any quinone species bound at the Q<sub>o</sub>-site. Therefore, modeling of quinone or quinol occupancy is based on occupancy of inhibitors.

Because the rate-limiting reaction involves reduction of the oxidized ISP (ISP<sub>ox</sub>), requiring a relatively short electron transfer path, the most obvious choice of bound inhibitor structure has been the stigmatellin structure, which shows a direct H-bond between N<sub>ε</sub> of His-152 of the reduced ISP (ISPH) and a carbonyl group of the Q<sub>o</sub>-site occupant. A quinol modeled with H-bonds to the same ligands as stigmatellin can replace the inhibitor in the structure without strain, and fits within the electron density of the inhibitor (22) and (2); the quinone species modeled in 1ntz is in a similar configuration. Models of this sort have been the starting point for most discussions of the *ES*-complex (23), (2), and (24). The relative pK values for quinol (pK >11.5) and ISP<sub>ox</sub> (pK<sub>ox1</sub> ~7.6) would favor an H-bond with the quinol –OH as donor, and the N<sub>ε</sub> of His-152 of ISP<sub>ox</sub> in the dissociated form as H-bond acceptor.

From the kinetics in chromatophores of the oxidation of the bound cyt *c*<sub>1</sub> and cyt *c*<sub>2</sub> in the uninhibited complex, or with different inhibitors bound, it could be concluded that for all complexes with ISPH initially bound with Q in the Q<sub>o</sub>-site (the *ISPb* configuration), the reaction time for oxidation of the ISPH complex is relatively rapid with a half-time in the range <30 μs (4); a more precise value (~10 μs) was subsequently determined in the isolated complex using flash-excitation of a ruthenium dimer bound to cyt *c*<sub>1</sub> (25). The Rieske ISP protein consists of three portions. One portion is an inter membrane helix anchoring the protein (resid 9-37 in the *Rba. sphaeroides* numbering). A tether region (resid 37-49) attaches the head group (resid 49-187) to the anchor portion. The ISP head group constitutes the mobile domain because its movement delivers an electron to cyt *c*<sub>1</sub> in a rapid process which is not rate limiting. The ISP head group moves from a position proximal to the cyt *b* and binding the quinol substrate to a second position proximal to the bound cyt *c*<sub>1</sub>. The distance traveled by the ISP head group is thought to be in the range of 16 to 22 Å. This distance is defined around the pivot of the tether region which seems to flex in response to the release of the ISP head group from the cyt *b*

position to the position close to the cyt  $c_1$ . This motion will be further explored in Chapter 6 and defined in the context of the model generated and discussed therein.

The  $Q_o$ -site is the catalytic site where the quinol is oxidized to form quinone. The  $Q_o$ -site is located in cyt  $b$  and has a larger volume than one quinol head group. Accordingly, the regions within the  $Q_o$ -site are designated proximal and distal domains with respect to heme  $b_L$ . The occupancy of these domains has been model in terms of the reaction coordinate. The  $ES$ -complex with  $QH_2$  H-boned to H152 of  $ISP_{ox}$  must be in the distal domain, and the  $SQ$  product of the first electron transfer, initially the neutral  $QH^*$ , must be formed in the distal domain, but likely diffuses to the proximal domain (a distance of  $\sim 5.5$  Å) to facilitate rapid electron transfer. The subject of much of this work focuses on the  $ES$ -complex from which for the first electron transfer on oxidation of the quinol occurs. After the first electron transfer, the  $SQ$  intermediate separates from the  $ISPH$ , a proton is released and transfer of the second electron to heme  $b_L$  occurs. However, the sequence of events is not known. Most of the evidence suggests that the proton from  $QH^*$  is released early, and the semiquinone anion ( $Q^{\bullet-}$ ) moves, but scenarios in which the neutral semiquinone ( $QH^*$ ) separates from the  $ISPH$ , and then moves to donate the electron to heme  $b_L$  cannot be ruled out. In either case, all these rearrangements lead to a molecular ballet, which results in the rapid transfer of a second electron up the low potential chain of hemes in cyt  $b$ . The proton released on oxidation of  $QH^*$  leaves the  $Q_o$ -site through a group of residues, - Y147, E295, N279, - connected to a water chain through the protein to the P-phase water, which also connects to R94 and the heme propionates. Transfer of the electron and release of the proton leaves the quinone in the site to diffuse out and be replaced by another quinol to be oxidized in a second turnover of the  $Q_o$ -site reaction.

The different scenarios for the sequencing are discussed in (26), based on recent information from experiment and MD simulation. A rate constant for oxidation of  $SQ_o$  has been

determined in a mutant strain E295W, in which the bulk of the sidechain likely constrains it to the distal domain. The rate of reduction of heme  $b_L$  was so severely inhibited that the heme remained oxidized over the time in which  $SQ_o$  occupancy could be measured. The value estimated for  $k$  was  $\sim 10^3 \text{ s}^{-1}$ , 1000-fold too low to account for the rate observed in wildtype at the occupancy expected in normal flux. The paradox could be resolved if the  $SQ_o$  could move closer to heme  $b_L$ . Movement to the proximal volume occupied by myxothiazol in known structures, a distance of  $\sim 5.5 \text{ \AA}$ , would increase the rate constant to  $k \sim 4 \times 10^9 \text{ s}^{-1}$ . Such a movement would require rapid diffusion in the  $Q_o$ -site volume, and our MD simulations have allowed us to estimate a value. What remains to be determined is the point in the sequence at which the  $H^+$  is released from the initial neutral form,  $QH^*$ .

The two cyt  $b$  hemes, cyt  $b_L$  (low  $E_m \sim -90 \text{ mV}$ ) and cyt  $b_H$  (higher  $E_m \sim 40 \text{ mV}$ ), are arranged along the path (the low potential chain) from the  $Q_o$ -site to the  $Q_i$ -site (see Fig. 1.1 and Fig 1.2), where reduction of quinone to quinol by two electrons coming from the  $b_H$  heme occurs. The requirement for two electrons from the low potential chain means that two quinols must be oxidized in the bifurcated reaction at the  $Q_o$ -site and transferred to the  $Q_i$ -site to complete the reaction there. The kinetic model previously proposed, and further extended here, is intended to simulate experimental conditions under which kinetic parameters were determined as will be discussed in greater detail with respect to the outcomes of the studies described herein. Most of the experimental data was generated with chromatophores using inhibitors, especially antimycin, to observe the accumulation of reduced hemes under various conditions after flash activation. Antimycin is an inhibitor at the  $Q_i$ -site that blocks the transfer of electrons from the heme  $b_H$  in the low potential chain by displacing quinone. In the MD model through which we are investigating atomistic processes, we have also simulated these experimental conditions by modelling antimycin in the  $Q_i$ -site. This allows us to examine changes in configuration

associated with different binding partners in protein surrounding the  $Q_i$ -site when Q is replaced by the inhibitor, and their role in the trajectories produced herein.

## Crystallographic Void in the $bc_1$ Complex and Chromatophore Membrane

Previous MD simulations of the  $bc_1$  complex have been based on non-native membranes, and have in some cases incorporated an artificial feature of the crystallographic structures, which has led to some distortion on MD relaxation. This latter problem relates to a large void volume in the protein structures, likely resulting from disorder of the endogenous material, likely lipid, filling the void. In the *Rb. sphaeroides* model proposed here, we have set up the membrane with the complement of lipids reported for the chromatophore membrane, and have taken steps to ameliorate the structural distortions on relaxation of the protein by populating the void with a appropriate lipids. These two steps provide an improved model, and we expect that this will give us a more realistic picture of the functional operation of the protein, and of a more native environment for interaction of the protein and its reactants.

Most MD simulations start from the crystallographic structures, which are artificial in that they are frozen in a lattice constrained by contacts with neighboring components of the unit cell. For membrane proteins, the prison is even more unnatural. There is no membrane, but instead ancillary lipids, detergent molecules, and waters filling the interstices. The MD simulation is set up to liberate the native structure from this prison, an essential preliminary to mechanistic exploration. Crystallographic models of the  $bc_1$  complex from vertebrate mitochondria or bacteria show in the dimeric structure a substantial volume in the dimer interface, to the N-side of the closely packed protein interface between the  $b_L$  hemes, which is devoid of resolved structure (Fig. 1.2). It is unlikely that this void represents a vacuum. In support of this, in higher resolution structures of the yeast mitochondrial complex, electron



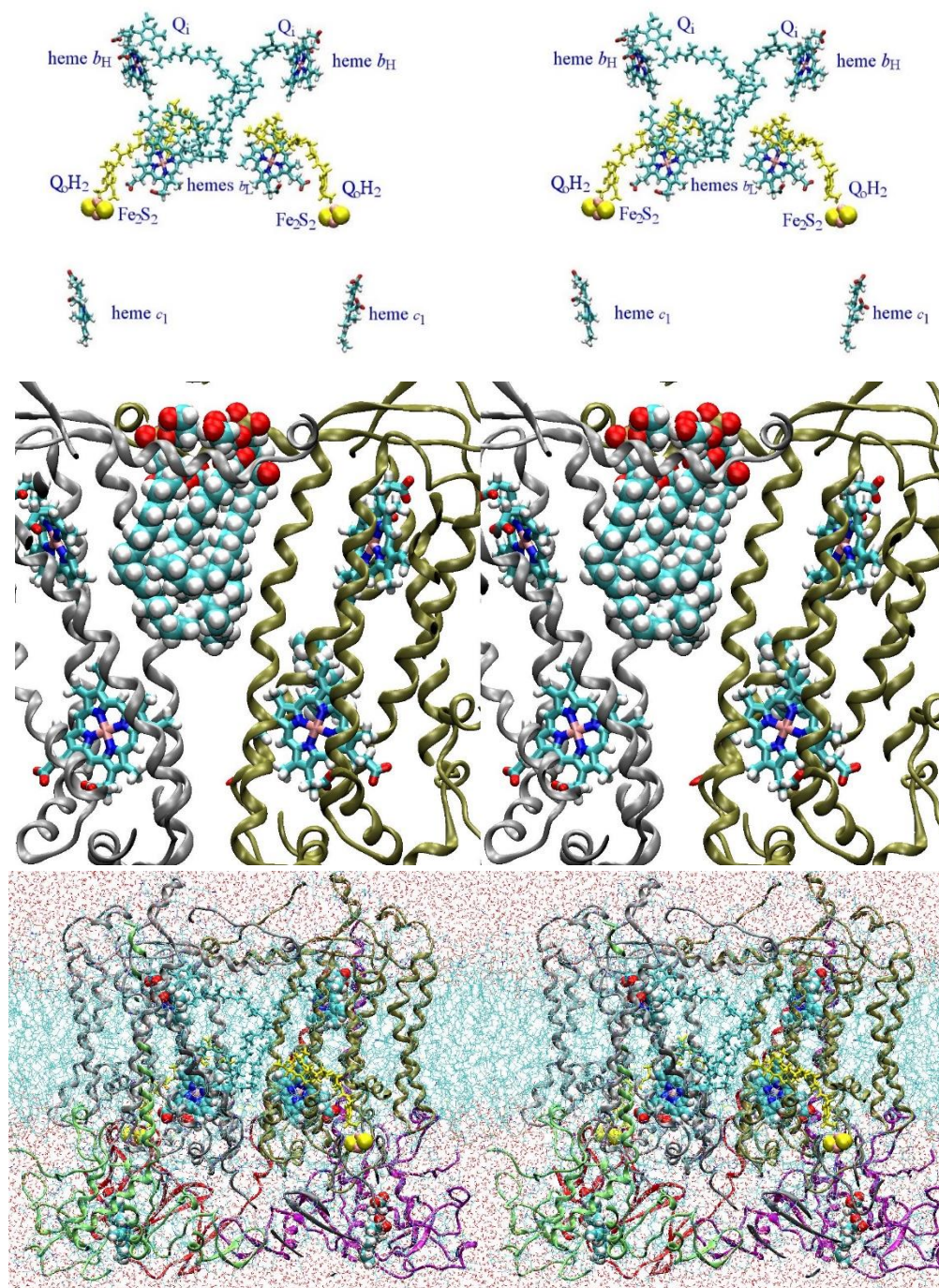


**Figure 1.2** Cross-section through the MD model of the *Rb. sphaeroides*  $bc_1$  complex after 31 ns of a production run. A (top). The initial occupants were replaced by parameterized molecules, with ubiquinone ( $Q_i$ ) in the  $Q_i$ -site and ubiquinol ( $Q_oH_2$ ) in the  $Q_o$ -site. A slice through the protein, shown as a cartoon, reveals the prosthetic groups colored by chain, embedded in the membrane between aqueous phases, with lipids and waters represented by lines for the bonds. The redox centers are shown by VDW spheres (for hemes and  $2Fe_2S_2$ -cluster), or by licorice bonds, colored as below. The “void” is the  $\nabla$ -shaped space defined by a scaffold of membrane spanning and transverse amphipathic helices (center, top of protein), here occupied by lipid. (Stereo pair for crossed-eye viewing.) B (center). The protein stripped away to show the redox centers, to facilitate identity: all redox groups except  $Fe_2S_2$  are shown by licorice bonds, the hemes are in CPK colors;  $QH_2$  at the  $Q_o$ -site is yellow;  $Q$  at the  $Q_i$ -site is cyan; the  $Fe_2S_2$  cluster is shown by VDW spheres. C (bottom). The same view of the protein, but zoomed to highlight two lipids (phosphatidylglycerol, shown by van der Waals spheres) occupying the void, with the  $b$ -type hemes (licorice bonds, CPK colors) for reference, and the scaffolding helices, showing how exchange of phospholipids would be impeded at the head group level. Structure taken from the trajectory exploring formation of the  $ES$ -complex, at a frame  $\sim 31$  ns, when the bond to H152 had stabilized.

density in the site has been resolved, and specific phospholipids identified. One cardiolipin

molecule occupies the central cavity, and tails from other lipids contribute more peripherally (27, 28). The protein scaffold supporting this volume, transmembrane helices, including those binding the hemes, and transverse amphipathic helices at the level of the hydrophilic head groups, one from each monomer, restricts access at this level, but allows access from the hydrophobic lipid phase (Fig. 1.2, bottom). The former restriction might be expected to impede ready diffusion of phospholipid from the membrane into the volume. It has also been suggested that the head groups of other cardiolipins play an important mechanistic role in directing protons to the quinone reduction reactions at the  $Q_i$ -site (discussed further below).

In earlier reports, and in two more recent MD simulations accessible to the author, it was assumed that the problem of the void would be addressed by “the physics”, as explored in MD simulation. In the earlier work, simulations were too short to reveal problems, but in the longer explorations possible now, the MD eliminated the void artificially. In one case, this was by partial collapse of the protein. Significantly, during 350 ns of simulation, although lipid tails explored and partly filled the volume, no phospholipid molecule diffused in. In another case, the void was filled by flooding with waters. Neither of these physical solutions is likely to be natural. In the former case, a partial unfolding of one of the transverse helices from the scaffolding seen in the crystallographic configuration disrupted the volume around one  $Q_i$ -site of the complex, precluding application to mechanistic studies involving that volume. In the latter, the waters would have introduced a high dielectric phase in a volume lined by hydrophobic residues suitable for lipid interactions. This volume is also close to the  $Q_i$ -site, which would significantly change the physical chemistry of the site. However, the focus in both the papers was the  $Q_o$ -site reaction, and since this is on the other side of the protein from the  $Q_i$ -site, it was supposed that disruption of structure at the latter would have little effect on the former. The problem of eliminating the void has been averted in simulations from the Róg group by introduction of a

cardiolipin molecule to occupy the void (29, 30), effectively simulating the yeast configuration in a *Rhodobacter capsulatus*  $bc_1$  complex.

A second set of problems lies in representation of the native membrane. Early MD simulations of the mitochondrial  $bc_1$  complex had used a simple POPC membrane (31), still preferred in some recent efforts using a *Rhodobacter* complex (32). A more natural membrane model was introduced by Postila et al. (29), with a composition based on that of mitochondrial membranes, also adopted in the recent simulation in collaboration with our lab (33). In addition to a different complement of lipids, with different location of the unsaturated bond, in equilibrating the membrane model, forces unfortunately came into play that converted the *cis* fatty acid sidechains to the unnatural *trans* configuration, thereby substantially altering the membrane properties. Whether or not this was important to simulation of function is not clear. The *Rhodobacter* are versatile bacteria, and like many other bacteria, can adapt their membrane composition to cope with environmental stress. For example, under phosphate-limited growth, much of the phospholipid component of the *Rb. sphaeroides* membrane (though not cardiolipin or phosphatidylglycerol) was substituted by non-phosphorus glycolipids, strains can be engineered mutation to eliminate synthesis of cardiolipin from phosphatidylglycerol ( $CD^-$  mutant). These conditions have been used to explore the dependence of growth, expression of cytochromes, and activity of respiratory and photosynthetic chains on membrane composition. The tested parameters were not attenuated, even when the  $CD^-$  mutants were grown under phosphate limiting conditions (34, 35). The only phospholipid present under the latter conditions was phosphatidylglycerol. In light of this versatility, it is not obvious that modifications in lipid content would alter the protein behavior. Nevertheless, a natural membrane is obviously preferable. Of special interest is the high ubiquinone content of the native membrane. Any



natural simulation should at least include this component, even though the diffusional processes involved in substrate or product activities are not yet accessible on the MD time scale.

The idea that the void discussed above is of importance physiologically as a chamber in which quinone species can be stored, allowing easier access to the catalytic sites, has been popularized in textbooks. Since the sites are also exposed through a more favorable diffusional path to the membrane lipid, and the ubiquinone is present in >30-fold excess over the complex (36-38), such a special function might seem superfluous. It seems much more likely that the void

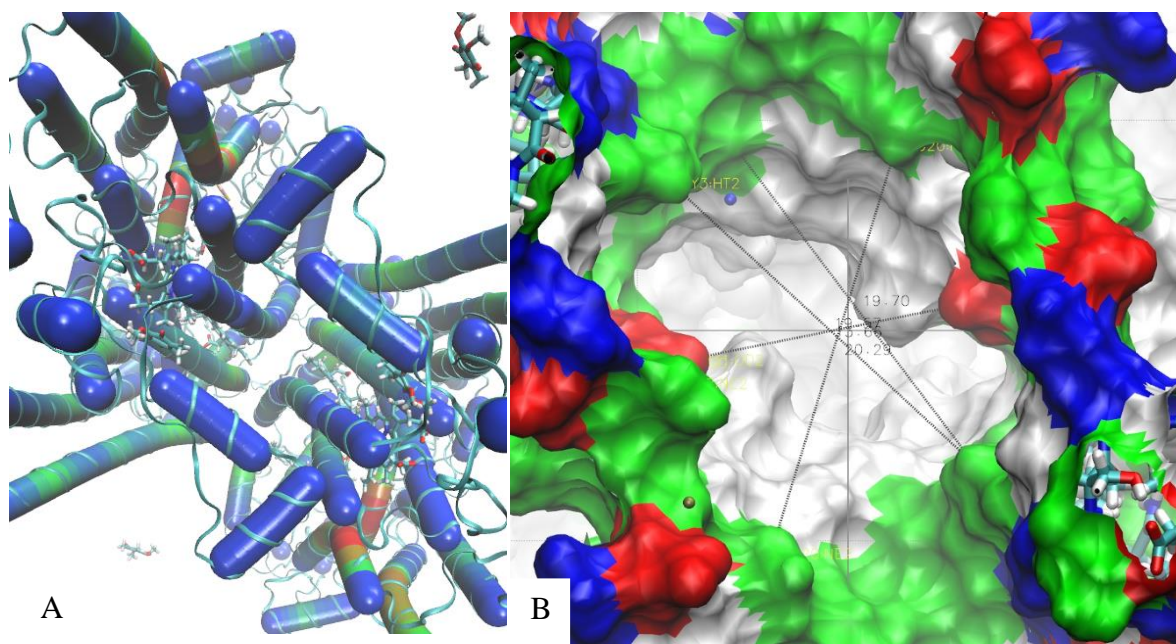


**Figure 1.3 A) View of void present in coordinates from crystal structure; and B) same view as (A) except rendered with Quick Surf and measurements added**

is accounted for by disorder in lipids which were naturally incorporated on assembly of the complex (perhaps including quinone species), which were not detected by X-ray diffraction.

Indeed, as noted above, a more stable structure has been achieved in *Rb. capsulatus* models by populating the void by a cardiolipins (29, 30), as seen in the yeast complex.

Figs. 1.3 A and B show the void in the middle of the  $bc_1$  complex crystal structure which was the starting point for the model of Fig 1.2 (accession code 2QJY) . Since nature abhors a vacuum, it has been assumed there detergent or lipids would fill this volume, which if

disordered would fail to be resolved as structured electron density in the X-ray crystallography study. As noted above, in earlier MD modeling studies of *bc*<sub>1</sub> complex in a solvated membrane system, the backbone was released early in the simulation with the void empty. In one study the site was flooded with water during the simulations and the protein collapsed inwards to reduce the void volume compared to the original crystallographic model (32). Another study found that reconfiguration of the protein around the void led to the collapse of the transmembrane helices inward and unfolding of one of the helices bordering the entry to the opening of the void from water layer (39)

Fig 1.3 A shows the view of the protein from above with helices depicted as tubes with ribbons wrapped around. Fig 1.3 B, from the same perspective, shows the central opening into the void with the protein rendered by its surface and distances between various points in a range close to where the membrane head groups line up in the membrane. The approximate dimension of the opening is 18 Å by 20 Å or 360 Å<sup>2</sup>. Lipid head groups occupy roughly 40 Å<sup>2</sup> of surface area, so theoretically 9 lipids could be fit in. The space under the opening is shared by crossing alpha helices, and quinone/quinol so as a guess it would seem that there would be fewer than 9 membrane lipids. Leaving the void empty when the backbone is released has produced the artifacts mentioned in the previous paragraph. Two membrane lipids were inserted into the void in preparation for minimizing the combined protein, water, substrate, and membrane system.

## Chapter 2 Methods and Materials

We have developed a new MD model using the *Rb. sphaeroides bc<sub>1</sub>* complex, in which the protein environment has been modeled in a native membrane, including ubiquinone. Under a startup XSEDE grant, we have validated the model running in the STAMPEDE environment, minimized energies, run equilibration protocols, and we have tested scaling parameters, and are currently using the refined model in production runs to explore mechanism at the atomistic level under additional XSEDE support.

Local computing resources were used for setting up structure files and testing whether system setups will run and begin equilibration but because of the size of the complete model (312,180 atoms) supercomputer resources are required to equilibrate and run the system and perform the associated calculations. This work uses the Extreme Science and Engineering Discovery Environment (XSEDE), which is supported by National Science Foundation grant number ACI-1053575(40). We received a startup allocation of 50,000 SUs of resources on Stampede in order to perform the minimization, restrained equilibration and initial runs described below. The Stampede platform is a TACC Dell PowerEdge C8220 Cluster with Intel Xeon Phi coprocessors. In order to perform these runs Python scripting was used to generate generic configuration files that were run in batch mode. The remote job submission was managed on the XSEDE platform by the Simple Linux Utility for Resource Management (SLURM) which is an open source, highly-scalable resource management and job scheduling system for submitting, executing, monitoring, and managing batch jobs (typically, parallel jobs) on high-performance Linux clusters.

Once the system was found to run on the local system then configuration scripts were prepared for the Stampede platform and SLURM scripts were prepared for remote batch

processing through XSEDE. The NAMD molecular dynamics (MD) package has historically had efficient performance on XSEDE resources. Fig 2.1 shows scaling calculations performed on TACC Stampede using NAMD 2.11 with a 1 fs time-step on the 312,320-atom system with a range of nodes. These were the second set of scaling calculations which were performed after changing the occupants of the Q<sub>o</sub>-site from stigmatellin to quinol which changed the number of atoms from 312,180 to 312,320. Efficiency was calculated per node,  $Efficiency = (T_{1\ node} \times N) / T_{N\ nodes}$ , where  $T_{1\ node}$  is the simulation time on a single node (16 cores on Stampede) and  $T_{N\ nodes}$  is the simulation time of the same systems on N nodes. With the molecular system in use, Stampede demonstrated efficiency of more than 74% for calculations on 256 - 400 cores (16 to 25 nodes).

Using 320 cores 7,903 SUs will be consumed for a 10 ns simulation. The visualization package VMD(41) and its associated plugins are used to visualize the model and results from the plugins. NAMD 2.11 (42) which was used for molecular dynamics calculations is a highly parallel, publicly available MD program, with demonstrated scalability on all XSEDE platforms.

Simulations involving lipids use the latest CHARMM36 force field in which the problem with consistency of lipid density has been resolved (43). The simulations with proteins and prosthetic groups will use CHARMM36 force field with CMAP corrections (44), supplemented by custom built topologies(45) (Appendix A and Appendix B). Water molecules are represented explicitly by the TIP3P model (46). In all simulations the temperature was maintained constant at 310 K using Langevin dynamics with a damping coefficient of 1 ps<sup>-1</sup> and the pressure at 1 atm using the Langevin Nose-Hoover method (47, 48). Long-range electrostatic forces will be calculated without truncating using the Particle Mesh Ewald (PME) method (49).

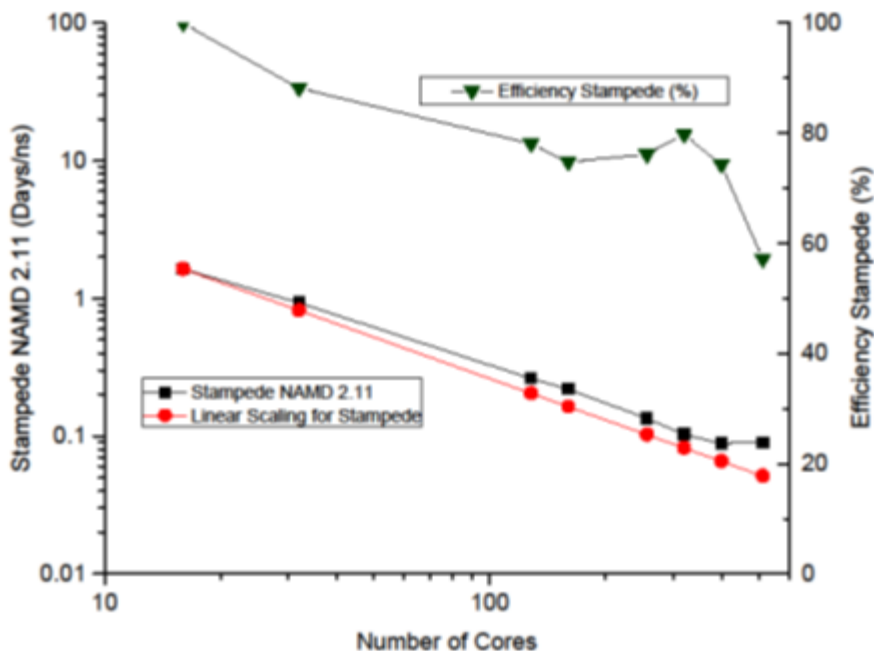


Figure 2.1 Performance of NAMD 2.11 with a 312,320-atom system on Stampede.

Topologies define the connections, relationships and charges which are then assigned by the VMD plugin called PSFGEN to create structure files (psf files) and coordinate files (pdb files). PSFGEN plugin in VMD was used to unite the protein structure fragments and ligate the hemes and iron sulfur cluster with the protein.

NAMD was used to perform molecular dynamics calculations based on a force field. Force field methods (also known as molecular mechanics) ignore the electronic motions and calculate the energy of a system as a function of the nuclear positions only.(50)

$$U(\vec{r}) = \sum U_{bonded}(\vec{r}) + \sum U_{nonbonded}(\vec{r})$$

After picking an appropriate set of coordinates for the  $bc_1$  complex from the protein data base (accession code 2QJY) the structural model of the  $bc_1$  complex was constructed.

During the equilibration phase the system is expected to evolve from the initial configuration to reach equilibrium in the new environment (50). Values of properties such as the



thermodynamic quantities of energy, temperature and pressure are monitored along with structural properties. Equilibration should continue until the monitored properties become stable.

## **Kinetic Model**

A kinetic model was initially developed for Dynafit, and has now been ported to the Matlab toolbox SimBiology. The model has also been implemented using the Gillespie algorithm for stochastic kinetic modelling. The kinetic model can be used to fit data to estimated parameters determined by experiments, by fitting kinetic data while varying critical parameters (rate constants, thermodynamic parameters, etc.). Also, in order to avoid lengthy stochastic simulations with time wasted on diffusion the stochastic solver should be modified to a hybrid stochastic system where the faster processes are represented by continuous process differential equations.

## Chapter 3 Membrane

In order to prepare a model of the *bc<sub>1</sub>* complex in a state as close as possible to its natural state in chromatophores, a selection of lipid types and fatty acid tails was made that resembles the experimentally determined quantities and falls within the accepted baselines which prior studies of membrane biosynthesis and composition establish. A large amount of data has been collected for the natural *Rb sphaeroides* chromatophore system. Two of the differences between prior membrane lipid types and membrane lipids found in the natural *Rb sphaeroides* chromatophore system include: 1) the fatty acid tails of *Rb sphaeroides* chromatophores membranes have different lengths; and 2) the saturation points differ from the fatty acids found in mitochondrial membrane lipids. The degree of saturation in fatty acids is an important factor in the behavior of the membrane and changes from those found in nature would subject the output of the molecular dynamics calculation to additional unnecessary variability. Furthermore, the consistency of the membrane seems to effect its components and larger issues of overall health, i.e., remote phenotypes, as is evidenced by current research into the importance of saturated vs. unsaturated fatty acids in human health. . While it seems obvious that using an unnatural membrane would be inappropriate for modelling a natural system, this study does not attempt to quantify the differences in behavior between an unnatural and a more natural membrane.

Studies of fatty acid biosynthesis of *Rb sphaeroides* found that the typical fatty acids were palmitate, stearate and vaccinate (51). Further, a lack of desaturases results in no reformation or change of saturation once the fatty acid chain is formed (51). The double bond is

located between carbon 11 and carbon 12 as shown below in the diagrams for the different membrane lipid types.

Similar to the issue of fatty acid content of the membrane, the larger issues of human health seem to intersect with concerns with the content of the membrane where cholesterol and cardiolipin is concerned. Many different lipid types are found in bacterial membrane, some of which might have important functional roles in purple bacteria and *Rba. sphaeroides*, specifically. Ornithine and glutamine lipids have been extracted from *Rba. sphaeroides* membranes and characterized (52). Ornithine lipids have been reported as required for optimal steady-state amounts of *c*-type cytochromes (53).

Another membrane component, cardiolipin (CL) has been suggested to be important to functions relevant to the operation of membrane proteins such as cyt *bc*<sub>1</sub> complex or cytochrome *c* oxidase (*CcO*). A recent atom-scale simulation study by Róg et al. cites numerous studies pointing to the physiological involvement of CL in electron and proton transfer by membrane proteins, apoptosis, aging and oxidative stress (54). The charged nature of CL seems to be particularly important to its effect because when the gene for the production of CL was knocked out in *Rb. sphaeroides* non-phospholipid substitutions of the similar charge were found around functioning *CcO* in membranes from the knock out organisms (34). Although the selection of specific types of membrane lipids may be flexible, the overall composition is important at least in terms of charge composition.

In order to produce a realistic natural membrane a combination of lipid types and fatty acids tails were chosen that best covered the variety found in various studies of the *Rb sphaeroides* membrane. The articles mentioned above surveyed and reported on membrane content in their investigations. Additional sources were investigated to gauge the appropriate

content for the photosynthetic *Rb sphaeroides* membrane since there are differences in the acyl lipid concentration for photosynthetic bacteria grown under photosynthetic and non-photosynthetic conditions (55). In switching from non-photosynthetic conditions to photosynthetic conditions the membranes in *Rb sphaeroides* exhibited a shift in CL to a higher percentage (6.2 % to 11.3 %); a shift in phosphatidylcholine choline (PC) to a slightly lower percentage; and a shift in phosphatidylethanolamine (PE) to a lower percentage (35.0 % to 21.4%), inter alia (55). It is worth noting that the magnitude and even direction of acyl lipid concentration shifts were in some cases different for *Rb capsulatus* which is the species of bacteria for which the redox center topologies and parameters were calculated in forming the topologies used in this study (45, 55). Since much of the data generated for the *Rb. sphaeroides bc<sub>1</sub>* complex was done with chromatophores utilizing flash activation, the chromatophore membrane composition is the most natural and realistic basis for a useful model which hopes to simulate function of the complex and so uses an acyl tail composition which have been found in the *Rb. sphaeroides* membrane.

There are no CHARMM 36 force field topology files which match the specific membrane lipids with corresponding and fatty acids tails of the *Rb. sphaeroides* membrane. Given resource constraints only a limited number of lipid types were chosen. The topology files for the following six lipid types were created from the head groups of lipids from the CHARMM 36 force field and the double bond positions were shifted in the tails: DVPG di-vaccenoyl phosphatidylglycerol (2,3-divacenyl-D-glycero-1-phosphatidylglycerol); VSPG (1-vaccenoyl 2-steroyl-D-glycero-1-phosphatidylglycerol); DVPE divaccenoyl phosphatidylethanolamine (2,3-divaccenoyl-D-glycero-1-phosphatidylethanolamine); VSPE vaccenoyl steroyl phosphatidylethanolamine (2,3-vacenoyl- steroyl D-glycero-1-phosphatidylethanolamine - steroyl D-glycero-1-phosphatidylethanolamine); DVPC di-vaccenoyl phosphatidylcholine (2,3-

divaccenyl-D-glycero-1-phosphatidylcholine); and VSPC vaccenoyl steroyl phosphatidylcholine (3-vaccenoyl-2-steroyl-D-glycero-1-phosphatidylcholine). For each lipid type (PG, PE, PC) the dioleoyl (DO) and the palmitoyl-oleoyl (PO) corresponding respective topology files were used to generate the formatted topology sections which were then modified to reflect the correct head type, desaturation point, bonding, and interconnect files. The topology files for TVCL (tetra vaccenoyl cardio lipin) and SQDG were assembled but not formatted and tested in time for inclusion. (Appendix A)

Preparation of the membrane and solvation around the protein for running by NAMD was performed by utilizing the web-based graphical user interface for CHARMM (CHARMM-GUI) (56). The CHARMM-GUI resource hosts several programs to assemble and run the membrane protein complex model to produce input files for NAMD, i.e., structure files, assembled pdb, and configuration files (57, 58). The Membrane Builder utilized the designated Protein Data Bank accession code 2QJY to look up the protein coordinates aligned within membrane boundaries and then proceed with several steps of membrane lipid selection, solvation parameter selection and insertion of selected membrane lipids into the membrane boundaries (59-61). The files output from CHARMM-GUI which were used include structure files (.psf) and coordinate files (.pdb) for the solvation layers and the membrane structure. The output files from CHARMM-GUI were combined with other files using the animate command and psfgen and molefacture plugins of VMD to unite these pieces with the protein, cofactors, substrates, and quinones.

The CHARMM-GUI membrane lipid library did not include the membrane lipids for which topologies had been made. During the membrane building process in CHARMM-GUI membrane lipids found in the library were used in place of the lipids whose topologies were developed to match the *Rb. sphaeroides* chromatophore. The last section of Table 1 details the lipid present in the CHARMM-GUI membrane segment output and the new lipid that replaced it.

The new membrane lipids were inserted into the membrane by replacing the lipids from membrane segment of the CHARMM-GUI output, e.g., our new lipid DVPG was substituted for DOPG as shown in Table 1. The corresponding library lipids chosen had the same connection of atoms in the head group and same fatty acid tail length as the new membrane lipids but the double bond shifted down to the C11-C12 position. Accordingly, tcl scripts were used to first rotate the dihedral of the new double bond to its cis conformation. Since this would have rotated the subject tail out of its original position into other occupied areas of the membrane segment, after setting the correct dihedral for the new double bond the other bonds starting from above the original double bond were rotated 360 degrees to find the point at which the end of the new tail was closest to the end of the original tail. This process was repeated for every carbon of every chain for every new lipid so that the resulting lipid tails would occupy roughly the same space as the original lipids they replaced.

Similar processes were used to i) fit and then renumber the Qi site UQ2 occupant and thread the additional isoprenoid units out of the active site; and ii) substitute quinones into the membrane for the cholesterol molecules inserted by CHARMM-GUI. A realistic chromatophore membrane includes quinones. Ubiquinone is the substrate for *bc<sub>1</sub>* complex in *Rb. sphaeroides*. Although substrate turnover or membrane diffusion is not within the timescale of a molecular dynamic simulation generally, the properties of the membrane are physiologically affected in important ways by constituents as can be imagined by the importance of cholesterol in human physiology. Accordingly, since there was no ubiquinone in the CHARMM-GUI Membrane Builder library, a number of cholesterols equal to the number of ubiquinones appropriate to the approximate concentration in the chromatophore were added to the membrane segment and then UQ10 substituted in with isoprenoid tail positioned toward the center of the membrane between the lipid tails.

Lipid Type	Zhang, X, et al (34)		Russell, J and Harwood, L (55)					Model Resname and source		
	Fatty Acid	(A) %	Fatty Acid	(B) %	(C) %	(D) %	(E) %	Residue name	(F)%	Charm-gui lipid library
CL	All (18:1)	5.2%		11.3%		13.0%		TOCL2	11%	TOCL2(18:1/18:1)
			16:0				6.9%		0%	PVCL2(18:1/16:0)
			16:1				0.8%			
			18:0				14.2%			
			18:1				78.0%			
			Others				2.1%			
PG	Combined	9.1%	combined	44.4%		44.4%		DVPG	40%	DOPG (18:1/18:1)
	18:1/18:1	7.4%	16:0		4.9%		9.3%	VSPG	6%	SOPG (18:1/18:0)
	18:0/18:1	1.4%	16:1		1%		1.4%			
	18:1/19:1	0.3%	18:0		9.7%		16.3%			
			18:1		80.8%		72.9%			
			Others		3.6%		2.1%			
PE	Combined	35.1%		21.4%		28.3%		DVPE	23%	DOPE (18:1/18:1)
	18:1/18:1	29.8%	16:0		4.2%		7.2%	VSPE	7%	SOPE (18:1/18:0)
	18:0/18:1	5.3%	16:1		0.9%		1.6%			
			18:0		8.4%		15.8%			
			18:1		82.0%		71.2%			
			Others		4.5%		4.2%			
PC	Combined	14.1%		11.9%		10.0%		DVPC	12%	DOPC (18:1/18:1)
	16:0/18:0	0.8%	16:0		4.8%		10.6%	VSPC	1%	SOPC (18:1/18:0)
	18:1/18:1	9.0%	16:1		2.2%		1.5%			
	18:0/18:1	1.0%	18:0		4.1%		13.8%			
	18:1/19:1	3.3%	18:1		84.2%		71.9%			
			Others		4.7%		2.2%			
SQDG	Combined	5.9%		4.2%		3.7%				
	16:0/16:0	0.5%	16:0		20.2%		21.5%			
	16:0/18:1	1.5%	16:1		0.9%		0.6%			
	16:0/18:0	0.7%	18:0		15.4%		14.5%			
	18:1/18:1	2.0%	18:1		62.4%		54.4%			
	18:0/18:1	1.0%	Others		1.1%		9.0%			
	18:0/18:0	0.2%								
OL	Total	9.6%		2.3%		na				
	20:1/18:1	2.7%								
	20:1/19:1	5.8%								
	20:0/21:1	1.2%								
QL	Combined	0.5%		na		na				
MMPE*	Combined	20.6%		na		na				
Acyl lipids**	Combined			4.5%						

**Table 3.1** Columns: (A) percentage of total of type of lipid and fatty acid tails for *Rb sphaeroides* grown under aerobic chemoheterotrophic conditions; (B) percentage of total for each type of lipid from *Rb sphaeroides* grown under photosynthetic conditions; (C) percentage of total of fatty acid for each type of lipid from *Rb sphaeroides* grown under photosynthetic conditions; (D) percentage of total for each type of lipid from *Rb sphaeroides* chromatophores grown under photosynthetic conditions; ; (E) percentage of total of fatty acid for each type of lipid from *Rb sphaeroides* chromatophores grown under photosynthetic conditions; and (F) percentage of each type in the membrane built for the molecular dynamics model. The CHARMM-Gui lipid library column refers to the specific types found in the CHARMM-Gui library which were used to construct the topologies for the model lipids. . CL – cardiolipin; PG – phosphatidylglycerol; PC – phosphatidylcholine; PE – phosphatidylethanolamine; SQDG – sulfoquinovosyldiacylglycerol; OL – ornithine lipid; QL – glutamine lipid. \* Includes MMPE, DMPE, and PE. \*\* Includes neutral acyl lipids and other polar acyl lipids.

The lateral diffusion coefficient of membrane lipid molecules, ubiquinone, ubiquinol and the protein in the xy plane  $D$  was calculated by fitting the time-dependent mean square displacement of the center of mass of the lipid headgroups using the Einstein equation (62):

(eq 3.1)

$$D = \frac{1}{2d} \lim_{t \rightarrow \infty} \frac{\langle dr^2 \rangle}{t}$$

The results of the calculation by equation 2.1 of the two dimensional diffusion coefficient for the new lipids across the course of a trajectory for the completely oxidized configuration (conf1\_3) is shown in Figure 3.1. The calculations were performed using the script listed in Appendix C.

The results of the calculation by equation 3.1 of the two dimensional diffusion coefficient for ubiquinone (UQ10) (UBIQ) and ubiquinol (UQ10) (UQL) across the course of a trajectory for the completely oxidized configuration is shown in Figure 3.2. The approximate value for  $D$ , the diffusion constant is  $3 \mu\text{m}^2/\text{s}$  from Figure 3.2. One group has found a value of 190 to 290  $\mu\text{m}^2/\text{s}$  in combination of phospholipid vesicles (63) while values of 2 orders of magnitude less are found with photobleaching measurements (64).

The results of the calculation by equation 3.1 of the protein center of mass diffusion constant for each conf1\_2 and conf1\_3 trajectory is shown in Figure 3.3. There is a difference between the movement of the protein by a factor of 2X but given the small sampling space this difference is probably statistically insignificant. The two dimensional diffusion constant can vary quite a bit for proteins depending on their size and environment but the apparent diffusion constant reached in our calculation is within the approximate values reported experimentally for similar proteins and environments.



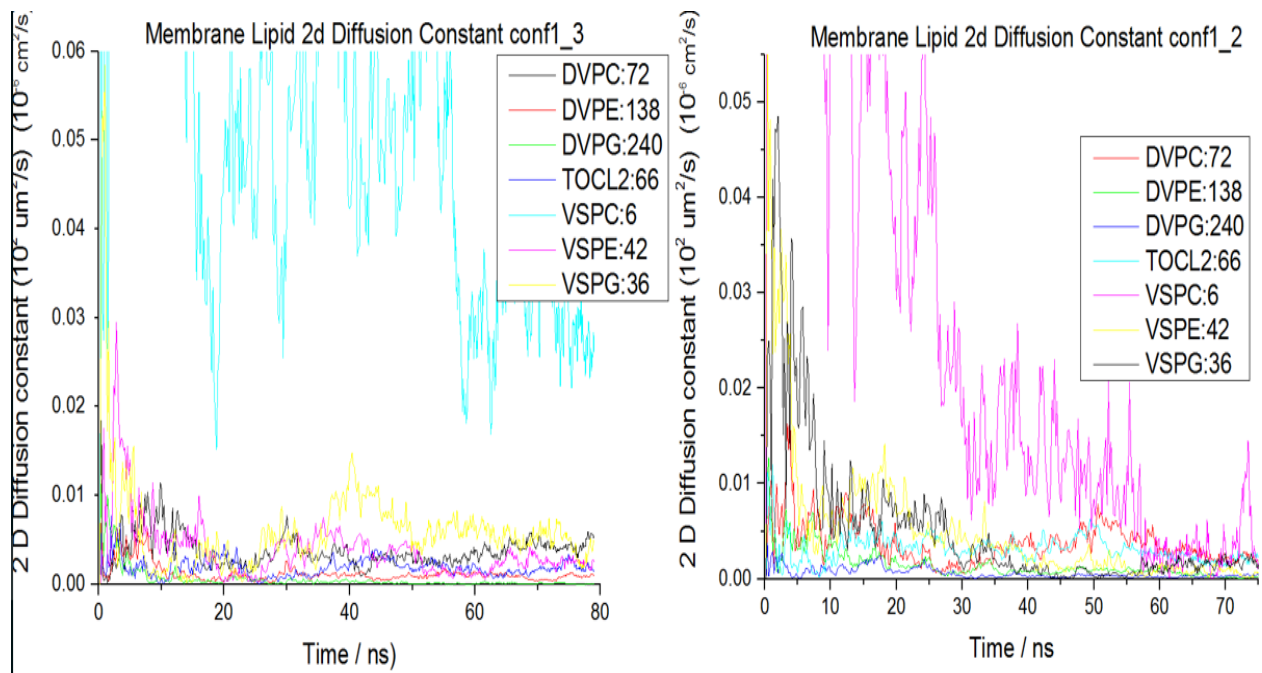


**Figure 3.1** Graph of 2 dimension ( $q=4$ ) diffusion constant for trajectory of conf1\_3 and conf1\_2 from Einstein's relationship for diffusion (eq-3.1). The legend indicates the name of the membrane lipid and the number of lipids in the membrane

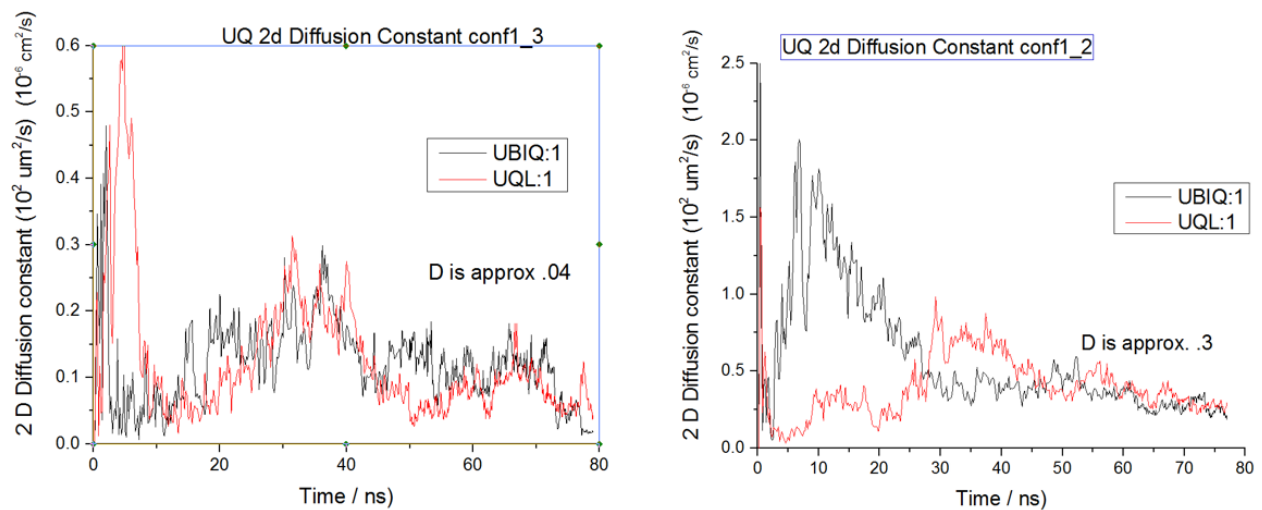


**Figure 3.2** Ubiquinone (UBIQ) head group center of mass and ubiquinol (UQL) head group center of mass two dimensional (2d) diffusion constant calculated from Einstein equation (eq. 3.1).

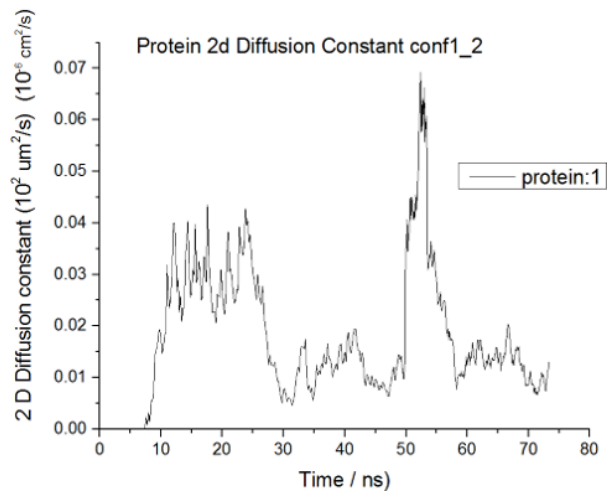
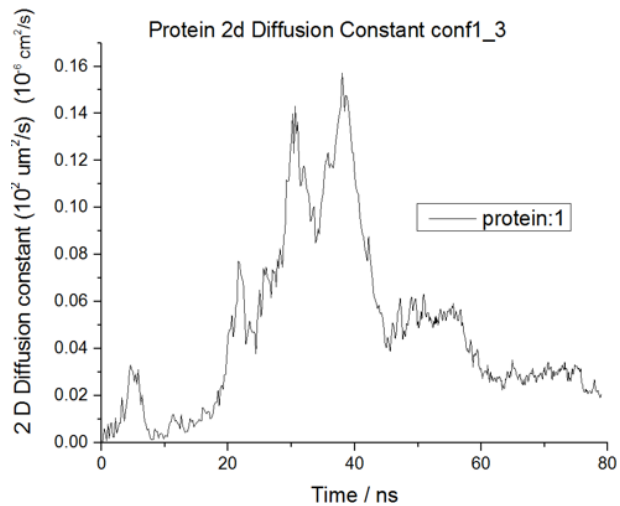


Figure 3.3 Protein diffusion constant graphed from Einstein equation ( eq. 2.1) for protein center of mass in conf1\_2 trajectory and conf1\_3 trajectory.

# Chapter 4 Simulation Set Up and Configurations

## Equilibration and Preparation

The currently running model is part of a lipid stabilized simulation and includes (i) the model of the *bc<sub>1</sub>* complex with two lipids inside of the interior space, quinol (UQ10) in the Q<sub>o</sub>-site (the inhibitor stigmatellin was originally in the crystal structure) and UQ10 in the Q<sub>i</sub>-site; (ii.) the membrane with new lipids, cardiolipin, and UQ10; and (iii.) water box solvated with sufficient charges to counter the charge in the membrane and the protein. The Q<sub>o</sub>-site occupant stigmatellin was replaced with the substrate UQ10 and after a 10000 steps of minimization the system was released again and continue to equilibrate while running for another 15 ns approximately to a total run time of about 50 ns. After about 50 ns the “production run” starts with the protein and bonds unconstrained at a 1 fs time step.

Table 4.1 shows these first stages of running the simulation. Initial equilibration runs (Run No. 0, conf file eq\_0 and No. 1, conf file eqR\_0) were at 1 fs time step with 10, 000 minimization steps. The energy stabilized and the equilibration was continued after the initial scaling. Run Nos. 1-6 were harmonically restrained equilibration cycles where the restraints were gradually released.. An extra bonds file was generated with dihedral angles and improper angles. These extra bonds were subject to additional restraining forces so that the double bonds are maintained in a natural cis- configuration so there is no isomerization even during extended minimization.

The dihedral force constant (‘dihed fc’) is applied to dihedral and improper angles of the components of the membrane which include membrane lipids and quinols . This harmonic force constant is in units of kcal/rad<sup>2</sup>. The force constant was started at 500 and then stepped down to

50 in the last equilibration run before being released. The backbone, head groups of substrate stigmatellin and quinone ‘head’ group were restrained to their initial positions with a force constant starting at 10 kcal\*mol<sup>-1</sup>/Å<sup>2</sup> and stepping down to 0.5 10 kcal\*mol<sup>-1</sup>/Å<sup>2</sup>.

The final equilibration runs and first production runs have been run with a 2 fs time step. All runs were conducted with the rigidBonds parameter set to ‘yes’ to keep the bonds between atoms from vibrating. The protein movement is shown as stabilizing at a fairly low rmsd value in Fig. 4.1.

Run No.	conf file	timestep(fs)	dihed fc*	bb*	steps	Actual Steps	Time (ps)
0	eq_0	1	500	10		258000	258
0	eqR_0	1	500	10		2758000	2758
1	eq_01	1	500	10		2769000	2769
2	eq_02	2	500	10	2500000	5269000	7769
3	eq_03	2	200	5	1250000	6519000	10269
4	eq_04	2	200	2.5	1250000	7769000	12769
5	eq_05	2	100	1	1250000	9019000	15269
6	eq_06	2	50	0.5	1250000	10269000	17769
7	run_01	2	0	0	1250000	11519000	20269
8	run_02	2	0	0	2500000	14019000	25269
<b>Insert Q</b>							
0	prod_eq_0	1	500	10	200000	210000	210
1	prod_eq_1	2	500	10	90000	300000	390
2	prod_eq_2	2	200	5	105000	405000	600
3	prod_eq_3	2	100	2.5	100000	505000	800
4	prod_eq_4	2	50	1	100000	605000	1000

Table 4.1 Restraining forces, steps executed, and clock time model run. The 'bb' restraints are applied to protein backbone, substrates and quinone head groups. \*The dihed fc is applied to a list of dihed and improper angles so that the double bonds and impropers of the membrane lipids and quinones are maintained and the units are kcal/rad<sup>2</sup>. \*\*The units of 'bb' are kcal\*mol<sup>-1</sup>/Å<sup>2</sup>.

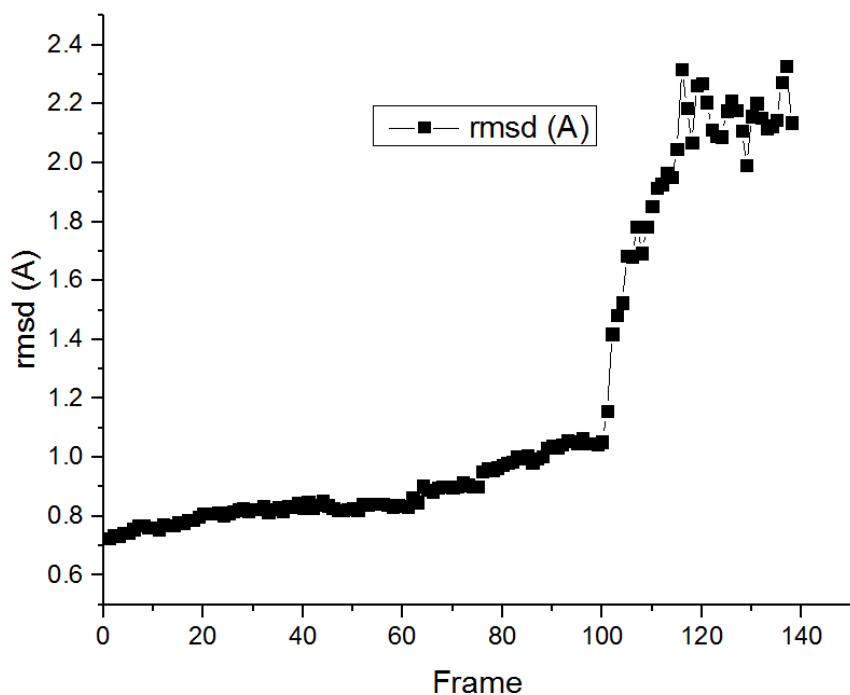


Figure 4.1 Plot of rmsd from NAMD energy for protein from the first frame to frame 140 (25269ps)

Three different configurations or simulations were run from the end of the preparation described above: conf1\_1, conf1\_2, conf1\_3 (Table 4.2). These first three are versions of the first intended configurations which represent states of the bc<sub>1</sub> complex as indicated by Table 4.3. Conf1 represents the fully oxidized state of the system with a substrate in the Q<sub>o</sub>-site as a precursor to the process of forming the enzyme substrate complex (ES complex). Conf2 models the system after the first oxidation of this substrate to a neutral semiquinone and reduced ISP head group with protonated liganding histidine (His152). The first three versions of Conf1 originate from the same starting state and each have slight errors in topologies and coordinates such as conf1\_1 used a topology with only eight isoprenoid units and slight irregularities in the head group which had to be corrected by creating new topologies.

Conf1\_2 represents a fortunate accident in that a mistake with inserting the inhibitor antimycin in the Q<sub>i</sub>-site caused the quinol in the Q<sub>o</sub>-site to withdraw from hydrogen bonding with

the ISP head group and release the ISP head group to move away. The mistake which caused this was the positioning of the antimycin such that a lipid tail of one of the two void-filling lipids intersected a ring of the antimycin structure. Although ring crossings should generate fatal errors on attempt to minimized, the Con1\_2 simulation did minimized, and ran without error messages for the times indicated. The lasso configuration generated an asymmetry in the central volume, which was likely the cause of the displacement of QH<sub>2</sub>, but we did not attempt to analyze the mechanism. This configuration can be used to examine ISP head group movement in preparation for deriving replicas for replica exchange.

The next state of Conf2 has started running but for less than 5 ns so no relevant data has been gathered yet. The initial few nanoseconds show the neutral semiquinone moving away from the ISP head group.

config	Run #	Config file	Timestep(fs)	Dihed fc	bb	steps
conf1_1						
Reverse Quinone to quinol assignment						
	0	prod_conf1_1_eq_0	2	0	0	2010000
	1	prod_conf1_1_eq_1	2	0	0	5342000
	2	prod_conf1_1_eq_2	2	0	0	9342000
	3	prod_conf1_1_eq_3	2	0	0	13114000
	4	prod_conf1_1_eq_4	2	0	0	17114000
	5	prod_conf1_1_eq_5	2	0	0	21114000
	6	prod_conf1_1_run_6	1	0	0	26114000
	7	prod_conf1_1_run_7	1	0	0	36114000
	8	prod_conf1_1_run_8	1	0	0	46114000
	9	prod_conf1_1_run_9	1	0	0	56114000
	10	prod_conf1_1_run_10	1	0	0	66114000
	11	prod_conf1_1_run_11	1	0	0	
conf1_2						
FixQH2 + inh(ANT)					bb+Q(head)	
	0	prod_conf1_2_eq_0	2	0	10	510000
	1	prod_conf1_2_eq_1	2	0	5	1510000
	2	prod_conf1_2_eq_2	2	0	2	2510000
	3	prod_conf1_2_eq_3	2	0	1	3510000
	4	prod_conf1_2_eq_4	2	0	0	8510000
	5	prod_conf1_2_eq_5	2	0	0	18510000
	6	prod_conf1_2_eq_6	2	0	0	28510000
	7	prod_conf1_2_run_7	1	0	0	38510000
	8	prod_conf1_2_run_8	1	0	0	48510000
	9	prod_conf1_2_run_9	1	0	0	
conf1_2a						
	0	prod_conf1_2a_eq_0	2	20 (+H)	0	510000
	1	prod_conf1_2a_run_1	1	0	0	
conf1_3						
	0	prod_conf1_3_eq_0	2	0	10	510000
	1	prod_conf1_3_eq_1	2	0	5	1510000
	2	prod_conf1_3_eq_2	2	0	2	2510000
	3	prod_conf1_3_eq_3	2	0	1	3510000
	4	prod_conf1_3_eq_4	2	0	0	8510000
	5	prod_conf1_3_eq_5	2	0	0	18510000
	6	prod_conf1_3_eq_6	2	0	0	28510000
	7	prod_conf1_3_run_7	1	0	0	38510000
	8	prod_conf1_3_run_8	1	0	0	48510000
	9	prod_conf1_3_run_9	1	0	0	58510000

Table 4.2 Restraining forces and steps executed. The 'bb' restraints are applied to protein backbone, substrates and quinone head groups. \*The dihed fc is applied to a list of dihed and improper angles so that the double bonds and improper.

Conf1		Monomer		Conf2		Monmer	
		First	Second			First	Second
	cyt c	O	O		cyt c	O	O
	cyt b-bL	O	O		cyt b-bL	O	O
	cytb-bH	O	O		cytb-bH	O	O
	FES	O	O		FES	R	O
	Qo	QH2	QH2		Qo	UQS (neutral)	QH2
	Qi	Q /Ant	Q/Ant		Qi	Q	Q
	Glu295	O <sup>-</sup>	O <sup>-</sup>		Glu295	O <sup>-</sup>	O <sup>-</sup>

**Table 4.3 Redox states /species in each monomer for the first two simulation configurations**



# Chapter 5 Modified Q-cycle: ES complex Formation<sup>2</sup>

Crofts lab has developed a kinetic model for the reaction at the Q<sub>o</sub>-site that includes kinetic and thermodynamic parameters for 15 partial processes determined directly using conventional protocols. The model was implemented in the Dynafit software environment (65, 66). In this work, I have extended the model by porting it to the Matlab toolbox SimBiology, and developed an implementation using the Gillespie algorithm for stochastic kinetic modelling.

Typically, reactions are kinetically modeled using differential solvers, which essentially find the limit of the difference equation for small  $\Delta t$  ( $dt$ ) and large population, i.e., a continuous sampling, but in modeling the reactions within a complex, the differential approximation can be considered inaccurate in a sense. Direct repeated calculation of the master equation is not possible but a stochastic algorithm was proposed by Gillespie for numerical simulation of the time evolution of a given set of kinetic equations (67). This method has been used by Ransac et al. (68), and they were able to model the main features of the Q-cycle using Moser-Dutton based rate constants, and driving forces from thermodynamic parameters. However, they failed to take into account the features of the mechanism associated with control and gating, and their model failed under conditions where these are important. In our version of a Gillespie model, these features could be included through explicit partial processes, and then reproduced the same

---

<sup>2</sup> Some of this material was previously published in 5.A. R. Crofts, Lhee, S., Crofts, S.B., Cheng, J. and Rose, S., Proton pumping in the *bc*<sub>1</sub> complex: A new gating mechanism that prevents short circuits. *Biochim. Biophys. Acta* **1757**, 1019-1034 (2006).and 26. A. R. Crofts *et al.*, The Q-cycle Mechanism of the bc<sub>1</sub> Complex: a Biologist's Perspective on Atomistic Studies. *The Journal of Physical Chemistry B*, (2017).

kinetics as the model using differential equations. In exploring the potential for integration of this approach into MD simulation in our own models, we found that when timescales became large, steps like diffusion, where the atomistic timescales are small, would consume enormous amounts of processor time in unnecessary recalculation of reaction probabilities, and this points to at least one aspect that is challenging.

In the present study, we would like to examine kinetics in the context of a molecular dynamics model of a system consisting of the enzyme, the substrate, and a membrane representing the natural membrane in relative proportion of membrane lipid types and approximate proportion of fatty acid tails. Our aim is to use the kinetic model in iterative mode, in conjunction with differential and stochastic solvers and data from experiments, to incorporate values calculated from the molecular dynamics into the traditional physicochemical representation by means of fitting procedures.

The kinetic model for the monomeric  $bc_1$  complex developed for this study is shown diagrammatically in Fig. 5.1 by its different states. The model for the dimeric complex including electron transfer across the interface between dimers is not shown and will be used in the future for the iterative parameter fitting and simulations discussed *infra*. The model includes 15 partial processes and includes various other partial processes which have rate constants estimated based on thermodynamic constraints. The model is based on an antimycin inhibited  $bc_1$  complex where full reduction of all components would involve two quinols being reduced at the Qo-site to deliver two electrons to  $b_L$  and  $b_H$  hemes. The resultant model has 54 reactions including diffusion reactions and proton distribution 'reactions'. The model shows the reactions advancing from state to state in the process of two quinols being oxidized. In the current model parameters can be selected for fitting to experimental data. This model represents an improvement because



membrane, diffusing stochastically (Fig. 1.2a). The modifications to correct previous defects therefore appeared to have been effectively implemented. Both the overall structure, and configurations for both the  $Q_o$ - and  $Q_i$ -sites (occupied in the initial crystallographic model respectively by stigmatellin and ubiquinone), retained configurations close to those seen in the starting crystallographic model when occupied by UQ-10 respectively in reduced or oxidized

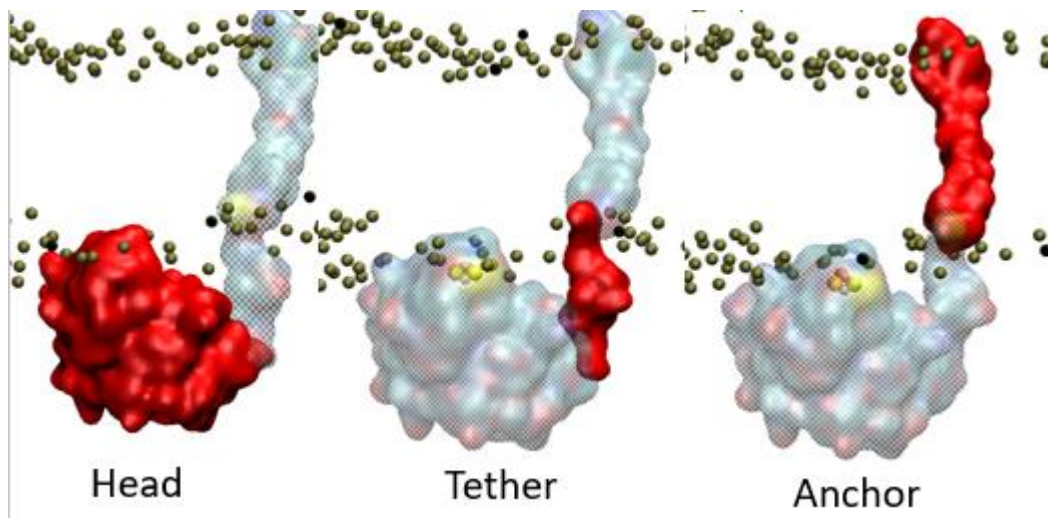


**Figure 5.2** ISP head group, Tether and Anchor in red with gold potassium ions from membrane lipids to indicate membrane location.

form at  $Q_o$ - and  $Q_i$ -sites (Fig. 1.2), a state appropriate to steady-state turnover. This is in line with the recent simulations reported by Postila et al. (29), in which the  $Q_i$ -site mechanism was simulated in a *Rb. capsulatus* model of the  $bc_1$  complex with cardiolipin in the void.

Confl, the versions of our oxidized  $bc_1$  complex shows properties which include significant differences from those previously reported. The basis of these differences obviously needs to be resolved. In the Barragan et al.(33) complex leading to productive forward chemistry, three H-bonds stabilized the structure: from H156  $N_\epsilon$  to  $QH_2$  -OH, from Y147 -OH to  $QH_2$  -OH (the other end), and from Y147 -OH to E295  $-COO^-$ . On the positive side, the three residues involved in stabilizing the *ES*-complex were all found to participate in H-bond pairing, suggesting that drastic revision of previous work might not be necessary. However, the configuration in which all three H-bonds were engaged, which formed the basis of the QC

calculations, has not yet been reached in our simulation after 87 ns (conf1\_3). Fig. 5.3, 5.4 A and show states of the Q<sub>o</sub>-site in which important H-bonds or potential H-bonding are highlighted, and (in Fig. 5.4 B and C), the distances for the H-bonds above, read from the trajectory of conf1\_3 as it evolves. In the time courses shown, ISP<sub>ox</sub> and QH<sub>2</sub> are start separate (monomer 2) or start together (monomer 1), but over the first 130 frames (26 ns), the H-bond from QH<sub>2</sub> -OH to ISP<sub>ox</sub> N<sub>e</sub> of H152 forms in monomer 2, and stabilizes the *ES*-complex. During the entire trajectory, Y147, E295, and N279 explore configurations in which Y147 visits QH<sub>2</sub>. Mostly, E295 is busy swapping its association between the other two residues. This volume of the protein also includes several exchangeable waters which are involve in H-bonding with the polar residues, and connecting to the heme *b<sub>L</sub>* propionates and Arg-94, likely providing H<sup>+</sup> conducting pathways, including one to the P-phase water. Over the remaining time captured in

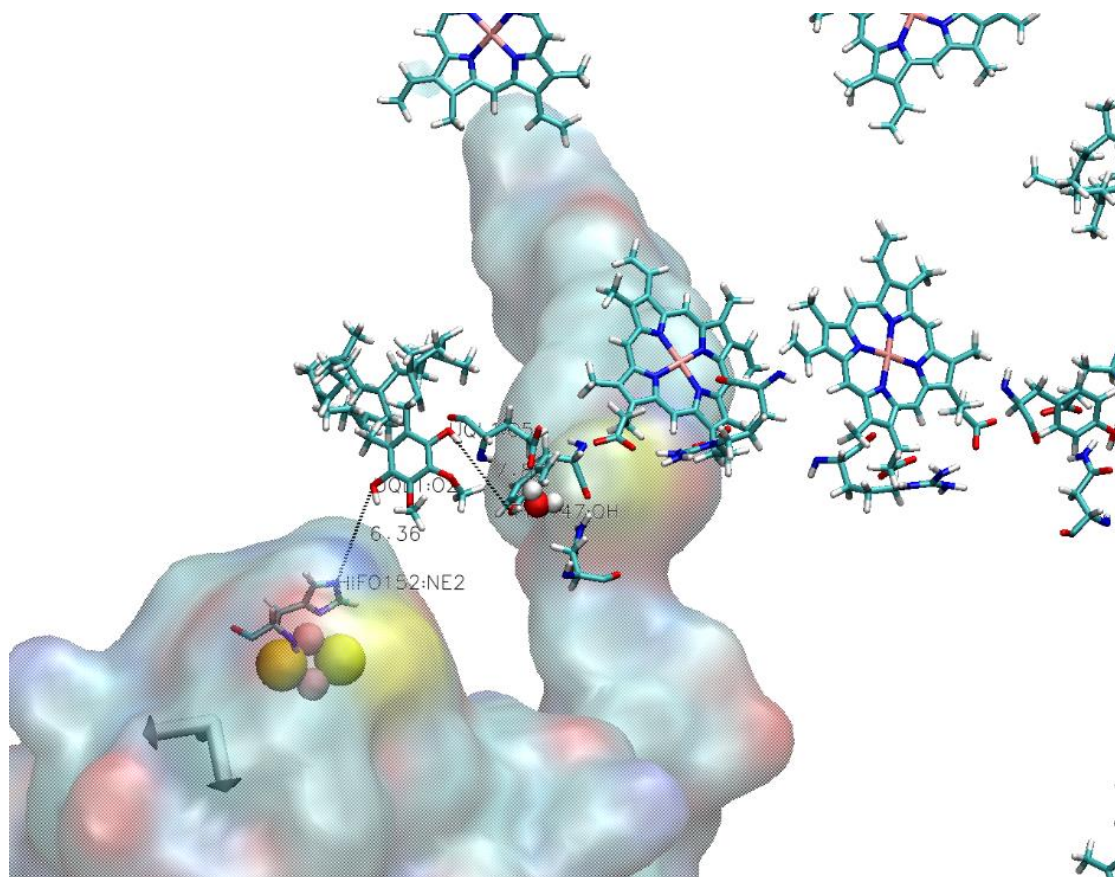


**Figure 5.3** Formation of *ES*-complex H-bond network from conf1\_1 being formed early in the trajectory

this trajectory, Y147 occasionally H-bonds with QH<sub>2</sub> as shown in A, about only 30% of the time (see time course in Fig. 5.4 B and C) although Y147 of monomer 1 seems to stay in the neighbor of QH<sub>2</sub> for most of the trajectory. In the frame captured in Fig 5.4 A, the two primary H-bonds to QH<sub>2</sub> stabilizing the *ES*-complex (from H152 and Y147) are both present, but E295 is distant. This pattern persists, though we should note that the *ES*-complex at the Q<sub>o</sub>-site of monomer 2 was somewhat less stable than monomer 1, with an interesting time dependence that might suggest some interaction between sites.

Our current simulation with antimycin occupying the Q<sub>i</sub>-site (conf1\_3), a commonly used experimental situation since it allows ready measurement of turnover of the Q<sub>o</sub>-site through reduction of heme *b<sub>H</sub>*. The measured rate of QH<sub>2</sub> oxidation (in the first turnover) when heme *b<sub>H</sub>* is initially oxidized is the same in the absence or presence of antimycin(13, 69). In line with this, the configuration of the *ES*-complex followed essentially the same pattern (not shown). If this pattern is confirmed in additional runs, it would require at least a modest change in interpretation of the previous result; that the release of a H<sup>+</sup> from QH<sup>•</sup> involves collisional exchange via stochastic H-bonding, rather than the direct relay previously suggested(70). However, more extensive revision could be justified; it is possible that the earlier modeling (2-4, 23) of the *ES*-complex as involving E295 as a direct ligand to QH<sub>2</sub> has biased thinking towards an emphasis on a direct role in H<sup>+</sup> release. If so, an alternative scenario would be that the product state QH<sup>•</sup>.ISPH dissociates to release the neutral SQ to diffuse in the site, and that E295 is involved only in transfer of the H<sup>+</sup> to the heme propionate after the QH<sup>•</sup> is close enough to transfer the electron, thus facilitating an electrostatically linked PCET. The stochastic proton exchanges among this group of residues would enable transfers fast enough to make these last two models indistinguishable experimentally from the earlier model. One consideration in deciding between these scenarios is the need to contain the SQ in the Q<sub>o</sub>-site. Preference might depend on a simple



physical principle; the low probability (high energy cost) of solvating a charged species, favors mechanisms involving  $Q^{\bullet}$  as the liberated form, rather than  $QH^{\bullet}$ , since the former would have a much lower probability of escape into the lipid phase via the hydrophobic entrance channel.

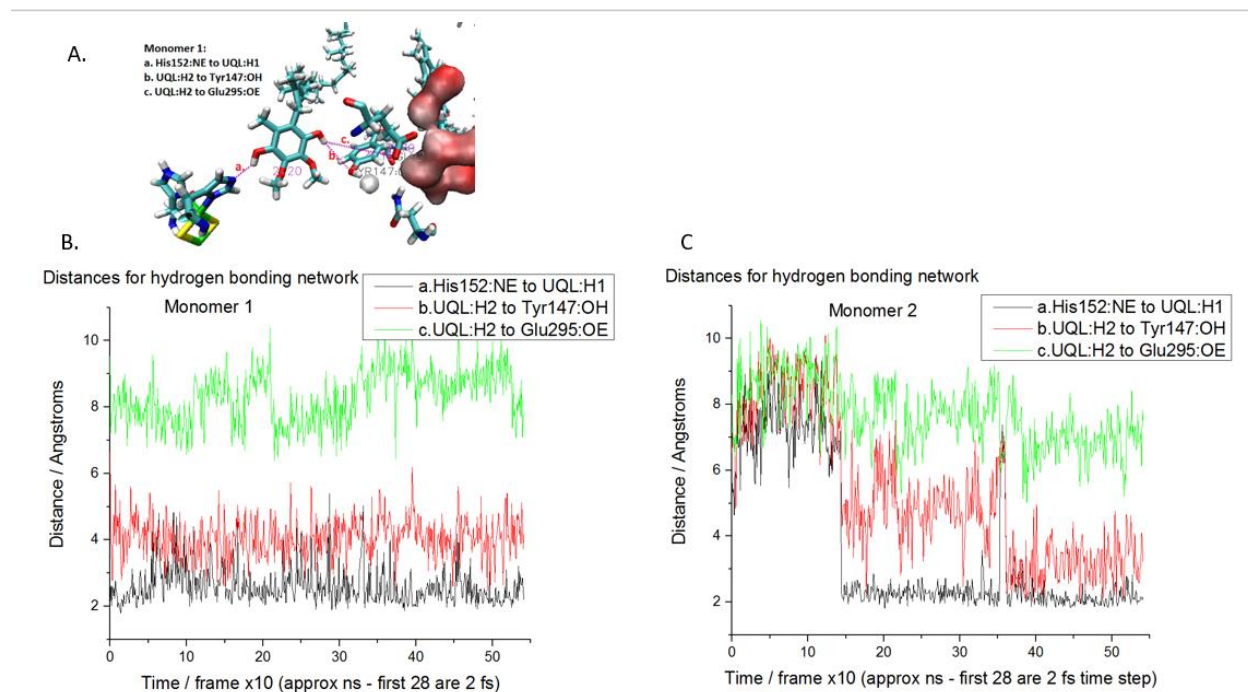


**Figure 5.4 ES complex formation. A.** The Hbond network around the quinol with the potential hbonds indicated including the distance to Glu295. **B and C)** Graph of the distances across the conf1\_3 trajectory of the Hbonds for the corresponding, respective monomers, monomer 1 and monomer 2.

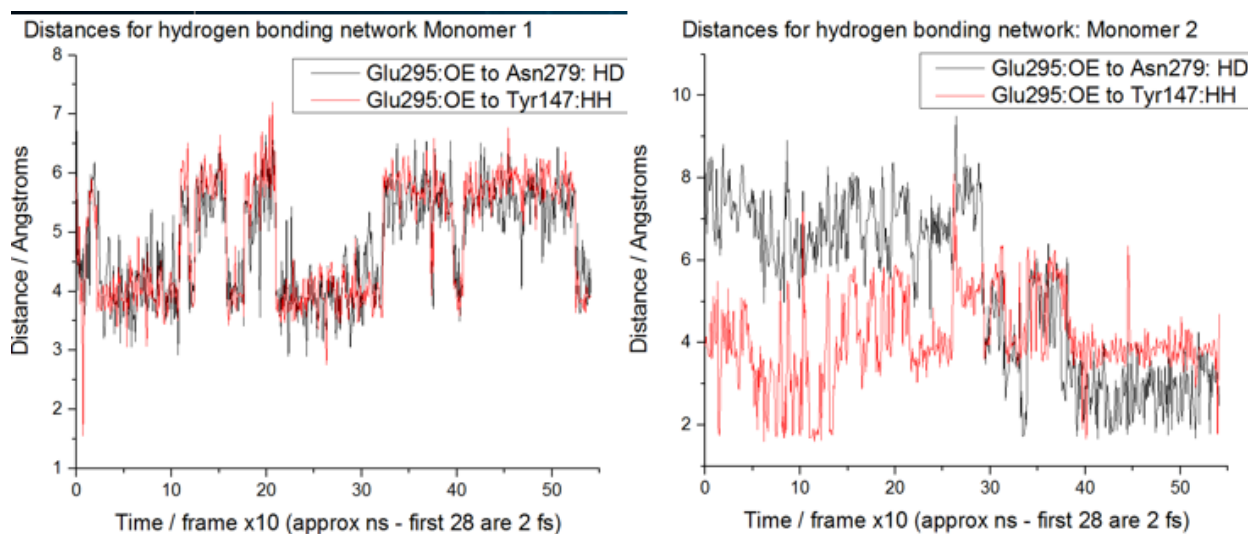


**Figure 5.5 Details of the trajectory (conf1\_3) showing other potential H-bonding partners for the Glu295.**

# Chapter 6 ISP Head Group Dynamics<sup>3</sup>

Molecular dynamics simulations of the  $bc_1$  complex will be run in different redox states in order to sample a range of conformations which may be used to calculate a variety of potentials of mean force (PMF). Umbrella sampling (US) (71) with the weighted histogram analysis method (WHAM) (72-74) can be used in the study goals set forth below to calculate the energetics associated with the studied processes. However, before Umbrella sampling can be used effectively the motions of all parts of the simulation must be understood.

One goal of the calculations will be the *C. elegans* mutations which have focused attention in the role of ISP and movement of its extrinsic head-domain in control and gating of ROS production. Using molecular modeling the potential mean force of diffusion of the ISP head group and energy parameters of the ‘hinge region’ or tether during the constrained motion of the head group will be calculated for each redox state of the headgroup, i.e., before and after the reduction of the ISP. The physicochemical underpinnings of our spring-loaded model (6, 7) are based on studies of changes in binding free-energy in these complexes in ISP tether-span mutants (75). The Hamiltonian replica exchange (RE) method will be used to access otherwise inaccessible thermodynamic states orthogonal to the reaction path (76). The distance of the path is approximately 30 angstroms and will require windows of about 1 angstrom.

Additional PMF umbrella calculations will study diffusional displacements of the quinone/quinol substrates and semiquinone intermediate. Diffusion of the semiquinone within the  $Q_o$ -site is important to the proposed mechanism. The diffusional distance is 6-7 angstroms,

---

<sup>3</sup> Some of this material was published in: 5. A. R. Crofts, Lhee, S., Crofts, S.B., Cheng, J. and Rose, S., Proton pumping in the  $bc_1$  complex: A new gating mechanism that prevents short circuits. *Biochim. Biophys. Acta* **1757**, 1019-1034 (2006).and 26. A. R. Crofts *et al.*, The Q-cycle Mechanism of the  $bc_1$  Complex: a Biologist’s Perspective on Atomistic Studies. *The Journal of Physical Chemistry B*, (2017).



and the diffusion occurs under varying conditions of coulombic steering due to the redox state of heme  $b_L$ .

## Set Up of Pathway of Head Group Movement

The “spring” is physicochemical, with the forces determined by configuration of the tether region, mainly by the stretching or collapse to helical form, as the headgroup of the ISP moves between the  $Q_o$ -site and the electron-acceptor with heme  $c_1$ . Structures showing different configurations of the tether (cf. (3)) a crystallographic database for intermediate states in the forward reaction trajectory (see Figure 6.1). Movement of the head group is shown from differences found in crystallographic studies. Figure 6.1 shows the first and last position of the ISP head group on the left from four mitochondrial crystal structures which were assembled and aligned according to their anchor portions.

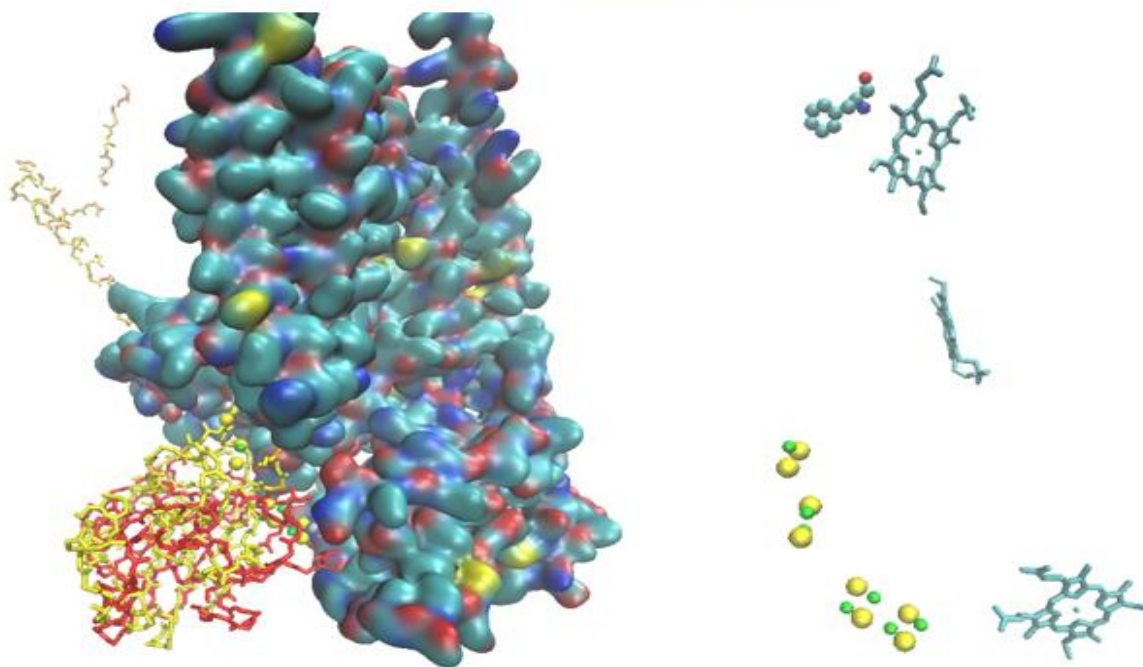


**Figure 6.1** Mitochondrial  $bc_1$  complex with ISP structures from four mitochondrial  $bc_1$  complexes aligned to the anchor portion. The figure on the left has the first and last head group positions indicated by corresponding, respective yellow and red head group backbone representations. On the right the protein has been removed leaving the FES clusters for the four positions and the cyt  $c_1$ , and the cyt  $b$  hemes (heme  $b_L$  and heme  $b_H$ ).

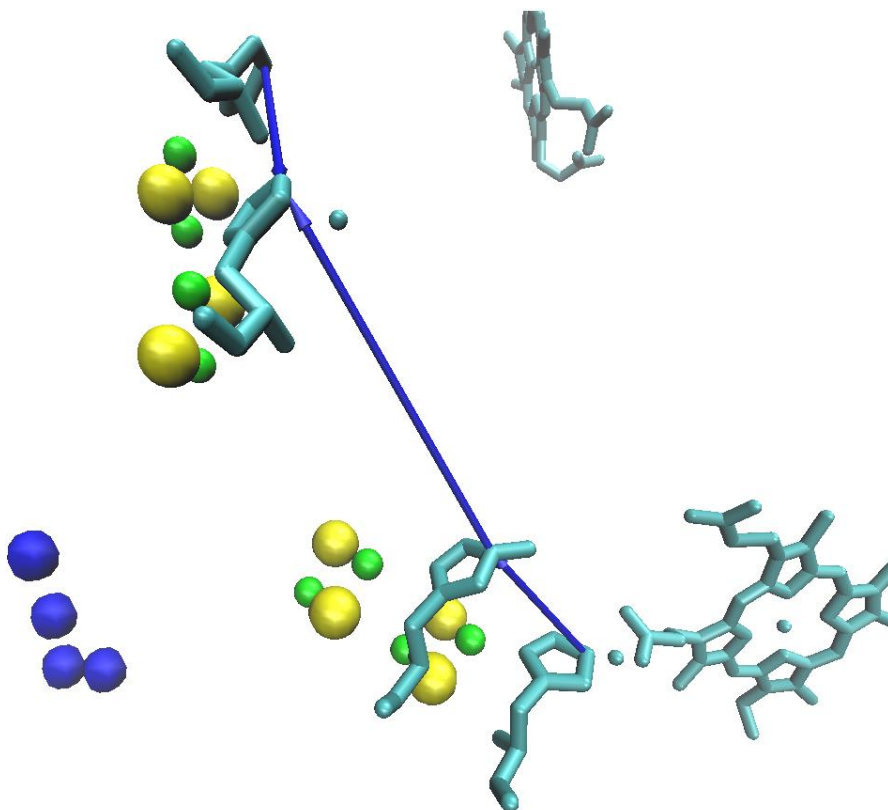


**Figure 6.2** The center of mass of the ISP head group of each position of the four aligned head group position is shown as blue spheres and blue vectors are drawn connecting the liganding histidine of the FeS cluster.

The head displacement appears to be a complicated process included in the dynamic process of gating the electron transfer (Fig. 6.2). The process is more complicated than a group rotation of the ISP head group around a pivot. An example of the way the motion is complex is shown by the difference in the paths taken by the liganding His152 of the FeS cluster (blue arrows) vs the path of the center of mass of the ISP head group (blue spheres) in Figure 6.2. The blue spheres located at the calculated center of mass for the head group show a boomerang shaped trajectory where the center of mass turns sharply upward in the last frame where the head group achieves closest approach to the propionate of cytochrome  $c_1$ .

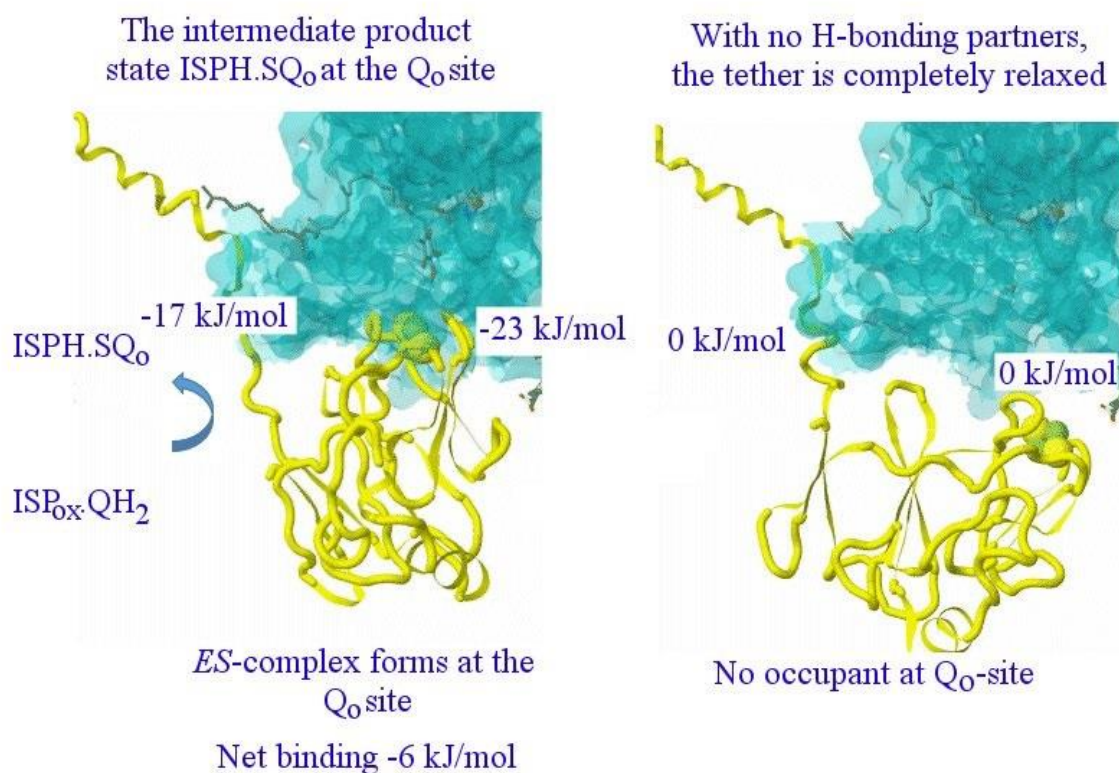


**Figure 6.3** The ISP subunit from structures of mitochondrial *bc*<sub>1</sub> complexes showing conformations that change with the occupancy of the Q<sub>0</sub>-site (adapted from (1-4)). The structures show ISP with the fully extended tether (left) on binding at the Q<sub>0</sub>-site (here with stigmatellin) and with the fully relaxed tether (right) when no bond is formed with a Q<sub>0</sub>-site occupant.

The extrinsic head of ISP moves to dock on cyt *b*, and the driving force is associated with substrate binding (predominantly, the H-bond with His-152) and the protein interfaces involved. The work involved in binding contributes one set of the counteracting forces in the spring-loaded scenario. The other set of forces is associated with a change from helical to elongated chain in the tether span where the suppressor mutations are located. The binding force pulls on the tether to extend it. In the spring-loaded mechanism (6, 7, 77), the experimentally determined binding free-energy (~-6 kJ/mol) is the difference between the work involved in binding (-23 kJ/mol), and the work needed to extend the tether (-17 kJ/mol), referred to the relaxed state. The values shown are estimated from work on ISP mutants in *Rb. capsulatus* and *Rb. Sphaeroides* (77-80). The curved arrow shows the first electron transfer reaction after formation of the *ES*-complex.

## ES-complex Separation: A Fortunate Accident

When the antimycin was inserted to replace Q in the fully oxidized configuration (conf1) it was positioned (through carelessness) in such a way that one of the DVPG lipid tails was lassoed by the ring of the antimycin, as shown in the top portion of Fig. 6.4. During extensive minimization after setup, no error message was generated by the software to indicate that

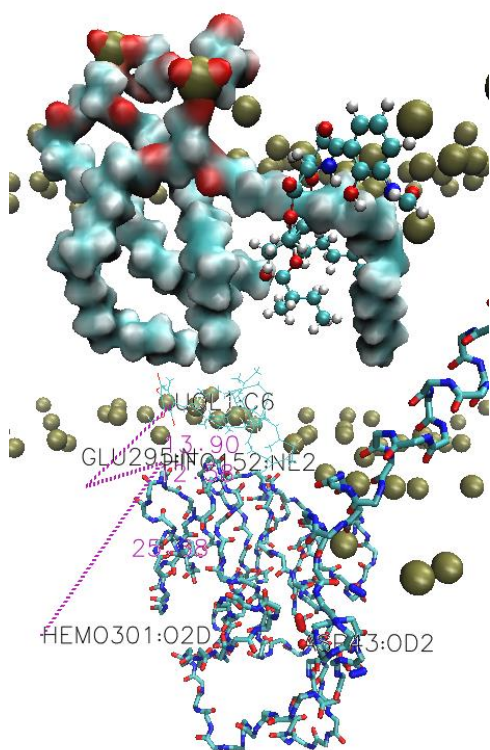


**Figure 6.4** Lipid fatty acid tail of a DVPG membrane lipid penetrates one of the rings of the antimycin in the Q<sub>i</sub>-site.

improper steric constraints were involved, and no error was indicated during the subsequent simulation, and the lassoed lipid tail in the antimycin ring was not detected until the trajectory generated by the simulation (conf1\_2, run for 77 ns) was examined; the anomalous exit of QH<sub>2</sub> from one of the Q<sub>o</sub>-sites required an asymmetric driving force, and the cause then became apparent. After the mistake was detected, the antimycin position was corrected so the lipid tail did not intersect the antimycin ring. The resultant configuration (conf1\_3) was then run. The major difference between these two configuration trajectories was the release of the ES complex observed in conf1\_2.

The first and last frames of the conf1\_2 trajectory are shown in Figure 6.5. With regard to the separation of the ES complex the conf1\_2 trajectory shows a small amount of movement of the FeS cluster toward the electron acceptor of the cyt c<sub>1</sub> propionate located at the second catalytic interface for the ISP head group. The distance from the cluster liganding His152: NE to



the cyt  $c_2$  heme propionate changes 2.24 Å from the time zero through to 77 ns. The quinol pulls away from the ISP head group and then leaves the channel leading out of  $Q_o$ -site.

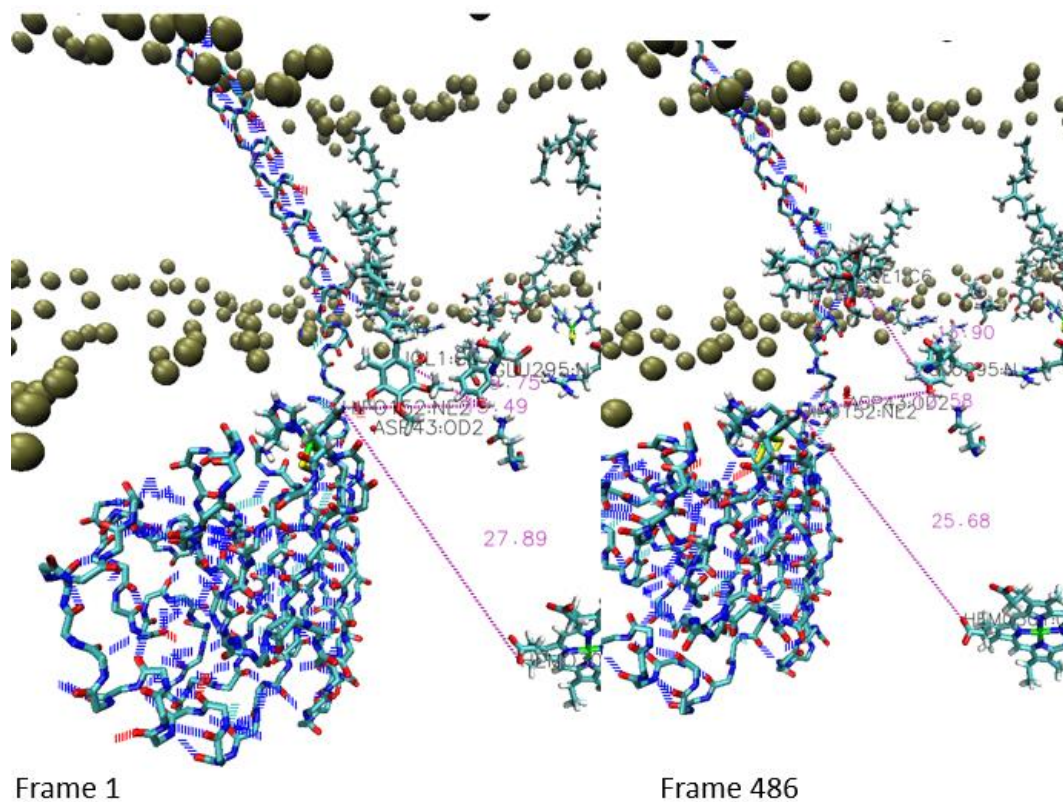


**Figure 6.5** Representations from the first and last frames of the conf1\_2 configuration trajectory

The absolute motion of the quinol head group relative to its position in the first frame fails to show the relative motions of the head group and the quinol. Figure 6.6 shows the absolute motion of the ISP center of mass (ISP\_CofM), ISP FeS cluster (FES2\_vo), and the quinol head group (UqH2head\_movement). All of these motions appear substantial and relatively fast compared to the time frame in which they are required to occur in. However, the distance the center of mass of the protein moves from its initial position explains much of the large scale absolute movement of the ISP head group.

During the 77 ns trajectory of conf1\_2 the net motion is consistent with ranges defined by experiments observing effects of different experimental conditions on rate limiting processes which occur after ES complex separation. So a better way to observe the motions is by looking

at the separation distance between the participants in the ES complex, i.e., ISP head group, ubiquinol, and cyt b (Fig. 6.6). The destination of the ISP head group for passing an electron, as indicated by the bond shown to the propionate in Fig 6.5, is cyt  $c_1$  and constitutes a second catalytic interface for the ISP head group.

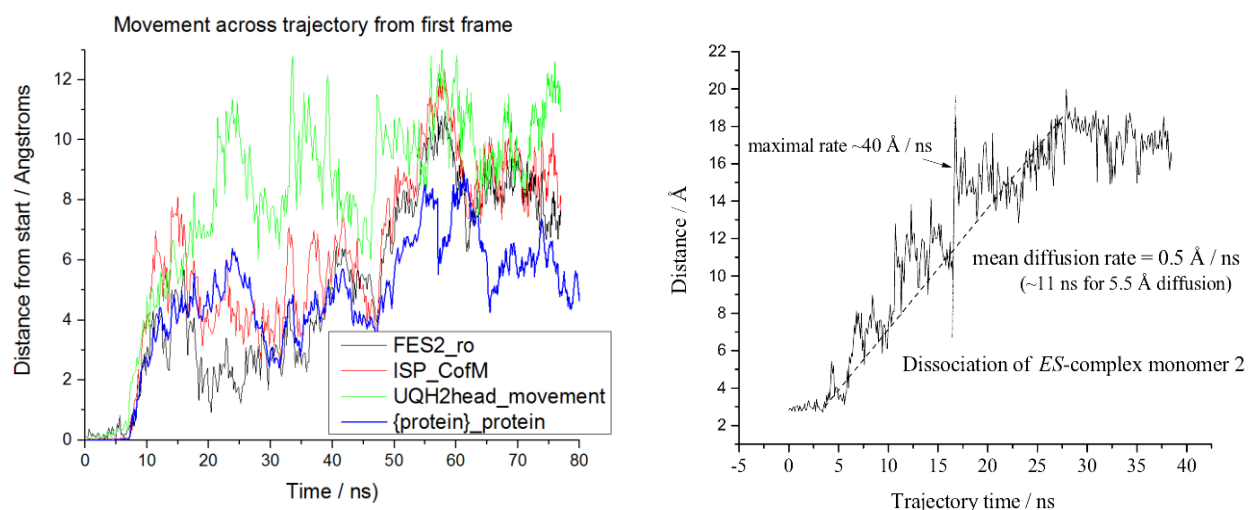


**Figure 6.6 Left:** Movement of the FES cluster center of mass (FES2\_ro), the ISP head group center of mass (ISP\_CofM), ubiquinol head center of mass movement (UQH2head\_movement) and protein center of mass movement (protein\_protein) where the movement in Angstroms is the magnitude of the displacement vector measured from the initial position at time 0 ns. **Right:** Exit of QH<sub>2</sub> measured by the distance between QH<sub>2</sub>-O and ISP H152 N $\epsilon$ .

Relative distances or separation distances between His152: NE (the epsilon nitrogen) and QH<sub>2</sub> (right) allows visualization of the diffusion of the QH<sub>2</sub> out of the Q<sub>o</sub>-site. The pathway followed is through the access channel from the lipid phase, so this diffusion is essentially 1-D. The kinetic parameters from measurements of turnover of partial processes show that entry and exit of Q or QH<sub>2</sub> is rapid compared to the rate limiting step ( $10^3 \text{ s}^{-1}$ ), so the diffusional rate shown here would certainly allow rapid passage. However, this needs to be applied in determination of collisional frequency to relate it to kinetics. The diffusional rates are also relevant in the Q<sub>o</sub>-site mechanism, where the SQ<sub>o</sub> must move closer to heme  $b_L$  to transfer the electron rapidly. In the kinetic model, this process has a rate  $\sim 10^7 \text{ s}^{-1}$  and the SQ<sub>o</sub> moves through  $\sim 5.5 \text{ \AA}$ , so the mean rate seen here is quite sufficient (see Fig.6.6, right). Also shown are

distances to the heme propionate of cyt  $c_1$  (Hem:O) and a relatively fixed point near the opening of the  $Q_o$ -site, Tyr147, are shown in Fig. 6.7. The distance between the quinol and the point picked to represent a fixed position relative to the protein, Tyr147, is also shown in Fig. 6.7. The ISP head group moves about 5 Å closer to the heme propionate of cyt  $c_1$  within 13 frames and then oscillates within 2 to 5 Å for the rest of the trajectory (Fig. 6.7). The His152: NE of the ISP head group moves at much as 3 Å from the Tyr147 in 8 frames and then oscillates between that distance and 1 Å separation. The distance of separation of the quinol head group from proximate to the Tyr147 to outside the  $Q_o$ -site entry way shows an abrupt quick change and then gradual steps in and out of the entry way until the head group of UQH<sub>2</sub> is situated well outside the  $Q_o$ -site after 20 frames which is about 40 ns of simulation time since the trajectory starts at a 2 fs time step (Fig. 6.7)

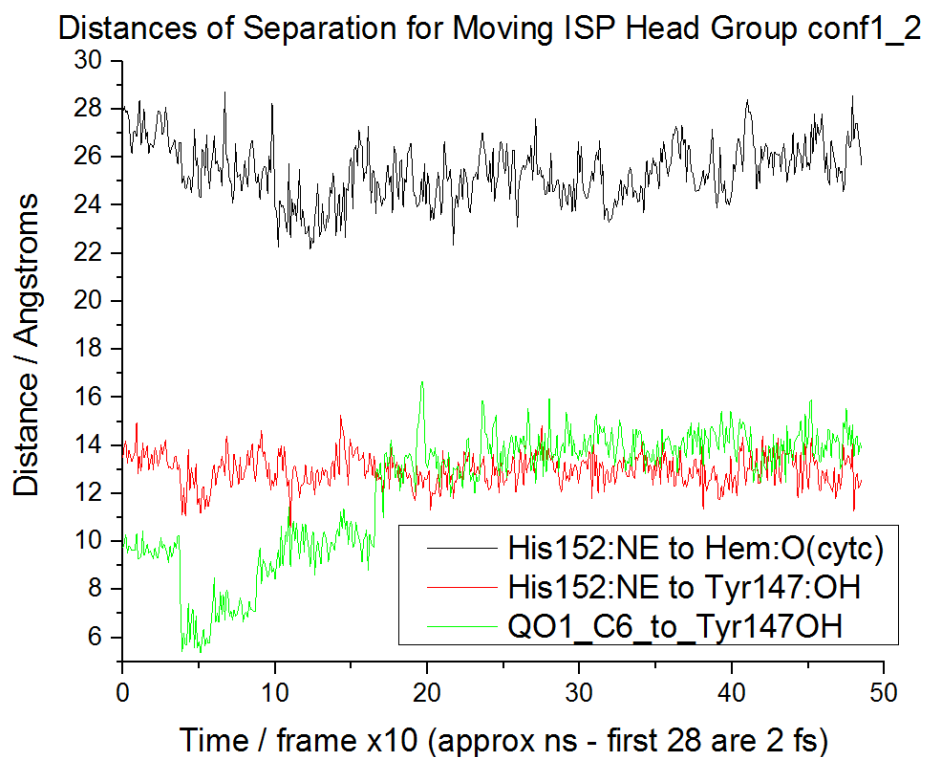
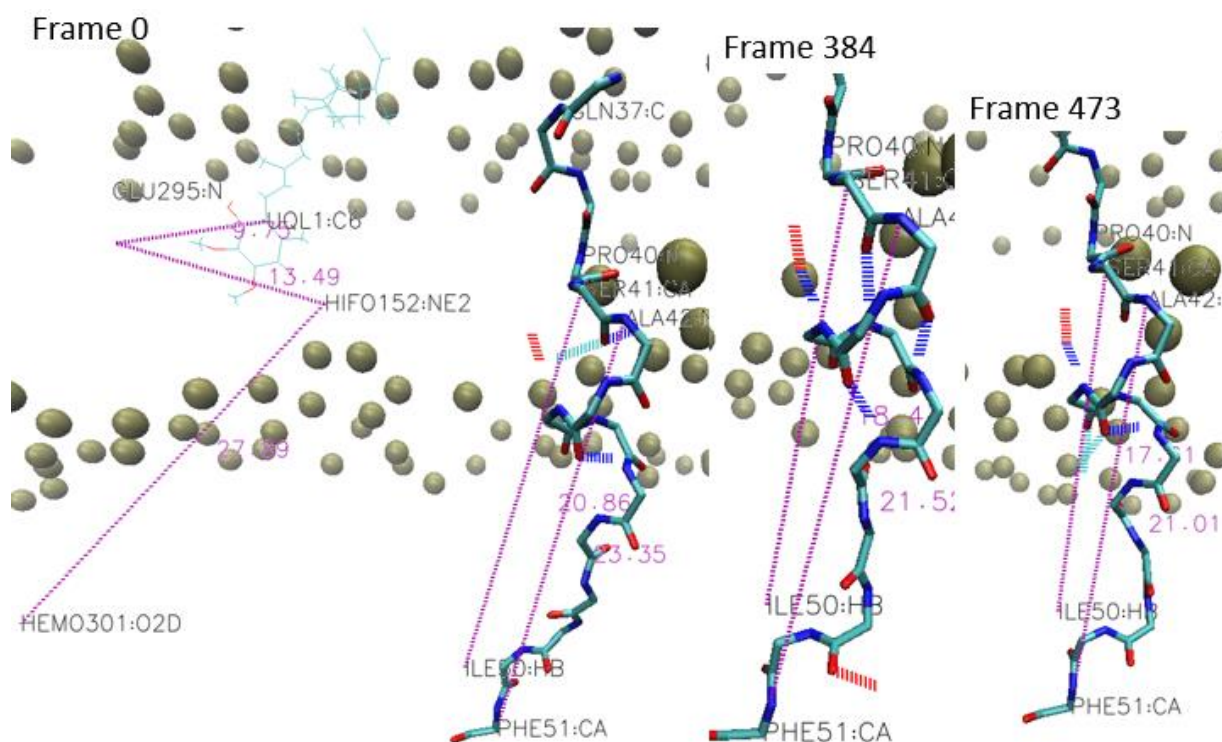


Figure 6.7 distances of separation between the indicated protein residue Tyr147, liganding His152 and cyt  $c_1$  propionate.

Changes in the tether region are shown in Figure 6.8 which shows the formation of various hydrogen bond from before ES complex separation (frame 0) to after ES – complex formation. The ISP tether region is represented with only the backbone atoms. The hydrogen bonds can be seen more easily but since some hydrogen bonds are forming with side chains and surrounding residues, they seem to float proximate to the ISP tether region representation. The indicated bonds between arbitrarily picked pairs of points along the tether region have their separation distances graphed in Fig 6.10. As seen in Fig. 6.10 this portion of the tether region seems to be relaxing toward a more structured configuration with more interlinking hydrogen



**Figure 6.8** Changes in the ISP tether region for conf1\_2 with bond indications from Fig. 6.5 left in to give context to the ISP tether region represented with only the back bone and hydrogen bonds indicated with thick broken red and blue lines.

bonds. These additional hydrogen bonds are part of the gating force for the ES complex as discussed above with reference to the calculation of these relative forces shown in Fig. 6.3. The number and frequency of hydrogen bonds can be tracked with the VMD timeline plugin shown in Fig. 6.10.



## Distances for ISP hinge region extension

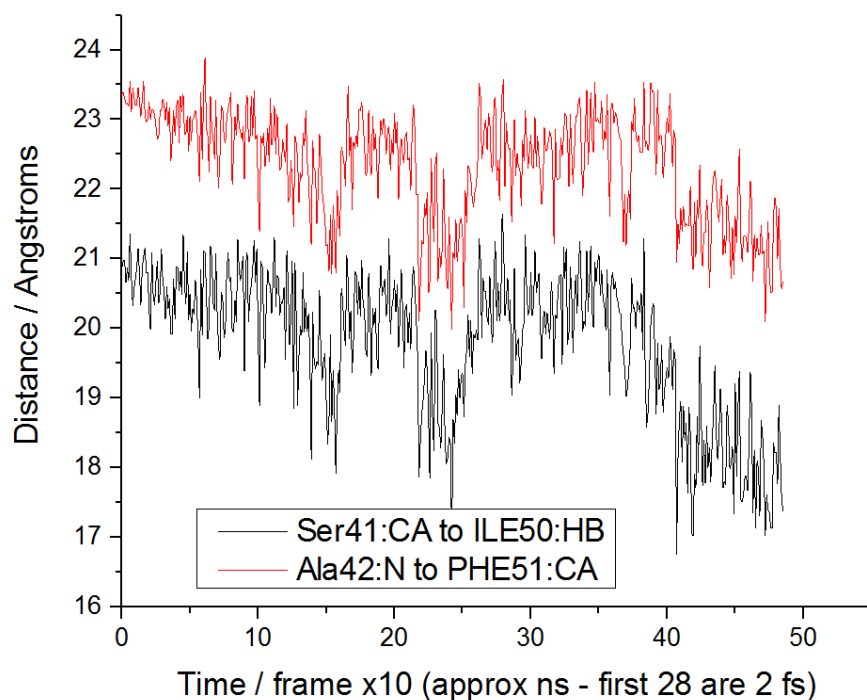


Figure 6.9 Distances between the two pairs of arbitrarily selected points along the ISP tether region as indicated in Figure 6.8.

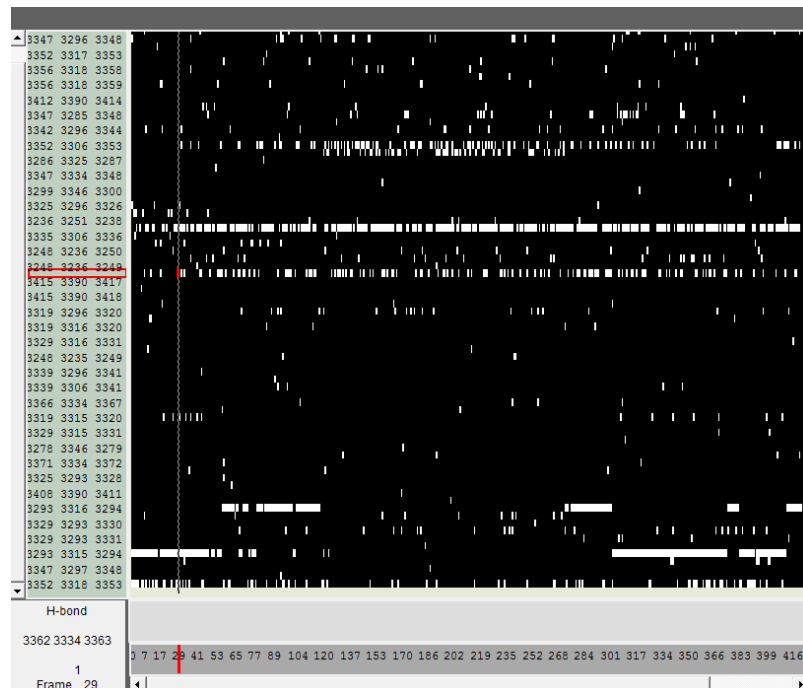


Figure 6.10 Timeline representation of H-bonding across conf1\_2 trajectory where the color scheme is a binary representation of the presence or absence of an H-bond according to the H-bond definition so that white portions show frames in which an H-bond exists and black portions show when there is no H-bond.

The energy parameters can be entered into the kinetic model to (i.) compare to earlier guesses based on different assumptions; and (ii.) adjust other parameters by using these energy terms change the other terms by changing the partitioning of energy between partial processes in the kinetic model. These experiments will help characterize a mechanism which is predicted to be 'spring-loaded' with respect to the ISP headgroup involvement.

# References

1. A. R. Crofts *et al.*, Mechanism of ubiquinol oxidation by the bc<sub>1</sub> complex: Different domains of the quinol binding pocket and their role in the mechanism and binding of inhibitors. *Biochemistry* **38**, 15807-15826 (1999).
2. A. R. Crofts *et al.*, Pathways for proton release during ubihydroquinone oxidation by the bc<sub>1</sub> complex. *P Natl Acad Sci USA* **96**, 10021-10026 (1999).
3. A. R. Crofts *et al.*, The mechanism of ubiquinol oxidation by the bc<sub>1</sub> complex: the role of the iron sulfur protein, and its mobility. *Biochemistry* **38**, 15791-15806 (1999).
4. A. R. Crofts, S. Hong, Z. Zhang, E. A. Berry, Physicochemical aspects of the movement of the Rieske iron sulfur protein during quinol oxidation by the bc<sub>1</sub> complex. *Biochemistry* **38**, 15827-15839 (1999).
5. A. R. Crofts, Lhee, S., Crofts, S.B., Cheng, J. and Rose, S., Proton pumping in the bc<sub>1</sub> complex: A new gating mechanism that prevents short circuits. *Biochim. Biophys. Acta* **1757**, 1019-1034 (2006).
6. G. Jafari *et al.*, Tether mutations that restore function and suppress pleiotropic phenotypes of the *C. elegans* isp-1(qm150) Rieske iron-sulfur protein. *P Natl Acad Sci USA* **112**, E6148-E6157 (2015).
7. G. Jafari, B. M. Wasko, M. Kaeberlein, A. R. Crofts, New functional and biophysical insights into the mitochondrial Rieske iron-sulfur protein from genetic suppressor analysis in *C. elegans*. *Worm* **5**, e1174803 (2016).
8. E. A. Berry, H. De Bari, L.-S. Huang, Unanswered questions about the structure of cytochrome bc<sub>1</sub> complexes. *Biochim. Biophys. Acta* **1827**, 1258-1277 (2013).
9. E. A. Berry, D.-W. Lee, L.-S. Huang, F. Daldal, in *The Purple Phototrophic Bacteria*, C. N. Hunter, F. Daldal, M. C. Thurnauer, J. T. Beatty, Eds. (Springer, Dordrecht, The Netherlands, 2009), chap. 22.
10. C. Hunte, S. Solmaz, H. Palsdóttir, T. Wenz, in *Bioenergetics*. (Springer, Berlin / Heidelberg, 2008), vol. 45, pp. 253-278.
11. D. Xia *et al.*, Structural analysis of cytochrome bc<sub>1</sub> complexes: Implications to the mechanism of function. *Biochim. Biophys. Acta* **1827**, 1278-1294 (2013).
12. J. B. Jackson, A. R. Crofts, The high energy state in chromatophores from *Rhodospseudomonas spheroides*. *FEBS Lett.* **4**, 185-189 (1969).
13. A. R. Crofts, S. W. Meinhardt, K. R. Jones, M. Snozzi, The role of the quinone pool in the cyclic electron-transfer chain of *Rhodospseudomonas sphaeroides*: A Modified Q-cycle Mechanism. *Biochim. Biophys. Acta* **723**, 202-218 (1983).
14. J. B. Jackson, A. R. Crofts, The kinetics of light induced carotenoid changes in *Rhodospseudomonas spheroides* and their relation to electrical field generation across the chromatophore membrane. *Eur. J. Biochem.* **18**, 120-130 (1971).
15. E. G. Glaser, A. R. Crofts, A new electrogenic step in the ubiquinol: Cytochrome c<sub>2</sub> oxidoreductase complex of *Rhodospseudomonas sphaeroides*. *Biochimica et Biophysica Acta (BBA) - Bioenergetics* **766**, 322-333 (1984).
16. G. Venturoli, M. Virgili, B. A. Melandri, A. R. Crofts, Kinetic measurements of electron transfer in coupled chromatophores from photosynthetic bacteria: A method of correction for the electrochromic effects. *FEBS Lett.* **219**, 477-484 (1987).
17. Y. Chen, University of Illinois at Urbana-Champaign, (1989).
18. Y. Chen, A. R. Crofts, in *Current Research in Photosynthesis*, M. Baltscheffsky, Ed. (Kluwer Academic Publishers, Dordrecht/Boston/London., 1990), vol. III, pp. 287-290.

19. A. R. Crofts *et al.*, in *Highlights in Ubiquinone Research*, G. Lenaz, O. Barnabei, A. Rabbi, M. Battino, Eds. (Taylor & Francis, Ltd, London, 1990), pp. 98-103.
20. J. J. Lemasters, W. H. Billica, Non-equilibrium thermodynamics of oxidative phosphorylation by inverted inner membrane vesicles of rat liver mitochondria. *Journal of Biological Chemistry* **256**, 12949-12957 (1981).
21. X. Gao *et al.*, Structural Basis for the Quinone Reduction in the bc<sub>1</sub> Complex: A Comparative Analysis of Crystal Structures of Mitochondrial Cytochrome bc<sub>1</sub> with Bound Substrate and Inhibitors at the Q<sub>i</sub> Site. *Biochemistry* **42**, 9067-9080 (2003).
22. E. A. Berry, and Huang, L. S., Observations concerning the quinol oxidation site of the cytochrome bc<sub>1</sub> complex. *FEBS Lett.* **555**, 13-20 (2003).
23. A. R. Crofts *et al.*, The mechanism of ubiquinol oxidation by the bc<sub>1</sub> complex: the different domains of the quinol binding pocket, and their role in mechanism, and the binding of inhibitors. *Biochemistry* **38**, 15807-15826 (1999).
24. C. Hunte, J. Koepke, C. Lange, T. Roßmanith, H. Michel, Structure at 2.3 Å resolution of the cytochrome bc<sub>1</sub> complex from the yeast *Saccharomyces cerevisiae* co-crystallized with an antibody F<sub>v</sub> fragment. *Structure* **8**, 669-684 (2000).
25. G. Engstrom *et al.*, Photoinduced electron transfer between the Rieske iron-sulfur protein and cytochrome c<sub>1</sub> in the *Rhodobacter sphaeroides* cytochrome bc<sub>1</sub> complex: effects of pH, temperature, and driving force. *J. Biol.Chem.* **277**, 31072-31078 (2002).
26. A. R. Crofts *et al.*, The Q-cycle Mechanism of the bc<sub>1</sub> Complex: a Biologist's Perspective on Atomistic Studies. *The Journal of Physical Chemistry B*, (2017).
27. C. Lange, J. H. Nett, B. L. Trumpower, C. Hunte, Specific roles of protein-phospholipid interactions in the yeast bc<sub>1</sub> complex structure. *EMBO J.* **23**, 6591-6600 (2001).
28. S. R. N. Solmaz, C. Hunte, Structure of Complex III with Bound Cytochrome c in Reduced State and Definition of a Minimal Core Interface for Electron Transfer. *Journal of Biological Chemistry* **283**, 17542-17549 (2008).
29. P. A. Postila *et al.*, Key role of water in proton transfer at the Q<sub>o</sub>-site of the cytochrome bc<sub>1</sub> complex predicted by atomistic molecular dynamics simulations. *Biochim. Biophys. Acta* **1827**, 761-768 (2013).
30. S. Pöyry *et al.*, Atomistic simulations indicate cardiolipin to have an integral role in the structure of the cytochrome bc<sub>1</sub> complex. *Biochimica et Biophysica Acta (BBA) - Bioenergetics* **1827**, 769-778 (2013).
31. S. Izrailev, A. R. Crofts, E. A. Berry, K. Schulten, Steered Molecular Dynamics Simulation of the Rieske Subunit Motion in the Cytochrome bc<sub>1</sub> Complex. *Biophys. J.* **77**, 1753-1768 (1999).
32. D. R. Martin, D. N. LeBard, D. V. Matyushov, Coulomb Soup of Bioenergetics: Electron Transfer in a Bacterial bc<sub>1</sub> Complex. *The Journal of Physical Chemistry Letters* **4**, 3602-3606 (2013).
33. A. M. Barragan, A. R. Crofts, K. Schulten, I. A. Solov'yov, Identification of ubiquinol binding motifs at the Q<sub>o</sub>-site of the cytochrome bc<sub>1</sub> complex. *J. Phys. Chem. B*, (2014).
34. X. Zhang *et al.*, Combined genetic and metabolic manipulation of lipids in *Rhodobacter sphaeroides* reveals non-phospholipid substitutions in fully active cytochrome c oxidase. *Biochemistry* **50**, 3891-3902 (2011).
35. C. Benning, Z. H. Huang, D. A. Gage, Accumulation of a Novel Glycolipid and a Betaine Lipid in Cells of *Rhodobacter sphaeroides* Grown under Phosphate Limitation. *Archives of Biochemistry and Biophysics* **317**, 103-111 (1995).
36. A. Baccarini-Melandri *et al.*, Differential Extraction and Structural Specificity of Specialized Ubiquinone Molecules in Secondary Electron Transfer in Chromatophores from *Rps. sphaeroides* GA. *Arch. Biochem. Biophys.* **216**, 566-580 (1982).

37. A. Baccarini-Melandri, B. A. Melandri, A role for ubiquinone-10 in the b---c2 segment of the photosynthetic bacterial electron transport chain. *FEBS Letters* **80**, 459-464 (1977).
38. K.-I. Takamiya, P. L. Dutton, Ubiquinone in *Rhodospseudomonas sphaeroides*. Some thermodynamic properties. *Biochimica et Biophysica Acta (BBA) - Bioenergetics* **546**, 1-16 (1979).
39. A. M. Barragan, A. R. Crofts, K. Schulten, I. A. Solov'yov, Identification of Ubiquinol Binding Motifs at the Q(o)-Site of the Cytochrome bc(1) Complex. *The Journal of Physical Chemistry. B* **119**, 433-447 (2015).
40. T. John, C. Timothy *et al.*, Eds. (2014), vol. 16, pp. 62-74.
41. W. Humphrey, A. Dalke, K. Schulten, VMD: Visual molecular dynamics. *Journal of Molecular Graphics* **14**, 33-38 (1996).
42. J. C. Phillips *et al.*, Scalable molecular dynamics with NAMD. *J. Computational Chem.* **26**, 1781-1802 (2005).
43. J. B. Klauda *et al.*, Update of the CHARMM all-atom additive force field for lipids: Validation on six lipid types. *Journal of Physical Chemistry B.* **114**, 7830-7843. (2010).
44. J. MacKerell, A. D. , M. Feig, C. L. Brooks III, Extending the treatment of backbone energetics in protein force fields: Limitations of gas-phase quantum mechanics in reproducing protein conformational distributions in molecular dynamics simulations. *Journal of Computational Chemistry* **25**, 1400-1415 (2004).
45. K. Kaszuba *et al.*, Parameterization of the prosthetic redox centers of the bacterial cytochrome bc 1 complex for atomistic molecular dynamics simulations. *Theor Chem Acc* **132**, 1-13 (2013).
46. W. L. Jorgensen, J. Chandrasekhar, J. D. Madura, R. W. Impey, M. L. Klein, Comparison of simple potential functions for simulating liquid water. *Journal of Chemical Physics* **79**, 926-935 (1983).
47. T. Martinetz, K. Schulten, Topology representing networks. *Neural Networks* **7**, 507-522 (1994).
48. S. E. Feller, Y. Zhang, R. W. Pastor, B. R. Brooks, Constant pressure molecular dynamics simulation: The Langevin piston method. *Journal of Chemical Physics* **103**, 4613-4621 (1995).
49. T. Darden, D. York, L. G. Pedersen, Particle mesh Ewald: An N.log(N) method for Ewald sums in large systems. *Journal of Chemical Physics* **98**, 10089-10092 (1993).
50. A. Leach, *Molecular Modelling: Principles and Applications (2nd Edition)*. (Prentice Hall, 2001).
51. B. Tamot, C. Benning, in *The Purple Phototrophic Bacteria*, C. N. Hunter, F. Daldal, M. C. Thurnauer, J. T. Beatty, Eds. (Springer Netherlands, Dordrecht, 2009), pp. 119-134.
52. X. Zhang, S. M. Ferguson-Miller, G. E. Reid, Characterization of ornithine and glutamine lipids extracted from cell membranes of *Rhodobacter sphaeroides*. *Journal of the American Society for Mass Spectrometry* **20**, 198-212 (2009).
53. S. Aygun-Sunar *et al.*, Ornithine lipid is required for optimal steady-state amounts of c-type cytochromes in *Rhodobacter capsulatus*. *Molecular Microbiology* **61**, 418-435 (2006).
54. T. Róg *et al.*, Role of Cardiolipins in the Inner Mitochondrial Membrane: Insight Gained through Atom-Scale Simulations. *The Journal of Physical Chemistry B* **113**, 3413-3422 (2009).
55. N. J. Russell, J. L. Harwood, Changes in the acyl lipid composition of photosynthetic bacteria grown under photosynthetic and non-photosynthetic conditions. . *Biochem. J.* **181**, 339-345 (1979).
56. S. Jo, T. Kim, V. G. Iyer, W. Im, CHARMM-GUI: A web-based graphical user interface for CHARMM. *Journal of Computational Chemistry* **29**, 1859-1865 (2008).
57. B. R. Brooks *et al.*, CHARMM: The biomolecular simulation program. *Journal of Computational Chemistry* **30**, 1545-1614 (2009).
58. J. Lee *et al.*, CHARMM-GUI Input Generator for NAMD, GROMACS, AMBER, OpenMM, and CHARMM/OpenMM Simulations Using the CHARMM36 Additive Force Field. *Journal of Chemical Theory and Computation* **12**, 405-413 (2016).

59. E. L. Wu *et al.*, CHARMM-GUI Membrane Builder toward realistic biological membrane simulations. *Journal of Computational Chemistry* **35**, 1997-2004 (2014).
60. S. Jo, J. B. Lim, J. B. Klauda, W. Im, CHARMM-GUI Membrane Builder for Mixed Bilayers and Its Application to Yeast Membranes. *Biophysical Journal* **97**, 50-58 (2009).
61. S. Jo, T. Kim, W. Im, Automated Builder and Database of Protein/Membrane Complexes for Molecular Dynamics Simulations. *PLoS ONE* **2**, e880 (2007).
62. L. Janosi, Z. Li, J. F. Hancock, A. A. Gorfe, Organization, dynamics, and segregation of Ras nanoclusters in membrane domains. *Proceedings of the National Academy of Sciences* **109**, 8097-8102 (2012).
63. R. Fato, M. Battino, G. P. Castelli, G. Lenaz, Measurement of the lateral diffusion coefficients of ubiquinones in lipid vesicles by fluorescence quenching of 12-(9-anthroyl)stearate. *FEBS Letters* **179**, 238--242 (1985).
64. M. F. Blackwell, J. Whitmarsh, Effect of integral membrane proteins on the lateral mobility of plastoquinone in phosphatidylcholine proteoliposomes. *Biophysical Journal* **58**, 1259-1271 (1990).
65. A. R. Crofts *et al.*, The mechanism of ubihydroquinone oxidation at the Q<sub>o</sub>-site of the cytochrome *bc*<sub>1</sub> complex. *Biochim. Biophys. Acta* **1827**, 1362-1377 (2013).
66. D. Victoria, R. Burton, A. R. Crofts, Role of the -PEWY- glutamate in catalysis at the Q<sub>o</sub>-site of the *cyt bc*<sub>1</sub> complex. *Biochim. Biophys. Acta* **1827**, 365-386 (2012).
67. D. T. Gillespie, Exact Stochastic Simulation of Coupled Chemical Reactions. *J. Phys. Chem.* **81**, 2340-2361 (1977).
68. S. Ransac, N. Parisey, J.-P. Mazat, The loneliness of the electrons in the *bc*<sub>1</sub> complex. *Biochim. Biophys. Acta* **1777**, 1053-1059 (2008).
69. A. R. Crofts, V. P. Shinkarev, D. R. J. Kolling, S. Hong, The modified Q-cycle explains the apparent mismatch between the kinetics of reduction of cytochromes *c*<sub>1</sub> and *b*<sub>H</sub> in the *bc*<sub>1</sub> complex. *J. Biol. Chem.* **278**, 36191-36201 (2003).
70. A. M. Barragan, K. Schulten, I. A. Solov'yov, Mechanism of the Primary Charge Transfer Reaction in the Cytochrome *bc*<sub>1</sub> Complex. *The Journal of Physical Chemistry B* **120**, 11369-11380 (2016).
71. G. M. Torrie, J. P. Valleau, Nonphysical sampling distributions in Monte Carlo free-energy estimation: Umbrella sampling. *Journal of Computational Physics* **23**, 187-199. (1977).
72. A. Kumar, V. Kothekar, Stereochemical aspects of interactions of DNA binding domain of human progesterone receptor with d(AGGTCATGCT)<sub>2</sub>. *Indian Journal of Biochemistry and Biophysics* **29**, 236-244 (1992).
73. M. Souaille, B. Roux, Extension to the weighted histogram analysis method: combining umbrella sampling with free energy calculations. *Computer Physics Communications* **135**, 40-57 (2001).
74. D. Frenkel, B. Smit, *Understanding Molecular Simulation From Algorithms to Applications*. (Academic Press, San Diego, California, 2002).
75. A. R. Crofts, V. P. Shinkarev, S. A. Dikanov, R. I. Samoilova, D. Kolling, Interactions of quinone with the iron-sulfur protein of the *bc*<sub>1</sub> complex: Is the mechanism spring-loaded? *Biochim. Biophys. Acta* **1555**, 48-53 (2002).
76. Y. Sugita, A. Kitao, Y. Okamoto, Multidimensional replica-exchange method for free-energy calculations. *The Journal of Chemical Physics* **113**, 6042-6051 (2000).
77. A. R. Crofts, V. P. Shinkarev, S. A. Dikanov, R. I. Samoilova, D. Kolling, Interactions of quinone with the iron-sulfur protein of the *bc*(1) complex: is the mechanism spring-loaded? *Biochimica Et Biophysica Acta-Bioenergetics* **1555**, 48-53 (2002).
78. E. Darrouzet, Valkova-Valchanova, M., and Daldal, F., The [2Fe-2S] Cluster E<sub>m</sub> as an Indicator of the Iron-Sulfur Subunit Position in the Ubihydroquinone Oxidation Site of the Cytochrome *bc*<sub>1</sub> Complex. *J. Biol. Chem* **277**, 3464-3470 (2002).

79. E. Darrouzet, F. Daldal, Protein-protein interactions between cytochrome b and the Fe-S protein subunits during QH<sub>2</sub> oxidation and large-scale domain movement in the bc<sub>1</sub> complex. *Biochemistry* **42**, 1499-1507 (2003).
80. E. Darrouzet, M. Valkova-Valchanova, F. Daldal, Probing the role of the Fe-S rubunit hinge region during Q<sub>o</sub> site catalysis in *Rhodobacter capsulatus* bc<sub>1</sub> complex. *Biochemistry* **39**, 15475-15483 (2000).





ATOM H14C	HL	0.25 !			
ATOM C15	CTL5	-0.35 !			
ATOM H15A	HL	0.25 !	H12A--C12---H12B		
ATOM H15B	HL	0.25 !			
ATOM H15C	HL	0.25 !			
GROUP		!		alpha5	
ATOM C11	CTL2	-0.08 !			
ATOM H11A	HAL2	0.09 !	H11A--C11---H11B		
ATOM H11B	HAL2	0.09 !		alpha4	
ATOM P	PL	1.50 !	(-) O13 O12		
ATOM O13	O2L	-0.78 !	\ /	alpha3	
ATOM O14	O2L	-0.78 !	P (+)		
ATOM O12	OSLP	-0.57 !	/ \	alpha2	
ATOM O11	OSLP	-0.57 !	(-) O14 O11		
ATOM C1	CTL2	-0.08 !		alpha1	
ATOM HA	HAL2	0.09 !	HA---C1---HB		
ATOM HB	HAL2	0.09 !		theta1	
GROUP		!			
ATOM C2	CTL1	0.17 !	HS---C2-----		
ATOM HS	HAL1	0.09 !	beta1		
ATOM O21	OSL	-0.49 !	O22 O21	theta3	
ATOM C21	CL	0.90 !	\ \ / beta2		
ATOM O22	OBL	-0.63 !	C21		
ATOM C22	CTL2	-0.22 !	beta3		
ATOM H2R	HAL2	0.09 !	H2R---C22---H2S		
ATOM H2S	HAL2	0.09 !			
GROUP		!		beta4	
ATOM C3	CTL2	0.08 !			
ATOM HX	HAL2	0.09 !		HX---C3---HY	
ATOM HY	HAL2	0.09 !			gamma1
ATOM O31	OSL	-0.49 !		O32 O31	
ATOM C31	CL	0.90 !		\ \ /	gamma2
ATOM O32	OBL	-0.63 !		C31	
ATOM C32	CTL2	-0.22 !			gamma3
ATOM H2X	HAL2	0.09 !		H2X---C32---H2Y	
ATOM H2Y	HAL2	0.09 !			
GROUP		!			gamma4
ATOM C23	CTL2	-0.18 !			
ATOM H3R	HAL2	0.09 !	H3R ---C23---H3S		
ATOM H3S	HAL2	0.09 !			
GROUP		!			
ATOM C24	CTL2	-0.18 !			
ATOM H4R	HAL2	0.09 !	H4R ---C24---H4S		
ATOM H4S	HAL2	0.09 !			
GROUP		!			
ATOM C25	CTL2	-0.18 !			
ATOM H5R	HAL2	0.09 !	H5R ---C25---H5S		
ATOM H5S	HAL2	0.09 !			
GROUP		!			
ATOM C26	CTL2	-0.18 !			
ATOM H6R	HAL2	0.09 !	H6R ---C26---H6S		
ATOM H6S	HAL2	0.09 !			
GROUP		!			
ATOM C27	CTL2	-0.18 !			
ATOM H7R	HAL2	0.09 !	H7R ---C27---H7S		
ATOM H7S	HAL2	0.09 !			
GROUP		!			
ATOM C28	CTL2	-0.18 !			
ATOM H8R	HAL2	0.09 !	H8R ---C28---H8S		
ATOM H8S	HAL2	0.09 !			
GROUP		!			
ATOM C29	CTL2	-0.18 !			
ATOM H9R	HAL2	0.09 !	H9R ---C29---H9S		
ATOM H9S	HAL2	0.09 !			

GROUP		!		
ATOM C210	CTL2	-0.18		
ATOM H10R	HAL2	0.09	H10R---C210--H10S	
ATOM H10S	HAL2	0.09		
GROUP		!		
ATOM C211	CEL1	-0.15		
ATOM H11R	HEL1	0.15	H11R --C211	
GROUP		!	(CIS)	
ATOM C212	CEL1	-0.15		
ATOM H12R	HEL1	0.15	H12R---C212	
GROUP		!		
ATOM C213	CTL2	-0.18		
ATOM H13R	HAL2	0.09	H13R---C213--H13S	
ATOM H13S	HAL2	0.09		
GROUP		!		
ATOM C214	CTL2	-0.18		
ATOM H14R	HAL2	0.09	H14R---C214--H14S	
ATOM H14S	HAL2	0.09		
GROUP		!		
ATOM C215	CTL2	-0.18		
ATOM H15R	HAL2	0.09	H15R---C215--H15S	
ATOM H15S	HAL2	0.09		
GROUP		!		
ATOM C216	CTL2	-0.18		
ATOM H16R	HAL2	0.09	H16R---C216--H16S	
ATOM H16S	HAL2	0.09		
GROUP		!		
ATOM C217	CTL2	-0.18		
ATOM H17R	HAL2	0.09	H17R---C217--H17S	
ATOM H17S	HAL2	0.09		
GROUP		!		
ATOM C218	CTL3	-0.27		
ATOM H18R	HAL3	0.09	H18R---C218--H18S	
ATOM H18S	HAL3	0.09		
ATOM H18T	HAL3	0.09	H18T	
GROUP		!		
ATOM C33	CTL2	-0.18		
ATOM H3X	HAL2	0.09	H3X ---C33---H3Y	
ATOM H3Y	HAL2	0.09		
GROUP		!		
ATOM C34	CTL2	-0.18		
ATOM H4X	HAL2	0.09	H4X ---C34---H4Y	
ATOM H4Y	HAL2	0.09		
GROUP		!		
ATOM C35	CTL2	-0.18		
ATOM H5X	HAL2	0.09	H5X ---C35---H5Y	
ATOM H5Y	HAL2	0.09		
GROUP		!		
ATOM C36	CTL2	-0.18		
ATOM H6X	HAL2	0.09	H6X ---C36---H6Y	
ATOM H6Y	HAL2	0.09		
GROUP		!		
ATOM C37	CTL2	-0.18		
ATOM H7X	HAL2	0.09	H7X ---C37---H7Y	
ATOM H7Y	HAL2	0.09		
GROUP		!		
ATOM C38	CTL2	-0.18		
ATOM H8X	HAL2	0.09	H8X ---C38---H8Y	
ATOM H8Y	HAL2	0.09		
GROUP		!		
ATOM C39	CTL2	-0.18		
ATOM H9X	HAL2	0.09	H9X ---C39---H9Y	
ATOM H9Y	HAL2	0.09		
GROUP		!		

ATOM C310	CTL2	-0.18	!		
ATOM H10X	HAL2	0.09	!	H10X---	C310--H10Y
ATOM H10Y	HAL2	0.09	!		
GROUP			!		
ATOM C311	CEL1	-0.15	!		
ATOM H11X	HEL1	0.15	!	H11X---	C311
GROUP			!		
ATOM C312	CEL1	-0.15	!		
ATOM H12X	HEL1	0.15	!	H12X---	C312
GROUP			!		
ATOM C313	CTL2	-0.18	!		
ATOM H13X	HAL2	0.09	!	H13X---	C313--H13Y
ATOM H13Y	HAL2	0.09	!		
GROUP			!		
ATOM C314	CTL2	-0.18	!		
ATOM H14X	HAL2	0.09	!	H14X---	C314--H14Y
ATOM H14Y	HAL2	0.09	!		
GROUP			!		
ATOM C315	CTL2	-0.18	!		
ATOM H15X	HAL2	0.09	!	H15X---	C315--H15Y
ATOM H15Y	HAL2	0.09	!		
GROUP			!		
ATOM C316	CTL2	-0.18	!		
ATOM H16X	HAL2	0.09	!	H16X---	C316--H16Y
ATOM H16Y	HAL2	0.09	!		
GROUP			!		
ATOM C317	CTL2	-0.18	!		
ATOM H17X	HAL2	0.09	!	H17X---	C317--H17Y
ATOM H17Y	HAL2	0.09	!		
GROUP			!		
ATOM C318	CTL3	-0.27	!		
ATOM H18X	HAL3	0.09	!	H18X---	C318--H18Y
ATOM H18Y	HAL3	0.09	!		
ATOM H18Z	HAL3	0.09	!		H18Z

! Polar Head

BOND N	C13	N	C14	N	C15		
BOND C13	H13A	C13	H13B	C13	H13C		
BOND C14	H14A	C14	H14B	C14	H14C		
BOND C15	H15A	C15	H15B	C15	H15C		
BOND N	C12						
BOND C12	H12A	C12	H12B	C12	C11		
BOND C11	H11A	C11	H11B	C11	O12	O11	C1
BOND O12	P	P	O11	P	O13	P	O14

! Glycerol Backbone

BOND C1	HA	C1	HB	C1	C2
BOND C2	HS	C2	C3	C2	O21
BOND C3	HX	C3	HY	C3	O31

! Chain from C2

BOND O21	C21				
BOND C21	C22				
DOUBLE C21	O22				
BOND C22	H2R	C22	H2S	C22	C23
BOND C23	H3R	C23	H3S	C23	C24
BOND C24	H4R	C24	H4S	C24	C25
BOND C25	H5R	C25	H5S	C25	C26
BOND C26	H6R	C26	H6S	C26	C27
BOND C27	H7R	C27	H7S	C27	C28
BOND C28	H8R	C28	H8S	C28	C29
BOND C29	H9R	C29	H9S	C29	C210
BOND C210	H10R	C210	H10S	C210	C211
BOND C211	H11R				
DOUBLE C211	C212				
BOND C212	H12R	C212	C213		

```

BOND C213 H13R      C213 H13S      C213 C214
BOND C214 H14R      C214 H14S      C214 C215
BOND C215 H15R      C215 H15S      C215 C216
BOND C216 H16R      C216 H16S      C216 C217
BOND C217 H17R      C217 H17S      C217 C218
BOND C218 H18R      C218 H18S      C218 H18T
! Chain From C3
BOND O31 C31
BOND C31 C32
DOUBLE C31 O32
BOND C32 H2X      C32 H2Y      C32 C33
BOND C33 H3X      C33 H3Y      C33 C34
BOND C34 H4X      C34 H4Y      C34 C35
BOND C35 H5X      C35 H5Y      C35 C36
BOND C36 H6X      C36 H6Y      C36 C37
BOND C37 H7X      C37 H7Y      C37 C38
BOND C38 H8X      C38 H8Y      C38 C39
BOND C39 H9X      C39 H9Y      C39 C310
BOND C310 H10X    C310 H10Y    C310 C311
BOND C311 H11X
DOUBLE C311 C312
BOND C312 H12X    C312 C313
BOND C313 H13X    C313 H13Y    C313 C314
BOND C314 H14X    C314 H14Y    C314 C315
BOND C315 H15X    C315 H15Y    C315 C316
BOND C316 H16X    C316 H16Y    C316 C317
BOND C317 H17X    C317 H17Y    C317 C318
BOND C318 H18X    C318 H18Y    C318 H18Z

```

```

IMPR C21 O21 C22 O22      C31 O31 C32 O32

```

```

IC C15      N      C12      C11      1.5031  108.03  -62.19  116.82  1.5409
IC C13      C12     *N      C14      1.4955  110.60  122.73  109.67  1.4976
IC C13      C12     *N      C15      1.4955  110.60  -119.76  108.04  1.5032
IC C13      N      C12      C11      1.4955  110.60   57.52  116.83  1.5412
IC C11      N      *C12    H12A     1.5412  116.83  -126.40  111.94  1.0787
IC H12A     N      *C12    H12B     1.0787  111.94  -116.29  108.17  1.0974
IC C14      N      C13      H13A     1.4976  110.99  179.50  109.35  1.0869
IC H13A     N      *C13    H13B     1.0869  109.35  118.93  111.32  1.0813
IC H13A     N      *C13    H13C     1.0869  109.35  -119.04  111.19  1.0811
IC C13      N      C14      H14A     1.4955  110.99  -179.22  109.65  1.0877
IC H14A     N      *C14    H14B     1.0877  109.65  118.74  110.91  1.0820
IC H14A     N      *C14    H14C     1.0877  109.65  -119.76  111.49  1.0812
IC C13      N      C15      H15A     1.4955  109.44  -64.69  111.04  1.0951
IC H15A     N      *C15    H15B     1.0951  111.04  123.93  113.87  1.0740
IC H15A     N      *C15    H15C     1.0951  111.04  -112.38  110.25  1.0938
IC N        C12     C11      O12      1.5223  116.83  127.52  108.22  1.4232
IC O12      C12     *C11    H11A     1.4232  108.22  -123.07  113.25  1.1138
IC H11A     C12     *C11    H11B     1.1138  113.25  -118.71  109.20  1.1129
IC C12      C11     O12      P        1.5412  108.22  -67.94  118.41  1.5875
IC C11      O12     P        O11      1.4232  118.41  -166.85  104.05  1.5781
IC O11      O12     *P       O13      1.5781  104.05  117.80  108.05  1.4795
IC O11      O12     *P       O14      1.5781  104.05  -117.37  106.82  1.4822
IC O12      P       O11      C1        1.5875  104.05  167.61  118.26  1.4316
IC P        O11      C1        C2        1.5781  118.26  168.12  110.80  1.5508
IC C2      O11     *C1      HA        1.5508  110.80  -119.17  111.41  1.1170
IC HA      O11     *C1      HB        1.1170  111.41  -120.80  110.01  1.1146
IC O11     C1       C2        C3        1.4316  110.80  176.77  110.71  1.5573
IC C3      C1       *C2     O21      1.5573  110.71  120.62  108.02  1.4410 !defines S
chirality
IC C3      C1       *C2     HS        1.5573  110.71  -118.37  106.71  1.1170 !defines S
chirality
IC C1      C2       O21     C21      1.5508  108.02  147.52  115.15  1.3177
IC C2      O21     C21     C22      1.4410  115.15  179.16  108.63  1.5289

```

IC C22	O21	*C21	O22	1.5289	108.63	-178.85	126.55	1.2187	
IC O21	C21	C22	C23	1.3177	108.63	-177.70	112.21	1.5449	
IC C23	C21	*C22	H2R	1.5449	112.21	-121.72	107.88	1.1092	
IC H2R	C21	*C22	H2S	1.1092	107.88	-117.16	107.60	1.1093	
IC C1	C2	C3	O31	1.5508	110.71	176.05	112.62	1.4438	
IC O31	C2	*C3	HX	1.4438	112.62	-118.51	106.65	1.1128	
IC HX	C2	*C3	HY	1.1128	106.65	-115.12	109.46	1.1145	
IC C2	C3	O31	C31	1.5573	112.62	87.12	115.04	1.3313	
IC C3	O31	C31	C32	1.4438	115.04	-172.98	108.55	1.5288	
IC C32	O31	*C31	O32	1.5288	108.55	-178.89	125.60	1.2170	
IC O31	C31	C32	C33	1.3313	108.55	-166.73	113.05	1.5447	
IC C33	C31	*C32	H2X	1.5447	113.05	-121.10	107.23	1.1103	
IC H2X	C31	*C32	H2Y	1.1103	107.23	-117.00	108.11	1.1090	
IC C21	C22	C23	C24	1.5289	112.21	175.76	112.39	1.5338	
IC C24	C22	*C23	H3R		1.5360	113.21	-119.83	108.42	1.1148
IC C24	C22	*C23	H3S		1.5396	113.52	-123.43	110.53	1.1101
IC C22	C23	C24	C25		1.5450	113.21	-172.34	113.68	1.5399
IC C25	C23	*C24	H4R		1.5399	113.68	120.91	108.91	1.1136
IC C25	C23	*C24	H4S		1.5396	113.52	-123.43	110.53	1.1101
IC C23	C24	C25	C26		1.5360	113.68	-56.95	113.57	1.5353
IC C26	C24	*C25	H5R		1.5353	113.57	121.41	108.70	1.1129
IC C26	C24	*C25	H5S		1.5396	113.52	-123.43	110.53	1.1101
IC C24	C25	C26	C27		1.5399	113.57	-173.39	113.79	1.5375
IC C27	C25	*C26	H6R		1.5375	113.79	122.09	109.21	1.1127
IC C27	C25	*C26	H6S		1.5396	113.52	-123.43	110.53	1.1101
IC C25	C26	C27	C28		1.5353	113.79	177.45	113.35	1.5458
IC C28	C26	*C27	H7R		1.5458	113.35	119.87	108.07	1.1139
IC C28	C26	*C27	H7S		1.5396	113.52	-123.43	110.53	1.1101
IC C26	C27	C28	C29	1.5399	113.57	-173.39	113.79	1.5375	
IC C29	C27	*C28	H8R		1.5375	113.79	122.09	109.21	1.1127
IC C29	C27	*C28	H8S		1.5396	113.52	-123.43	110.53	1.1101
IC C27	C28	C29	C210		1.5353	113.79	177.45	113.35	1.5458
IC C210	C28	*C29	H9R		1.5458	113.35	119.87	108.07	1.1139
IC C210	C28	*C29	H9S		1.5396	113.52	-123.43	110.53	1.1101
IC C28	C29	C210	C211		1.5375	113.35	67.78	114.46	1.5115
IC C211	C29	*C210	H10R		1.5115	114.46	121.34	107.89	1.1131
IC C211	C29	*C210	H10S		1.5396	113.52	-123.43	110.53	1.1101
IC C29	C210	C211	C212		1.5458	114.46	180.00	126.91	1.3502
IC C212	C210	*C211	H11R		1.3502	126.91	-178.81	114.69	1.1010
IC C210	C211	C212	C213		1.5115	126.91	0.00	126.69	1.5092
!cis db									
IC C213	C210	*C212	H12R		1.5099	126.94	-177.42	118.69	1.1018
IC C211	C212	C213	C214	1.3502	126.69	180.00	111.86	1.5417	
IC C214	C212	*C213	H13R		1.5396	113.52	-123.43	110.53	1.1101
IC C214	C212	*C213	H13S		1.5097	125.28	121.00	119.65	1.1004
IC C212	C213	C214	C215		1.5092	111.86	180.00	113.99	1.5334
IC C215	C213	*C214	H14R		1.5396	113.52	-123.43	110.53	1.1101
IC C215	C213	*C214	H14S		1.5097	125.28	121.00	119.65	1.1004
IC C213	C214	C215	C216		1.5417	113.99	180.00	111.46	1.5365
IC C216	C214	*C215	H15R		1.5396	113.52	-123.43	110.53	1.1101
IC C216	C214	*C215	H15S	1.5097	125.28	121.00	119.65	1.1004	
IC C214	C215	C216	C217		1.5376	114.97	180.00	113.95	1.5347
IC C217	C215	*C216	H16R		1.5396	113.52	-123.43	110.53	1.1101
IC C217	C215	*C216	H16S		1.5097	125.28	121.00	119.65	1.1004
IC C215	C216	C217	C218		1.5385	113.95	180.00	113.05	1.5311
IC C218	C216	*C217	H17R		1.5396	113.52	-123.43	110.53	1.1101
IC C218	C216	*C217	H17S		1.5097	125.28	121.00	119.65	1.1004
IC C216	C217	C218	H18R		1.5347	113.05	180.00	110.58	1.1110
IC H18R	C217	*C218	H18S		1.5396	113.52	-123.43	110.53	1.1101
IC H18R	C217	*C218	H18T		1.5097	125.28	121.00	119.65	1.1004
IC C31	C32	C33	C34	1.5405	116.85	180.00	126.13	1.5951	
IC C34	C32	*C33	H3X	1.5410	113.36	-119.96	111.74	1.1148	
IC C34	C32	*C33	H3Y	1.5192	121.35	121.00	106.97	1.1128	
IC C32	C33	C34	C35	1.6060	126.13	180.00	113.36	1.5410	

IC C35	C33	*C34	H4X	1.5396	113.52	-123.43	110.53	1.1101
IC C35	C33	*C34	H4Y	1.5192	121.35	121.00	106.97	1.1128
IC C33	C34	C35	C36	1.5951	113.36	180.00	113.52	1.5396
IC C36	C34	*C35	H5X	1.5396	113.52	-123.43	110.53	1.1101
IC C36	C34	*C35	H5Y	1.5192	121.35	123.34	106.97	1.1128
IC C34	C35	C36	C37	1.5410	113.52	180.00	114.47	1.5397
IC C37	C35	*C36	H6X	1.5396	113.52	-123.43	110.53	1.1101
IC C37	C35	*C36	H6Y	1.5192	121.35	123.34	106.97	1.1128
IC C35	C36	C37	C38	1.5396	114.47	180.00	113.41	1.5386
IC C38	C36	*C37	H7X	1.5396	113.52	-123.43	110.53	1.1101
IC C38	C36	*C37	H7Y	1.5192	121.35	123.34	106.97	1.1128
IC C36	C37	C38	C39	1.5397	113.41	180.00	113.71	1.5382
IC C39	C37	*C38	H8X	1.5396	113.52	-123.43	110.53	1.1101
IC C39	C37	*C38	H8Y	1.5192	121.35	123.34	106.97	1.1128
IC C37	C38	C39	C310	1.5353	113.79	177.45	113.35	1.5458
IC C310	C38	*C39	H9X	1.5458	113.35	119.87	108.07	1.1139
IC C310	C38	*C39	H9Y	1.5396	113.52	-123.43	110.53	1.1101
IC C38	C39	C310	C311	1.5375	113.35	67.78	114.46	1.5115
IC C311	C39	*C310	H10X	1.5115	114.46	121.34	107.89	1.1131
IC C311	C39	*C310	H10Y	1.5396	113.52	-123.43	110.53	1.1101
IC C39	C310	C311	C312	1.5458	114.46	180.00	126.91	1.3502
IC C312	C310	*C311	H11X	1.3502	126.91	-178.81	114.69	1.1010
IC C310	C311	C312	C313	1.5115	126.91	0.00	126.69	1.5092 !cis db
IC C313	C310	*C312	H12X	1.5099	126.94	-177.42	118.69	1.1018
IC C311	C312	C313	C314	1.3502	126.69	180.00	111.86	1.5417
IC C314	C312	*C313	H13X	1.5396	113.52	-123.43	110.53	1.1101
IC C314	C312	*C313	H13Y	1.5097	125.28	121.00	119.65	1.1004
IC C312	C313	C314	C315	1.5092	111.86	180.00	113.99	1.5334
IC C315	C313	*C314	H14X	1.5396	113.52	-123.43	110.53	1.1101
IC C315	C313	*C314	H14Y	1.5097	125.28	121.00	119.65	1.1004
IC C313	C314	C315	C316	1.5377	113.85	180.00	111.81	1.5374
IC C316	C314	*C315	H15X	1.5396	113.52	-123.43	110.53	1.1101
IC C316	C314	*C315	H15Y	1.5192	121.35	123.34	106.97	1.1128
IC C314	C315	C316	C317	1.5357	111.81	180.00	114.29	1.5985
IC C317	C315	*C316	H16X	1.5396	113.52	-123.43	110.53	1.1101
IC C317	C315	*C316	H16Y	1.5192	121.35	123.34	106.97	1.1128
IC C315	C316	C317	C318	1.5374	114.29	180.00	130.92	1.5745
IC C318	C316	*C317	H17X	1.5396	113.52	-123.43	110.53	1.1101
IC C318	C316	*C317	H17Y	1.5192	121.35	123.34	106.97	1.1128
IC C316	C317	C318	H18X	1.5985	130.92	180.00	110.90	1.1113
IC H18X	C317	*C318	H18Y	1.5396	113.52	-123.43	110.53	1.1101
IC H18X	C317	*C318	H18Z	1.5192	121.35	123.34	106.97	1.1128

```

RESI VSPC      0.00 ! 3-vaccenoyl-2-steroyl-D-glycero-1-phosphatidylcholine
! Vaccenyl - CH2
!
! Vaccenyl - CH
!           |      (-)          (+)
!           CH2 - PO4 - CH2 - CH2 - N-(CH3)3!
!
!!Derived form the following files
!!   By Stuart Rose 9/10/2013 - Use of IC files was different between these two:
!!
!!RESI DOPC      0.00 ! 2,3-dioleoyl-D-glycero-1-phosphatidylcholine
!!
!!RESI POPC      0.00 ! 3-palmitoyl-2-oleoyl-D-glycero-1-Phosphatidylcholine
!!
!! Palmitoyl - CH2
!!           |
!!   Oleyol - CH
!!           |      (-)          (+)
!!           CH2 - PO4 - CH2 - CH2 - N-(CH3)3
!!

```



ATOM H6R	HAL2	0.09	!	H6R	---	C26	---	H6S						
ATOM H6S	HAL2	0.09	!											
GROUP			!											
ATOM C27	CTL2	-0.18	!											
ATOM H7R	HAL2	0.09	!	H7R	---	C27	---	H7S						
ATOM H7S	HAL2	0.09	!											
GROUP			!											
ATOM C28	CTL2	-0.18	!											
ATOM H8R	HAL2	0.09	!	H8R	---	C28	---	H8S						
ATOM H8S	HAL2	0.09	!											
GROUP			!											
ATOM C29	CTL2	-0.18	!											
ATOM H9R	HAL2	0.09	!	H9R	---	C29	---	H9S						
ATOM H9S	HAL2	0.09	!											
GROUP			!											
ATOM C210	CTL2	-0.18	!											
ATOM H10R	HAL2	0.09	!	H10R	---	C210	---	H10S						
ATOM H10S	HAL2	0.09	!											
GROUP			!											
ATOM C211	CEL1	-0.15	!											
ATOM H11R	HEL1	0.15	!	H11R	--	C211								
GROUP			!											
ATOM C212	CEL1	-0.15	!											
ATOM H12R	HEL1	0.15	!	H12R	---	C212								
GROUP			!											
ATOM C213	CTL2	-0.18	!											
ATOM H13R	HAL2	0.09	!	H13R	---	C213	---	H13S						
ATOM H13S	HAL2	0.09	!											
GROUP			!											
ATOM C214	CTL2	-0.18	!											
ATOM H14R	HAL2	0.09	!	H14R	---	C214	---	H14S						
ATOM H14S	HAL2	0.09	!											
GROUP			!											
ATOM C215	CTL2	-0.18	!											
ATOM H15R	HAL2	0.09	!	H15R	---	C215	---	H15S						
ATOM H15S	HAL2	0.09	!											
GROUP			!											
ATOM C216	CTL2	-0.18	!											
ATOM H16R	HAL2	0.09	!	H16R	---	C216	---	H16S						
ATOM H16S	HAL2	0.09	!											
GROUP			!											
ATOM C217	CTL2	-0.18	!											
ATOM H17R	HAL2	0.09	!	H17R	---	C217	---	H17S						
ATOM H17S	HAL2	0.09	!											
GROUP			!											
ATOM C218	CTL3	-0.27	!											
ATOM H18R	HAL3	0.09	!	H18R	---	C218	---	H18S						
ATOM H18S	HAL3	0.09	!											
ATOM H18T	HAL3	0.09	!					H18T						
GROUP			!											
ATOM C33	CTL2	-0.18	!											
ATOM H3X	HAL2	0.09	!					H3X	---	C33	---	H3Y		
ATOM H3Y	HAL2	0.09	!											
GROUP			!											
ATOM C34	CTL2	-0.18	!											
ATOM H4X	HAL2	0.09	!							H4X	---	C34	---	H4Y
ATOM H4Y	HAL2	0.09	!											
GROUP			!											
ATOM C35	CTL2	-0.18	!											
ATOM H5X	HAL2	0.09	!							H5X	---	C35	---	H5Y
ATOM H5Y	HAL2	0.09	!											
GROUP			!											
ATOM C36	CTL2	-0.18	!											
ATOM H6X	HAL2	0.09	!							H6X	---	C36	---	H6Y



ATOM H6Y	HAL2	0.09	!		
GROUP			!		
ATOM C37	CTL2	-0.18	!		
ATOM H7X	HAL2	0.09	!	H7X	---C37---H7Y
ATOM H7Y	HAL2	0.09	!		
GROUP			!		
ATOM C38	CTL2	-0.18	!		
ATOM H8X	HAL2	0.09	!	H8X	---C38---H8Y
ATOM H8Y	HAL2	0.09	!		
GROUP			!		
ATOM C39	CTL2	-0.18	!		
ATOM H9X	HAL2	0.09	!	H9X	---C39---H9Y
ATOM H9Y	HAL2	0.09	!		
GROUP			!		
ATOM C310	CTL2	-0.18	!		
ATOM H10X	HAL2	0.09	!	H10X	---C310--H10Y
ATOM H10Y	HAL2	0.09	!		
GROUP			!		
ATOM C311	CTL2	-0.18	!		
ATOM H11X	HAL2	0.09	!	H11X	---C311--H11Y
ATOM H12Y	HAL2	0.09	!		
GROUP			!		
ATOM C312	CTL2	-0.18	!		
ATOM H12X	HAL2	0.09	!	H12X	---C312--H12Y
ATOM H12Y	HAL2	0.09	!		
GROUP			!		
ATOM C313	CTL2	-0.18	!		
ATOM H13X	HAL2	0.09	!	H13X	---C313--H13Y
ATOM H13Y	HAL2	0.09	!		
GROUP			!		
ATOM C314	CTL2	-0.18	!		
ATOM H14X	HAL2	0.09	!	H14X	---C314--H14Y
ATOM H14Y	HAL2	0.09	!		
GROUP			!		
ATOM C315	CTL2	-0.18	!		
ATOM H15X	HAL2	0.09	!	H15X	---C315--H15Y
ATOM H15Y	HAL2	0.09	!		
GROUP			!		
ATOM C316	CTL2	-0.18	!		
ATOM H16X	HAL2	0.09	!	H16X	---C316--H16Y
ATOM H16Y	HAL2	0.09	!		
GROUP			!		
ATOM C317	CTL2	-0.18	!		
ATOM H17X	HAL2	0.09	!	H17X	---C317--H17Y
ATOM H17Y	HAL2	0.09	!		
GROUP			!		
ATOM C318	CTL3	-0.27	!		
ATOM H18X	HAL3	0.09	!	H18X	---C318--H18Y
ATOM H18Y	HAL3	0.09	!		
ATOM H18Z	HAL3	0.09	!		H18Z

! Polar Head

BOND N	C13	N	C14	N	C15		
BOND C13	H13A	C13	H13B	C13	H13C		
BOND C14	H14A	C14	H14B	C14	H14C		
BOND C15	H15A	C15	H15B	C15	H15C		
BOND N	C12						
BOND C12	H12A	C12	H12B	C12	C11		
BOND C11	H11A	C11	H11B	C11	O12	O11	C1
BOND O12	P	P	O11	P	O13	P	O14

! Glycerol Backbone

BOND C1	HA	C1	HB	C1	C2		
BOND C2	HS	C2	C3	C2	O21		
BOND C3	HX	C3	HY	C3	O31		

```

! Chain from C2
BOND O21 C21
BOND C21 C22
DOUBLE C21 O22
BOND C22 H2R      C22 H2S      C22 C23
BOND C23 H3R      C23 H3S      C23 C24
BOND C24 H4R      C24 H4S      C24 C25
BOND C25 H5R      C25 H5S      C25 C26
BOND C26 H6R      C26 H6S      C26 C27
BOND C27 H7R      C27 H7S      C27 C28
BOND C28 H8R      C28 H8S      C28 C29
BOND C29 H9R      C29 H9S      C29 C210
BOND C210 H10R    C210 H10S    C210 C211
BOND C211 H11R
DOUBLE C211 C212
BOND C212 H12R    C212 C213
BOND C213 H13R    C213 H13S    C213 C214
BOND C214 H14R    C214 H14S    C214 C215
BOND C215 H15R    C215 H15S    C215 C216
BOND C216 H16R    C216 H16S    C216 C217
BOND C217 H17R    C217 H17S    C217 C218
BOND C218 H18R    C218 H18S    C218 H18T

```

```

! Chain From C3
BOND O31 C31
BOND C31 C32
DOUBLE C31 O32
BOND C32 H2X      C32 H2Y      C32 C33
BOND C33 H3X      C33 H3Y      C33 C34
BOND C34 H4X      C34 H4Y      C34 C35
BOND C35 H5X      C35 H5Y      C35 C36
BOND C36 H6X      C36 H6Y      C36 C37
BOND C37 H7X      C37 H7Y      C37 C38
BOND C38 H8X      C38 H8Y      C38 C39
BOND C39 H9X      C39 H9Y      C39 C310
BOND C310 H10X    C310 H10Y    C310 C311
BOND C311 H11X    C311 H11Y    C311 C312
BOND C312 H12X    C312 H12Y    C312 C313
BOND C313 H13X    C313 H13Y    C313 C314
BOND C314 H14X    C314 H14Y    C314 C315
BOND C315 H15X    C315 H15Y    C315 C316
BOND C316 H16X    C316 H16Y    C316 C317
BOND C317 H17X    C317 H17Y    C317 C318
BOND C318 H18X    C318 H18Y    C318 H18Z

```

```

IMPR C21 O21 C22 O22      C31 O31 C32 O32

```

IC C15	N	C12	C11	1.5031	108.03	-62.19	116.82	1.5409
IC C13	C12	*N	C14	1.4955	110.60	122.73	109.67	1.4976
IC C13	C12	*N	C15	1.4955	110.60	-119.76	108.04	1.5032
IC C13	N	C12	C11	1.4955	110.60	57.52	116.83	1.5412
IC C11	N	*C12	H12A	1.5412	116.83	-126.40	111.94	1.0787
IC H12A	N	*C12	H12B	1.0787	111.94	-116.29	108.17	1.0974
IC C14	N	C13	H13A	1.4976	110.99	179.50	109.35	1.0869
IC H13A	N	*C13	H13B	1.0869	109.35	118.93	111.32	1.0813
IC H13A	N	*C13	H13C	1.0869	109.35	-119.04	111.19	1.0811
IC C13	N	C14	H14A	1.4955	110.99	-179.22	109.65	1.0877
IC H14A	N	*C14	H14B	1.0877	109.65	118.74	110.91	1.0820
IC H14A	N	*C14	H14C	1.0877	109.65	-119.76	111.49	1.0812
IC C13	N	C15	H15A	1.4955	109.44	-64.69	111.04	1.0951
IC H15A	N	*C15	H15B	1.0951	111.04	123.93	113.87	1.0740
IC H15A	N	*C15	H15C	1.0951	111.04	-112.38	110.25	1.0938
IC N	C12	C11	O12	1.5223	116.83	127.52	108.22	1.4232
IC O12	C12	*C11	H11A	1.4232	108.22	-123.07	113.25	1.1138
IC H11A	C12	*C11	H11B	1.1138	113.25	-118.71	109.20	1.1129

IC C12	C11	O12	P	1.5412	108.22	-67.94	118.41	1.5875	
IC C11	O12	P	O11	1.4232	118.41	-166.85	104.05	1.5781	
IC O11	O12	*P	O13	1.5781	104.05	117.80	108.05	1.4795	
IC O11	O12	*P	O14	1.5781	104.05	-117.37	106.82	1.4822	
IC O12	P	O11	C1	1.5875	104.05	167.61	118.26	1.4316	
IC P	O11	C1	C2	1.5781	118.26	168.12	110.80	1.5508	
IC C2	O11	*C1	HA	1.5508	110.80	-119.17	111.41	1.1170	
IC HA	O11	*C1	HB	1.1170	111.41	-120.80	110.01	1.1146	
IC O11	C1	C2	C3	1.4316	110.80	176.77	110.71	1.5573	
IC C3	C1	*C2	O21	1.5573	110.71	120.62	108.02	1.4410	!defines S
chirality									
IC C3	C1	*C2	HS	1.5573	110.71	-118.37	106.71	1.1170	!defines S
chirality									
IC C1	C2	O21	C21	1.5508	108.02	147.52	115.15	1.3177	
IC C2	O21	C21	C22	1.4410	115.15	179.16	108.63	1.5289	
IC C22	O21	*C21	O22	1.5289	108.63	-178.85	126.55	1.2187	
IC O21	C21	C22	C23	1.3177	108.63	-177.70	112.21	1.5449	
IC C23	C21	*C22	H2R	1.5449	112.21	-121.72	107.88	1.1092	
IC H2R	C21	*C22	H2S	1.1092	107.88	-117.16	107.60	1.1093	
IC C1	C2	C3	O31	1.5508	110.71	176.05	112.62	1.4438	
IC O31	C2	*C3	HX	1.4438	112.62	-118.51	106.65	1.1128	
IC HX	C2	*C3	HY	1.1128	106.65	-115.12	109.46	1.1145	
IC C2	C3	O31	C31	1.5573	112.62	87.12	115.04	1.3313	
IC C3	O31	C31	C32	1.4438	115.04	-172.98	108.55	1.5288	
IC C32	O31	*C31	O32	1.5288	108.55	-178.89	125.60	1.2170	
IC O31	C31	C32	C33	1.3313	108.55	-166.73	113.05	1.5447	
IC C33	C31	*C32	H2X	1.5447	113.05	-121.10	107.23	1.1103	
IC H2X	C31	*C32	H2Y	1.1103	107.23	-117.00	108.11	1.1090	
IC C21	C22	C23	C24	1.5289	112.21	175.76	112.39	1.5338	
IC C24	C22	*C23	H3R		1.5360	113.21	-119.83	108.42	1.1148
IC C24	C22	*C23	H3S		1.5396	113.52	-123.43	110.53	1.1101
IC C22	C23	C24	C25		1.5450	113.21	-172.34	113.68	1.5399
IC C25	C23	*C24	H4R		1.5399	113.68	120.91	108.91	1.1136
IC C25	C23	*C24	H4S		1.5396	113.52	-123.43	110.53	1.1101
IC C23	C24	C25	C26		1.5360	113.68	-56.95	113.57	1.5353
IC C26	C24	*C25	H5R		1.5353	113.57	121.41	108.70	1.1129
IC C26	C24	*C25	H5S		1.5396	113.52	-123.43	110.53	1.1101
IC C24	C25	C26	C27		1.5399	113.57	-173.39	113.79	1.5375
IC C27	C25	*C26	H6R		1.5375	113.79	122.09	109.21	1.1127
IC C27	C25	*C26	H6S		1.5396	113.52	-123.43	110.53	1.1101
IC C25	C26	C27	C28		1.5353	113.79	177.45	113.35	1.5458
IC C28	C26	*C27	H7R		1.5458	113.35	119.87	108.07	1.1139
IC C28	C26	*C27	H7S		1.5396	113.52	-123.43	110.53	1.1101
IC C26	C27	C28	C29		1.5399	113.57	-173.39	113.79	1.5375
IC C29	C27	*C28	H8R		1.5375	113.79	122.09	109.21	1.1127
IC C29	C27	*C28	H8S		1.5396	113.52	-123.43	110.53	1.1101
IC C27	C28	C29	C210		1.5353	113.79	177.45	113.35	1.5458
IC C210	C28	*C29	H9R		1.5458	113.35	119.87	108.07	1.1139
IC C210	C28	*C29	H9S		1.5396	113.52	-123.43	110.53	1.1101
IC C28	C29	C210	C211		1.5375	113.35	67.78	114.46	1.5115
IC C211	C29	*C210	H10R		1.5115	114.46	121.34	107.89	1.1131
IC C211	C29	*C210	H10S		1.5396	113.52	-123.43	110.53	1.1101
IC C29	C210	C211	C212		1.5458	114.46	180.00	126.91	1.3502
IC C212	C210	*C211	H11R		1.3502	126.91	-178.81	114.69	1.1010
IC C210	C211	C212	C213		1.5115	126.91	0.00	126.69	1.5092
!cis db									
IC C213	C210	*C212	H12R		1.5099	126.94	-177.42	118.69	1.1018
IC C211	C212	C213	C214		1.3502	126.69	180.00	111.86	1.5417
IC C214	C212	*C213	H13R		1.5396	113.52	-123.43	110.53	1.1101
IC C214	C212	*C213	H13S		1.5097	125.28	121.00	119.65	1.1004
IC C212	C213	C214	C215		1.5092	111.86	180.00	113.99	1.5334
IC C215	C213	*C214	H14R		1.5396	113.52	-123.43	110.53	1.1101
IC C215	C213	*C214	H14S		1.5097	125.28	121.00	119.65	1.1004
IC C213	C214	C215	C216		1.5417	113.99	180.00	111.46	1.5365

IC C216	C214	*C215	H15R		1.5396	113.52	-123.43	110.53	1.1101
IC C216	C214	*C215	H15S	1.5097	125.28	121.00	119.65	1.1004	
IC C214	C215	C216	C217		1.5376	114.97	180.00	113.95	1.5347
IC C217	C215	*C216	H16R		1.5396	113.52	-123.43	110.53	1.1101
IC C217	C215	*C216	H16S		1.5097	125.28	121.00	119.65	1.1004
IC C215	C216	C217	C218		1.5385	113.95	180.00	113.05	1.5311
IC C218	C216	*C217	H17R		1.5396	113.52	-123.43	110.53	1.1101
IC C218	C216	*C217	H17S		1.5097	125.28	121.00	119.65	1.1004
IC C216	C217	C218	H18R		1.5347	113.05	180.00	110.58	1.1110
IC H18R	C217	*C218	H18S		1.5396	113.52	-123.43	110.53	1.1101
IC H18R	C217	*C218	H18T		1.5097	125.28	121.00	119.65	1.1004
IC C31	C32	C33	C34	1.5405	116.85	180.00	126.13	1.5951	
IC C34	C32	*C33	H3X		1.5410	113.36	-119.96	111.74	1.1148
IC C34	C32	*C33	H3Y		1.5192	121.35	121.00	106.97	1.1128
IC C32	C33	C34	C35	1.6060	126.13	180.00	113.36	1.5410	
IC C35	C33	*C34	H4X		1.5396	113.52	-123.43	110.53	1.1101
IC C35	C33	*C34	H4Y		1.5192	121.35	121.00	106.97	1.1128
IC C33	C34	C35	C36	1.5951	113.36	180.00	113.52	1.5396	
IC C36	C34	*C35	H5X		1.5396	113.52	-123.43	110.53	1.1101
IC C36	C34	*C35	H5Y		1.5192	121.35	123.34	106.97	1.1128
IC C34	C35	C36	C37	1.5410	113.52	180.00	114.47	1.5397	
IC C37	C35	*C36	H6X		1.5396	113.52	-123.43	110.53	1.1101
IC C37	C35	*C36	H6Y		1.5192	121.35	123.34	106.97	1.1128
IC C35	C36	C37	C38	1.5396	114.47	180.00	113.41	1.5386	
IC C38	C36	*C37	H7X		1.5396	113.52	-123.43	110.53	1.1101
IC C38	C36	*C37	H7Y		1.5192	121.35	123.34	106.97	1.1128
IC C36	C37	C38	C39	1.5397	113.41	180.00	113.71	1.5382	
IC C39	C37	*C38	H8X		1.5396	113.52	-123.43	110.53	1.1101
IC C39	C37	*C38	H8Y		1.5192	121.35	123.34	106.97	1.1128
IC C37	C38	C39	C310	1.5353	113.79	177.45	113.35	1.5458	
IC C310	C38	*C39	H9X		1.5458	113.35	119.87	108.07	1.1139
IC C310	C38	*C39	H9Y		1.5396	113.52	-123.43	110.53	1.1101
IC C38	C39	C310	C311	1.5375	113.35	67.78	114.46	1.5115	
IC C311	C39	*C310	H10X		1.5115	114.46	121.34	107.89	1.1131
IC C311	C39	*C310	H10Y		1.5396	113.52	-123.43	110.53	1.1101
IC C39	C310	C311	C312	1.5458	114.46	180.00	126.91	1.3502	
IC C312	C310	*C311	H11X		1.3502	126.91	-178.81	114.69	1.1010
IC C310	C311	C312	C313	1.5115	126.91	0.00	126.69	1.5092	!cis db
IC C313	C310	*C312	H12X		1.5099	126.94	-177.42	118.69	1.1018
IC C311	C312	C313	C314	1.3502	126.69	180.00	111.86	1.5417	
IC C314	C312	*C313	H13X		1.5396	113.52	-123.43	110.53	1.1101
IC C314	C312	*C313	H13Y		1.5097	125.28	121.00	119.65	1.1004
IC C312	C313	C314	C315	1.5092	111.86	180.00	113.99	1.5334	
IC C315	C313	*C314	H14X		1.5396	113.52	-123.43	110.53	1.1101
IC C315	C313	*C314	H14Y		1.5097	125.28	121.00	119.65	1.1004
IC C313	C314	C315	C316	1.5377	113.85	180.00	111.81	1.5374	
IC C316	C314	*C315	H15X		1.5396	113.52	-123.43	110.53	1.1101
IC C316	C314	*C315	H15Y		1.5192	121.35	123.34	106.97	1.1128
IC C314	C315	C316	C317	1.5357	111.81	180.00	114.29	1.5985	
IC C317	C315	*C316	H16X		1.5396	113.52	-123.43	110.53	1.1101
IC C317	C315	*C316	H16Y		1.5192	121.35	123.34	106.97	1.1128
IC C315	C316	C317	C318	1.5374	114.29	180.00	130.92	1.5745	
IC C318	C316	*C317	H17X		1.5396	113.52	-123.43	110.53	1.1101
IC C318	C316	*C317	H17Y		1.5192	121.35	123.34	106.97	1.1128
IC C316	C317	C318	H18X		1.5985	130.92	180.00	110.90	1.1113
IC H18X	C317	*C318	H18Y	1.5396	113.52	-123.43	110.53	1.1101	
IC H18X	C317	*C318	H18Z	1.5192	121.35	123.34	106.97	1.1128	

! These are not done. IN PROGRESS  
! Cardiolipins

RESI TVCL2 -2.00 ! Tetravaccinyl Cardiolipin with head group charge = -2  
! Cardiolipin headgroup + 4 oleoly chains

```

GROUP          !
ATOM C3  CTL2  -0.08 !           HG11           OG12--HO12
HG31
ATOM HG31 HAL2  0.09 !           \           |           /
ATOM HG32 HAL2  0.09 !           C1-----C2-----
C3
ATOM P3  PL    1.50 !           / \           |           /
\
ATOM OP33 O2L  -0.78 !           /   HG12           HG22           HG32
\
ATOM OP34 O2L  -0.78 !           OP11
OP31
ATOM OP31 OSLP -0.57 !           |
|
ATOM OP32 OSLP -0.57 !           OP13 (-) --P1 (+) --OP14 (-)           OP33 (-) --
P3 (+) --OP34 (-)
ATOM C31  CTL2  -0.08 !           |
|
ATOM H31J HAL2  0.09 !           OP12
OP32
ATOM H31K HAL2  0.09 !           |
|
GROUP          !           H11J--C11--H11K           H31J-
-C31--H31K
ATOM C2  CTL1  0.14 !           |           |
ATOM HG22 HAL1  0.09 !           |           |
ATOM OG12 OHL  -0.65 !           H12J--C12-----O12-----           H32J-
-C32-----O32-----
ATOM HO12 HOL  0.42 !           |           |
|           |           |
GROUP          !           |           |           |
|           |           |           |
ATOM C1  CTL2  -0.08 !           H13J--C13--H13K           |           H33J--C33--
H33K
ATOM HG11 HAL2  0.09 !           |           |           |
|           |           |           |
ATOM HG12 HAL2  0.09 !           |           |           |
|           |           |           |
ATOM P1  PL    1.50 !           O13           |
O33           |
ATOM OP13 O2L  -0.78 !           |           |           |
|           |           |           |
ATOM OP14 O2L  -0.78 !           CB1=OB1           CA1=OA1
CD1=OD1           CC1=OC1
ATOM OP11 OSLP -0.57 !           |           |           |
|           |           |           |
ATOM OP12 OSLP -0.57 !           H2D--CB2--H2E           H2A--CA2--H2B           H2X-
-CD2--H2Y           H2R--CC2--H2S
ATOM C11  CTL2  -0.08 !           |           |           |
|           |           |           |
ATOM H11J HAL2  0.09 !           H3D--CB3--H3E           H3A--CA3--H3B           H3X-
-CD3--H3Y           H3R--CC3--H3S
ATOM H11K HAL2  0.09 !           |           |           |
|           |           |           |
GROUP          !           H4D--CB4--H4E           H4A--CA4--H4B           H4X-
-CD4--H4Y           H4R--CC4--H4S
ATOM C12  CTL1  0.17 !           |           |           |
|           |           |           |
ATOM H12J HAL1  0.09 !           H5D--CB5--H5E           H5A--CA5--H5B           H5X-
-CD5--H5Y           H5R--CC5--H5S
ATOM O12  OSL  -0.49 !           |           |           |
|           |           |           |
ATOM CA1  CL    0.90 !           H6D--CB6--H6E           H6A--CA6--H6B           H6X-
-CD6--H6Y           H6R--CC6--H6S

```

ATOM OA1	OBL	-0.63 !			
ATOM CA2	CTL2	-0.22 !			
ATOM H2A	HAL2	0.09 !	H7D--CB7--H7E	H7A--CA7--H7B	
H7X--CD7--H7Y		H7R--CC7--H7S			
ATOM H2B	HAL2	0.09 !			
GROUP		!	H8D--CB8--H8E	H8A--CA8--H8B	H8X-
-CD8--H8Y		H8R--CC8--H8S			
ATOM C13	CTL2	0.08 !			
ATOM H13J	HAL2	0.09 !	H9D--CB9	H9A--CA9	
H9X--CD9		H9R--CC9			
ATOM H13K	HAL2	0.09 !			
ATOM O13	OSL	-0.49 !			
ATOM CB1	CL	0.90 !	H10D--CB10	H10A--CA10	H10X-
-CD10		H10R--CC10			
ATOM OB1	OBL	-0.63 !			
ATOM CB2	CTL2	-0.22 !	H11D--CB11--H11E	H11A--CA11--H11B	H11X-
-CD11--H11Y		H11R--CC11--H11S			
ATOM H2D	HAL2	0.09 !			
ATOM H2E	HAL2	0.09 !	H12D--CB12--H12E	H12A--CA12--H12B	H12X-
-CD12--H12Y		H12R--CC12--H12S			
GROUP		!			
ATOM C32	CTL1	0.17 !			
ATOM H32J	HAL1	0.09 !	H13D--CB13--H13E	H13A--CA13--H13B	H13X-
-CD13--H13Y		H13R--CC13--H13S			
ATOM O32	OSL	-0.49 !			
ATOM CC1	CL	0.90 !	H14D--CB14--H14E	H14A--CA14--H14B	H14X-
-CD14--H14Y		H14R--CC14--H14S			
ATOM OC1	OBL	-0.63 !			
ATOM CC2	CTL2	-0.22 !	H15D--CB15--H15E	H15A--CA15--H15B	H15X-
-CD15--H15Y		H15R--CC15--H15S			
ATOM H2R	HAL2	0.09 !			
ATOM H2S	HAL2	0.09 !	H16D--CB16--H16E	H16A--CA16--H16B	H16X-
-CD16--H16Y		H16R--CC16--H16S			
GROUP		!			
ATOM C33	CTL2	0.08 !	H17D--CB17--H17E	H17A--CA17--H17B	H17X-
-CD17--H17Y		H17R--CC17--H17S			
ATOM H33J	HAL2	0.09 !			
ATOM H33K	HAL2	0.09 !	H18D--CB18--H18E	H18A--CA18--H18B	
H18X--CD18--H18Y		H18R--CC18--H18S			
ATOM O33	OSL	-0.49 !			
ATOM CD1	CL	0.90 !	H18F	H18C	
H18Z		H18T			
ATOM OD1	OBL	-0.63 !			
ATOM CD2	CTL2	-0.22 !			
ATOM H2X	HAL2	0.09 !			
ATOM H2Y	HAL2	0.09 !			
GROUP		!			
ATOM CA3	CTL2	-0.18 !			

ATOM H3A	HAL2	0.09	!
ATOM H3B	HAL2	0.09	!
GROUP			!
ATOM CA4	CTL2	-0.18	!
ATOM H4A	HAL2	0.09	!
ATOM H4B	HAL2	0.09	!
GROUP			!
ATOM CA5	CTL2	-0.18	!
ATOM H5A	HAL2	0.09	!
ATOM H5B	HAL2	0.09	!
GROUP			!
ATOM CA6	CTL2	-0.18	!
ATOM H6A	HAL2	0.09	!
ATOM H6B	HAL2	0.09	!
GROUP			!
ATOM CA7	CTL2	-0.18	!
ATOM H7A	HAL2	0.09	!
ATOM H7B	HAL2	0.09	!
GROUP			!
ATOM CA8	CTL2	-0.18	!
ATOM H8A	HAL2	0.09	!
ATOM H8B	HAL2	0.09	!
GROUP			!
ATOM CA9	CEL1	-0.15	!
ATOM H9A	HEL1	0.15	!
GROUP			!
ATOM CA10	CEL1	-0.15	!
ATOM H10A	HEL1	0.15	!
GROUP			!
ATOM CA11	CTL2	-0.18	!
ATOM H11A	HAL2	0.09	!
ATOM H11B	HAL2	0.09	!
GROUP			!
ATOM CA12	CTL2	-0.18	!
ATOM H12A	HAL2	0.09	!
ATOM H12B	HAL2	0.09	!
GROUP			!
ATOM CA13	CTL2	-0.18	!
ATOM H13A	HAL2	0.09	!
ATOM H13B	HAL2	0.09	!
GROUP			!
ATOM CA14	CTL2	-0.18	!
ATOM H14A	HAL2	0.09	!
ATOM H14B	HAL2	0.09	!
GROUP			!
ATOM CA15	CTL2	-0.18	!
ATOM H15A	HAL2	0.09	!
ATOM H15B	HAL2	0.09	!
GROUP			!
ATOM CA16	CTL2	-0.18	!
ATOM H16A	HAL2	0.09	!
ATOM H16B	HAL2	0.09	!
GROUP			!
ATOM CA17	CTL2	-0.18	!
ATOM H17A	HAL2	0.09	!
ATOM H17B	HAL2	0.09	!
GROUP			!
ATOM CA18	CTL3	-0.27	!
ATOM H18A	HAL3	0.09	!
ATOM H18B	HAL3	0.09	!
ATOM H18C	HAL3	0.09	!
GROUP			!
ATOM CB3	CTL2	-0.18	!
ATOM H3D	HAL2	0.09	!

ATOM H3E	HAL2	0.09	!
GROUP			!
ATOM CB4	CTL2	-0.18	!
ATOM H4D	HAL2	0.09	!
ATOM H4E	HAL2	0.09	!
GROUP			!
ATOM CB5	CTL2	-0.18	!
ATOM H5D	HAL2	0.09	!
ATOM H5E	HAL2	0.09	!
GROUP			!
ATOM CB6	CTL2	-0.18	!
ATOM H6D	HAL2	0.09	!
ATOM H6E	HAL2	0.09	!
GROUP			!
ATOM CB7	CTL2	-0.18	!
ATOM H7D	HAL2	0.09	!
ATOM H7E	HAL2	0.09	!
GROUP			!
ATOM CB8	CTL2	-0.18	!
ATOM H8D	HAL2	0.09	!
ATOM H8E	HAL2	0.09	!
GROUP			!
ATOM CB9	CEL1	-0.15	!
ATOM H9D	HEL1	0.15	!
GROUP			!
ATOM CB10	CEL1	-0.15	!
ATOM H10D	HEL1	0.15	!
GROUP			!
ATOM CB11	CTL2	-0.18	!
ATOM H11D	HAL2	0.09	!
ATOM H11E	HAL2	0.09	!
GROUP			!
ATOM CB12	CTL2	-0.18	!
ATOM H12D	HAL2	0.09	!
ATOM H12E	HAL2	0.09	!
GROUP			!
ATOM CB13	CTL2	-0.18	!
ATOM H13D	HAL2	0.09	!
ATOM H13E	HAL2	0.09	!
GROUP			!
ATOM CB14	CTL2	-0.18	!
ATOM H14D	HAL2	0.09	!
ATOM H14E	HAL2	0.09	!
GROUP			!
ATOM CB15	CTL2	-0.18	!
ATOM H15D	HAL2	0.09	!
ATOM H15E	HAL2	0.09	!
GROUP			!
ATOM CB16	CTL2	-0.18	!
ATOM H16D	HAL2	0.09	!
ATOM H16E	HAL2	0.09	!
GROUP			!
ATOM CB17	CTL2	-0.18	!
ATOM H17D	HAL2	0.09	!
ATOM H17E	HAL2	0.09	!
GROUP			!
ATOM CB18	CTL3	-0.27	!
ATOM H18D	HAL3	0.09	!
ATOM H18E	HAL3	0.09	!
ATOM H18F	HAL3	0.09	!
GROUP			!
ATOM CC3	CTL2	-0.18	!
ATOM H3R	HAL2	0.09	!
ATOM H3S	HAL2	0.09	!



GROUP			!
ATOM	CC4	CTL2	-0.18 !
ATOM	H4R	HAL2	0.09 !
ATOM	H4S	HAL2	0.09 !
GROUP			!
ATOM	CC5	CTL2	-0.18 !
ATOM	H5R	HAL2	0.09 !
ATOM	H5S	HAL2	0.09 !
GROUP			!
ATOM	CC6	CTL2	-0.18 !
ATOM	H6R	HAL2	0.09 !
ATOM	H6S	HAL2	0.09 !
GROUP			!
ATOM	CC7	CTL2	-0.18 !
ATOM	H7R	HAL2	0.09 !
ATOM	H7S	HAL2	0.09 !
GROUP			!
ATOM	CC8	CTL2	-0.18 !
ATOM	H8R	HAL2	0.09 !
ATOM	H8S	HAL2	0.09 !
GROUP			!
ATOM	CC9	CEL1	-0.15 !
ATOM	H9R	HEL1	0.15 !
GROUP			!
ATOM	CC10	CEL1	-0.15 !
ATOM	H10R	HEL1	0.15 !
GROUP			!
ATOM	CC11	CTL2	-0.18 !
ATOM	H11R	HAL2	0.09 !
ATOM	H11S	HAL2	0.09 !
GROUP			!
ATOM	CC12	CTL2	-0.18 !
ATOM	H12R	HAL2	0.09 !
ATOM	H12S	HAL2	0.09 !
GROUP			!
ATOM	CC13	CTL2	-0.18 !
ATOM	H13R	HAL2	0.09 !
ATOM	H13S	HAL2	0.09 !
GROUP			!
ATOM	CC14	CTL2	-0.18 !
ATOM	H14R	HAL2	0.09 !
ATOM	H14S	HAL2	0.09 !
GROUP			!
ATOM	CC15	CTL2	-0.18 !
ATOM	H15R	HAL2	0.09 !
ATOM	H15S	HAL2	0.09 !
GROUP			!
ATOM	CC16	CTL2	-0.18 !
ATOM	H16R	HAL2	0.09 !
ATOM	H16S	HAL2	0.09 !
GROUP			!
ATOM	CC17	CTL2	-0.18 !
ATOM	H17R	HAL2	0.09 !
ATOM	H17S	HAL2	0.09 !
GROUP			!
ATOM	CC18	CTL3	-0.27 !
ATOM	H18R	HAL3	0.09 !
ATOM	H18S	HAL3	0.09 !
ATOM	H18T	HAL3	0.09 !
GROUP			!
ATOM	CD3	CTL2	-0.18 !
ATOM	H3X	HAL2	0.09 !
ATOM	H3Y	HAL2	0.09 !
GROUP			!

```

ATOM CD4 CTL2 -0.18 !
ATOM H4X HAL2 0.09 !
ATOM H4Y HAL2 0.09 !
GROUP !
ATOM CD5 CTL2 -0.18 !
ATOM H5X HAL2 0.09 !
ATOM H5Y HAL2 0.09 !
GROUP !
ATOM CD6 CTL2 -0.18 !
ATOM H6X HAL2 0.09 !
ATOM H6Y HAL2 0.09 !
GROUP !
ATOM CD7 CTL2 -0.18 !
ATOM H7X HAL2 0.09 !
ATOM H7Y HAL2 0.09 !
GROUP !
ATOM CD8 CTL2 -0.18 !
ATOM H8X HAL2 0.09 !
ATOM H8Y HAL2 0.09 !
GROUP !
ATOM CD9 CEL1 -0.15 !
ATOM H9X HEL1 0.15 !
GROUP !
ATOM CD10 CEL1 -0.15 !
ATOM H10X HEL1 0.15 !
GROUP !
ATOM CD11 CTL2 -0.18 !
ATOM H11X HAL2 0.09 !
ATOM H11Y HAL2 0.09 !
GROUP !
ATOM CD12 CTL2 -0.18 !
ATOM H12X HAL2 0.09 !
ATOM H12Y HAL2 0.09 !
GROUP !
ATOM CD13 CTL2 -0.18 !
ATOM H13X HAL2 0.09 !
ATOM H13Y HAL2 0.09 !
GROUP !
ATOM CD14 CTL2 -0.18 !
ATOM H14X HAL2 0.09 !
ATOM H14Y HAL2 0.09 !
GROUP !
ATOM CD15 CTL2 -0.18 !
ATOM H15X HAL2 0.09 !
ATOM H15Y HAL2 0.09 !
GROUP !
ATOM CD16 CTL2 -0.18 !
ATOM H16X HAL2 0.09 !
ATOM H16Y HAL2 0.09 !
GROUP !
ATOM CD17 CTL2 -0.18 !
ATOM H17X HAL2 0.09 !
ATOM H17Y HAL2 0.09 !
GROUP !
ATOM CD18 CTL3 -0.27 !
ATOM H18X HAL3 0.09 !
ATOM H18Y HAL3 0.09 !
ATOM H18Z HAL3 0.09 !!

```

! Glycerol head

```

BOND C1 C2 C1 HG11 C1 HG12
BOND C2 OG12 C2 HG22 OG12 HO12 C2 C3
BOND C3 HG31 C3 HG32

```

! Phosphates

```

BOND C1  OP11 C3  OP31
BOND P1  OP11 P1  OP12  P1  OP13 P1  OP14
BOND P3  OP31 P3  OP32  P3  OP33 P3  OP34
! Glycerol Backbones
BOND OP12 C11  C11  H11J C11 H11K
BOND C11  C12
BOND C12  H12J C12  O12
BOND C12  C13
BOND C13  H13J C13  H13K C13 O13
BOND OP32 C31  C31  H31J C31 H31K
BOND C31  C32
BOND C32  H32J C32  O32
BOND C32  C33
BOND C33  H33J C33  H33K C33 O33
! Acyl chain 1
BOND O12  CA1  O13  CB1  O32  CC1  O33  CD1
BOND CA1  OA1  CA1  CA2
BOND CA2  H2A  CA2  H2B  CA2  CA3
BOND CA3  H3A  CA3  H3B  CA3  CA4
BOND CA4  H4A  CA4  H4B  CA4  CA5
BOND CA5  H5A  CA5  H5B  CA5  CA6
BOND CA6  H6A  CA6  H6B  CA6  CA7
BOND CA7  H7A  CA7  H7B  CA7  CA8
BOND CA8  H8A  CA8  H8B  CA8  CA9
BOND CA9  H9A  CA9  CA10
BOND CA10 H10A CA10 CA11
BOND CA11 H11A CA11 H11B CA11 CA12
BOND CA12 H12A CA12 H12B CA12 CA13
BOND CA13 H13A CA13 H13B CA13 CA14
BOND CA14 H14A CA14 H14B CA14 CA15
BOND CA15 H15A CA15 H15B CA15 CA16
BOND CA16 H16A CA16 H16B CA16 CA17
BOND CA17 H17A CA17 H17B CA17 CA18
BOND CA18 H18A CA18 H18B CA18 H18C
! Acyl chain 2
BOND CB1  OB1  CB1  CB2
BOND CB2  H2D  CB2  H2E  CB2  CB3
BOND CB3  H3D  CB3  H3E  CB3  CB4
BOND CB4  H4D  CB4  H4E  CB4  CB5
BOND CB5  H5D  CB5  H5E  CB5  CB6
BOND CB6  H6D  CB6  H6E  CB6  CB7
BOND CB7  H7D  CB7  H7E  CB7  CB8
BOND CB8  H8D  CB8  H8E  CB8  CB9
BOND CB9  H9D  CB9  CB10
BOND CB10 H10D CB10 CB11
BOND CB11 H11D CB11 H11E CB11 CB12
BOND CB12 H12D CB12 H12E CB12 CB13
BOND CB13 H13D CB13 H13E CB13 CB14
BOND CB14 H14D CB14 H14E CB14 CB15
BOND CB15 H15D CB15 H15E CB15 CB16
BOND CB16 H16D CB16 H16E CB16 CB17
BOND CB17 H17D CB17 H17E CB17 CB18
BOND CB18 H18D CB18 H18E CB18 H18F
! Acyl chain 3
BOND CC1  OC1  CC1  CC2
BOND CC2  H2R  CC2  H2S  CC2  CC3
BOND CC3  H3R  CC3  H3S  CC3  CC4
BOND CC4  H4R  CC4  H4S  CC4  CC5
BOND CC5  H5R  CC5  H5S  CC5  CC6
BOND CC6  H6R  CC6  H6S  CC6  CC7
BOND CC7  H7R  CC7  H7S  CC7  CC8
BOND CC8  H8R  CC8  H8S  CC8  CC9
BOND CC9  H9R  CC9  CC10
BOND CC10 H10R CC10 CC11

```

BOND CC11 H11R CC11 H11S CC11 CC12  
 BOND CC12 H12R CC12 H12S CC12 CC13  
 BOND CC13 H13R CC13 H13S CC13 CC14  
 BOND CC14 H14R CC14 H14S CC14 CC15  
 BOND CC15 H15R CC15 H15S CC15 CC16  
 BOND CC16 H16R CC16 H16S CC16 CC17  
 BOND CC17 H17R CC17 H17S CC17 CC18  
 BOND CC18 H18R CC18 H18S CC18 H18T  
 ! Acyl chain 4  
 BOND CD1 OD1 CD1 CD2  
 BOND CD2 H2X CD2 H2Y CD2 CD3  
 BOND CD3 H3X CD3 H3Y CD3 CD4  
 BOND CD4 H4X CD4 H4Y CD4 CD5  
 BOND CD5 H5X CD5 H5Y CD5 CD6  
 BOND CD6 H6X CD6 H6Y CD6 CD7  
 BOND CD7 H7X CD7 H7Y CD7 CD8  
 BOND CD8 H8X CD8 H8Y CD8 CD9  
 BOND CD9 H9X CD9 CD10  
 BOND CD10 H10X CD10 CD11  
 BOND CD11 H11X CD11 H11Y CD11 CD12  
 BOND CD12 H12X CD12 H12Y CD12 CD13  
 BOND CD13 H13X CD13 H13Y CD13 CD14  
 BOND CD14 H14X CD14 H14Y CD14 CD15  
 BOND CD15 H15X CD15 H15Y CD15 CD16  
 BOND CD16 H16X CD16 H16Y CD16 CD17  
 BOND CD17 H17X CD17 H17Y CD17 CD18  
 BOND CD18 H18X CD18 H18Y CD18 H18Z

!  
 ! IC TABLE  
 !

IMPR	CB1	O13	CB2	OB1					
IMPR	CA1	O12	CA2	OA1					
IMPR	CD1	O33	CD2	OD1					
IMPR	CC1	O32	CC2	OC1					
IC	OP31	C2	*C3	HG31	1.4633	109.99	126.99	106.69	1.1112
IC	HG31	C2	*C3	HG32	1.1112	106.69	120.70	112.94	1.1110
IC	C2	C3	OP31	P3	1.5211	109.99	154.06	117.47	1.5924
IC	C3	OP31	P3	OP32	1.4633	117.47	66.74	101.68	1.6525
IC	OP32	OP31	*P3	OP33	1.6525	101.68	-113.70	109.39	1.4926
IC	OP32	OP31	*P3	OP34	1.6525	101.68	112.29	106.74	1.4836
IC	OP31	P3	OP32	C31	1.5924	101.68	55.76	110.28	1.4698
IC	P3	OP32	C31	C32	1.6525	110.28	-172.41	110.74	1.5958
IC	C32	OP32	*C31	H31J	1.5958	110.74	116.75	110.82	1.1115
IC	H31J	OP32	*C31	H31K	1.1115	110.82	111.29	110.26	1.1103
IC	HG31	C3	C2	C1	1.1112	106.69	-61.74	114.49	1.5241
IC	C1	C3	*C2	OG12	1.5241	114.49	-122.33	108.64	1.4665
IC	C1	C3	*C2	HG22	1.5241	114.49	124.23	104.11	1.1108
IC	C3	C2	OG12	HO12	1.5211	108.64	-38.03	96.97	0.9599
IC	C3	C2	C1	OP11	1.5211	114.49	175.92	108.99	1.3945
IC	OP11	C2	*C1	HG11	1.3945	108.99	-131.04	104.78	1.1106
IC	HG11	C2	*C1	HG12	1.1106	104.78	-113.14	109.09	1.1119
IC	C2	C1	OP11	P1	1.5241	108.99	-84.99	120.20	1.5652
IC	C1	OP11	P1	OP12	1.3945	120.20	-27.24	102.68	1.5816
IC	OP12	OP11	*P1	OP13	1.5816	102.68	118.64	109.06	1.4705
IC	OP12	OP11	*P1	OP14	1.5816	102.68	-114.38	108.43	1.4438
IC	OP11	P1	OP12	C11	1.5652	102.68	-105.08	129.51	1.3844
IC	P1	OP12	C11	C12	1.5816	129.51	79.30	113.33	1.5572
IC	C12	OP12	*C11	H11J	1.5572	113.33	-123.60	109.70	1.1106
IC	H11J	OP12	*C11	H11K	1.1106	109.70	-125.75	111.37	1.1111
IC	OP12	C11	C12	C13	1.3844	113.33	172.10	111.92	1.5430
IC	C13	C11	*C12	O12	1.5430	111.92	120.38	106.67	1.4690
IC	O12	C11	*C12	H12J	1.4690	106.67	123.36	105.85	1.1110
IC	C11	C12	O12	CA1	1.5572	106.67	139.57	111.75	1.3546
IC	C12	O12	CA1	CA2	1.4690	111.75	-177.04	105.16	1.4819

IC CA2	O12	*CA1	OA1	1.4819	105.16	175.26	126.65	1.2359
IC O12	CA1	CA2	CA3	1.3546	105.16	-166.84	109.95	1.5144
IC CA3	CA1	*CA2	H2A	1.5144	109.95	-122.50	115.81	1.1105
IC H2A	CA1	*CA2	H2B	1.1105	115.81	-121.44	107.35	1.1109
IC C11	C12	C13	O13	1.5572	111.92	-172.11	107.78	1.5003
IC O13	C12	*C13	H13J	1.5003	107.78	-115.91	112.20	1.1109
IC H13J	C12	*C13	H13K	1.1109	112.20	-121.54	112.00	1.1122
IC C12	C13	O13	CB1	1.5430	107.78	77.67	115.10	1.2970
IC C13	O13	CB1	CB2	1.5003	115.10	-179.81	109.11	1.4434
IC CB2	O13	*CB1	OB1	1.4434	109.11	-173.82	130.35	1.2113
IC O13	CB1	CB2	CB3	1.2970	109.11	173.87	116.83	1.5195
IC CB3	CB1	*CB2	H2D	1.5195	116.83	-121.03	109.80	1.1112
IC H2D	CB1	*CB2	H2E	1.1112	109.80	-114.30	107.94	1.1107
IC OP32	C31	C32	C33	1.4698	110.74	-72.15	111.19	1.5682
IC C33	C31	*C32	O32	1.5682	111.19	124.56	112.11	1.3898
IC O32	C31	*C32	H32J	1.3898	112.11	122.90	114.56	1.1112
IC C31	C32	O32	CC1	1.5958	112.11	62.25	119.56	1.3075
IC C32	O32	CC1	CC2	1.3898	119.56	-174.92	104.05	1.4829
IC CC2	O32	*CC1	OC1	1.4829	104.05	-166.47	126.62	1.2264
IC O32	CC1	CC2	CC3	1.3075	104.05	170.64	115.59	1.5435
IC CC3	CC1	*CC2	H2R	1.5435	115.59	-124.86	107.06	1.1110
IC H2R	CC1	*CC2	H2S	1.1110	107.06	-105.63	111.30	1.1109
IC C31	C32	C33	O33	1.5958	111.19	-173.79	110.26	1.4370
IC O33	C32	*C33	H33J	1.4370	110.26	118.41	109.85	1.1107
IC H33J	C32	*C33	H33K	1.1107	109.85	116.35	110.86	1.1105
IC C32	C33	O33	CD1	1.5682	110.26	-82.05	116.23	1.3711
IC C33	O33	CD1	CD2	1.4370	116.23	156.92	111.58	1.5654
IC CD2	O33	*CD1	OD1	1.5654	111.58	-176.12	124.80	1.1850
IC O33	CD1	CD2	CD3	1.3711	111.58	79.99	113.19	1.5154
IC CD3	CD1	*CD2	H2X	1.5154	113.19	-122.11	106.99	1.1106
IC H2X	CD1	*CD2	H2Y	1.1106	106.99	-114.65	110.19	1.1109
IC CA1	CA2	CA3	CA4	1.4819	109.95	160.84	117.75	1.5645
IC CA4	CA2	*CA3	H3A	1.5645	117.75	-127.81	109.37	1.1111
IC H3A	CA2	*CA3	H3B	1.1111	109.37	-117.63	101.55	1.1105
IC CA2	CA3	CA4	CA5	1.5144	117.75	157.03	111.41	1.5424
IC CA5	CA3	*CA4	H4A	1.5424	111.41	-119.03	108.09	1.1114
IC H4A	CA3	*CA4	H4B	1.1114	108.09	-126.38	120.58	1.1101
IC CA3	CA4	CA5	CA6	1.5645	111.41	74.25	110.88	1.5499
IC CA6	CA4	*CA5	H5A	1.5499	110.88	-125.89	112.16	1.1114
IC H5A	CA4	*CA5	H5B	1.1114	112.16	-116.89	114.30	1.1106
IC CA4	CA5	CA6	CA7	1.5424	110.88	177.26	112.07	1.5702
IC CA7	CA5	*CA6	H6A	1.5702	112.07	-121.41	112.61	1.1107
IC H6A	CA5	*CA6	H6B	1.1107	112.61	-124.17	99.78	1.1108
IC CA5	CA6	CA7	CA8	1.5499	112.07	74.00	120.92	1.5501
IC CA8	CA6	*CA7	H7A	1.5501	120.92	-128.07	104.29	1.1105
IC H7A	CA6	*CA7	H7B	1.1105	104.29	-118.23	103.40	1.1112
IC CA6	CA7	CA8	CA9	1.5702	120.92	170.69	112.79	1.5329
IC CA9	CA7	*CA8	H8A	1.5329	112.79	-117.60	114.99	1.1111
IC H8A	CA7	*CA8	H8B	1.1111	114.99	-115.64	104.49	1.1114
IC CA7	CA8	CA9	CA10	1.5501	112.79	82.54	132.44	1.3410
IC CA10	CA8	*CA9	H9A	1.3410	132.44	-165.92	110.30	1.0996
IC CA8	CA9	CA10	CA11	1.5329	132.44	11.31	129.79	1.4668
IC CA11	CA9	*CA10	H10A	1.4668	129.79	173.10	113.82	1.1006
IC CA9	CA10	CA11	CA12	1.3410	129.79	-125.54	110.53	1.5132
IC CA12	CA10	*CA11	H11A	1.5132	110.53	-124.22	111.84	1.1109
IC H11A	CA10	*CA11	H11B	1.1109	111.84	-116.05	116.75	1.1107
IC CA10	CA11	CA12	CA13	1.4668	110.53	161.55	113.19	1.4862
IC CA13	CA11	*CA12	H12A	1.4862	113.19	-115.99	104.44	1.1104
IC H12A	CA11	*CA12	H12B	1.1104	104.44	-109.05	111.86	1.1114
IC CA11	CA12	CA13	CA14	1.5132	113.19	66.72	118.43	1.5736
IC CA14	CA12	*CA13	H13A	1.5736	118.43	-112.65	104.63	1.1114
IC H13A	CA12	*CA13	H13B	1.1114	104.63	-117.70	113.84	1.1109
IC CA12	CA13	CA14	CA15	1.4862	118.43	62.79	110.33	1.5584
IC CA15	CA13	*CA14	H14A	1.5584	110.33	-118.07	107.82	1.1108

IC H14A	CA13	*CA14	H14B	1.1108	107.82	-113.03	108.64	1.1112
IC CA13	CA14	CA15	CA16	1.5736	110.33	-175.93	102.80	1.5814
IC CA16	CA14	*CA15	H15A	1.5814	102.80	-121.30	114.89	1.1112
IC H15A	CA14	*CA15	H15B	1.1112	114.89	-125.40	120.38	1.1112
IC CA14	CA15	CA16	CA17	1.5584	102.80	-177.33	108.65	1.4920
IC CA17	CA15	*CA16	H16A	1.4920	108.65	-121.79	105.96	1.1117
IC H16A	CA15	*CA16	H16B	1.1117	105.96	-110.08	103.15	1.1108
IC CA15	CA16	CA17	CA18	1.5814	108.65	-168.13	114.64	1.5103
IC CA18	CA16	*CA17	H17A	1.5103	114.64	-123.69	105.58	1.1117
IC H17A	CA16	*CA17	H17B	1.1117	105.58	-117.14	106.96	1.1108
IC CA16	CA17	CA18	H18A	1.4920	114.64	-97.38	116.78	1.1116
IC H18A	CA17	*CA18	H18B	1.1116	116.78	-112.38	110.91	1.1109
IC H18A	CA17	*CA18	H18C	1.1116	116.78	124.13	107.97	1.1105
IC CB1	CB2	CB3	CB4	1.4434	116.83	-155.75	114.25	1.5868
IC CB4	CB2	*CB3	H3D	1.5868	114.25	-122.78	114.66	1.1117
IC H3D	CB2	*CB3	H3E	1.1117	114.66	-129.44	120.87	1.1109
IC CB2	CB3	CB4	CB5	1.5195	114.25	-52.65	114.56	1.5137
IC CB5	CB3	*CB4	H4D	1.5137	114.56	-115.68	101.27	1.1103
IC H4D	CB3	*CB4	H4E	1.1103	101.27	-119.02	105.41	1.1106
IC CB3	CB4	CB5	CB6	1.5868	114.56	-179.99	120.50	1.5634
IC CB6	CB4	*CB5	H5D	1.5634	120.50	-122.72	117.24	1.1113
IC H5D	CB4	*CB5	H5E	1.1113	117.24	-123.34	103.45	1.1107
IC CB4	CB5	CB6	CB7	1.5137	120.50	39.76	116.61	1.5133
IC CB7	CB5	*CB6	H6D	1.5133	116.61	-120.56	106.07	1.1110
IC H6D	CB5	*CB6	H6E	1.1110	106.07	-117.54	106.11	1.1114
IC CB5	CB6	CB7	CB8	1.5634	116.61	176.57	110.49	1.5173
IC CB8	CB6	*CB7	H7D	1.5173	110.49	-120.73	106.74	1.1106
IC H7D	CB6	*CB7	H7E	1.1106	106.74	-117.79	112.10	1.1106
IC CB6	CB7	CB8	CB9	1.5133	110.49	-82.21	120.66	1.5172
IC CB9	CB7	*CB8	H8D	1.5172	120.66	-115.86	108.05	1.1105
IC H8D	CB7	*CB8	H8E	1.1105	108.05	-111.89	111.52	1.1117
IC CB7	CB8	CB9	CB10	1.5173	120.66	-107.87	126.23	1.3089
IC CB10	CB8	*CB9	H9D	1.3089	126.23	177.32	108.46	1.0998
IC CB8	CB9	CB10	CB11	1.5172	126.23	-9.03	129.20	1.5488
IC CB11	CB9	*CB10	H10D	1.5488	129.20	-177.87	114.84	1.1001
IC CB9	CB10	CB11	CB12	1.3089	129.20	89.60	118.95	1.5198
IC CB12	CB10	*CB11	H11D	1.5198	118.95	-127.92	113.12	1.1108
IC H11D	CB10	*CB11	H11E	1.1108	113.12	-116.33	107.89	1.1110
IC CB10	CB11	CB12	CB13	1.5488	118.95	47.44	108.85	1.4805
IC CB13	CB11	*CB12	H12D	1.4805	108.85	-124.66	111.86	1.1106
IC H12D	CB11	*CB12	H12E	1.1106	111.86	-115.71	106.95	1.1117
IC CB11	CB12	CB13	CB14	1.5198	108.85	158.33	114.90	1.5460
IC CB14	CB12	*CB13	H13D	1.5460	114.90	-122.78	110.67	1.1114
IC H13D	CB12	*CB13	H13E	1.1114	110.67	-118.72	111.28	1.1107
IC CB12	CB13	CB14	CB15	1.4805	114.90	68.37	114.96	1.5755
IC CB15	CB13	*CB14	H14D	1.5755	114.96	-127.83	107.96	1.1104
IC H14D	CB13	*CB14	H14E	1.1104	107.96	-116.62	108.21	1.1111
IC CB13	CB14	CB15	CB16	1.5460	114.96	166.45	117.74	1.5429
IC CB16	CB14	*CB15	H15D	1.5429	117.74	-122.27	110.71	1.1109
IC H15D	CB14	*CB15	H15E	1.1109	110.71	-117.71	99.91	1.1101
IC CB14	CB15	CB16	CB17	1.5755	117.74	174.50	116.45	1.5273
IC CB17	CB15	*CB16	H16D	1.5273	116.45	-126.26	106.79	1.1119
IC H16D	CB15	*CB16	H16E	1.1119	106.79	-120.93	108.80	1.1106
IC CB15	CB16	CB17	CB18	1.5429	116.45	176.52	110.28	1.5697
IC CB18	CB16	*CB17	H17D	1.5697	110.28	-130.06	105.87	1.1105
IC H17D	CB16	*CB17	H17E	1.1105	105.87	-115.72	106.22	1.1106
IC CB16	CB17	CB18	H18D	1.5273	110.28	-159.07	103.32	1.1112
IC H18D	CB17	*CB18	H18E	1.1112	103.32	-120.33	105.93	1.1103
IC H18D	CB17	*CB18	H18F	1.1112	103.32	118.79	110.62	1.1116
IC CC1	CC2	CC3	CC4	1.4829	115.59	49.93	117.90	1.5366
IC CC4	CC2	*CC3	H3R	1.5366	117.90	-115.05	111.28	1.1107
IC H3R	CC2	*CC3	H3S	1.1107	111.28	-122.62	109.57	1.1107
IC CC2	CC3	CC4	CC5	1.5435	117.90	41.42	122.16	1.4856
IC CC5	CC3	*CC4	H4R	1.4856	122.16	-129.12	107.74	1.1116

IC H4R	CC3	*CC4	H4S	1.1116	107.74	-110.63	106.93	1.1114
IC CC3	CC4	CC5	CC6	1.5366	122.16	79.03	118.09	1.5779
IC CC6	CC4	*CC5	H5R	1.5779	118.09	-121.27	111.33	1.1111
IC H5R	CC4	*CC5	H5S	1.1111	111.33	-121.85	103.83	1.1116
IC CC4	CC5	CC6	CC7	1.4856	118.09	-175.62	114.14	1.5193
IC CC7	CC5	*CC6	H6R	1.5193	114.14	-112.92	99.65	1.1104
IC H6R	CC5	*CC6	H6S	1.1104	99.65	-115.34	114.89	1.1110
IC CC5	CC6	CC7	CC8	1.5779	114.14	86.04	111.08	1.5443
IC CC8	CC6	*CC7	H7R	1.5443	111.08	-126.84	118.56	1.1115
IC H7R	CC6	*CC7	H7S	1.1115	118.56	-116.67	107.70	1.1111
IC CC6	CC7	CC8	CC9	1.5193	111.08	-167.74	113.25	1.5955
IC CC9	CC7	*CC8	H8R	1.5955	113.25	-126.88	111.16	1.1113
IC H8R	CC7	*CC8	H8S	1.1113	111.16	-113.40	107.96	1.1105
IC CC7	CC8	CC9	CC10	1.5443	113.25	-109.87	126.39	1.3527
IC CC10	CC8	*CC9	H9R	1.3527	126.39	-170.92	110.56	1.0998
IC CC8	CC9	CC10	CC11	1.5955	126.39	15.86	128.70	1.4629
IC CC11	CC9	*CC10	H10R	1.4629	128.70	175.07	123.34	1.1002
IC CC9	CC10	CC11	CC12	1.3527	128.70	101.47	118.70	1.5861
IC CC12	CC10	*CC11	H11R	1.5861	118.70	-125.10	109.20	1.1112
IC H11R	CC10	*CC11	H11S	1.1112	109.20	-110.25	111.88	1.1101
IC CC10	CC11	CC12	CC13	1.4629	118.70	67.74	108.82	1.5353
IC CC13	CC11	*CC12	H12R	1.5353	108.82	-126.41	105.67	1.1103
IC H12R	CC11	*CC12	H12S	1.1103	105.67	-116.13	112.54	1.1110
IC CC11	CC12	CC13	CC14	1.5861	108.82	-177.19	124.76	1.5291
IC CC14	CC12	*CC13	H13R	1.5291	124.76	-126.31	102.56	1.1109
IC H13R	CC12	*CC13	H13S	1.1109	102.56	-101.72	109.52	1.1110
IC CC12	CC13	CC14	CC15	1.5353	124.76	-147.35	108.06	1.5835
IC CC15	CC13	*CC14	H14R	1.5835	108.06	-127.34	119.98	1.1117
IC H14R	CC13	*CC14	H14S	1.1117	119.98	-118.05	109.10	1.1109
IC CC13	CC14	CC15	CC16	1.5291	108.06	78.94	118.04	1.5648
IC CC16	CC14	*CC15	H15R	1.5648	118.04	-130.95	115.54	1.1114
IC H15R	CC14	*CC15	H15S	1.1114	115.54	-107.98	103.32	1.1109
IC CC14	CC15	CC16	CC17	1.5835	118.04	170.34	112.62	1.5605
IC CC17	CC15	*CC16	H16R	1.5605	112.62	116.67	109.09	1.1110
IC H16R	CC15	*CC16	H16S	1.1110	109.09	118.07	101.73	1.1110
IC CC15	CC16	CC17	CC18	1.5648	112.62	-160.59	113.48	1.5455
IC CC18	CC16	*CC17	H17R	1.5455	113.48	-119.35	112.75	1.1111
IC H17R	CC16	*CC17	H17S	1.1111	112.75	-118.74	109.01	1.1114
IC CC16	CC17	CC18	H18R	1.5605	113.48	-167.53	105.19	1.1114
IC H18R	CC17	*CC18	H18S	1.1114	105.19	123.30	114.77	1.1107
IC H18R	CC17	*CC18	H18T	1.1114	105.19	-120.49	105.29	1.1117
IC CD1	CD2	CD3	CD4	1.5654	113.19	-162.40	114.80	1.5512
IC CD4	CD2	*CD3	H3X	1.5512	114.80	-117.81	118.26	1.1102
IC H3X	CD2	*CD3	H3Y	1.1102	118.26	-125.60	110.95	1.1112
IC CD2	CD3	CD4	CD5	1.5154	114.80	63.81	109.67	1.6095
IC CD5	CD3	*CD4	H4X	1.6095	109.67	-112.22	109.63	1.1107
IC H4X	CD3	*CD4	H4Y	1.1107	109.63	-120.86	110.95	1.1109
IC CD3	CD4	CD5	CD6	1.5512	109.67	-171.66	110.10	1.5117
IC CD6	CD4	*CD5	H5X	1.5117	110.10	-113.98	105.23	1.1108
IC H5X	CD4	*CD5	H5Y	1.1108	105.23	-128.80	116.89	1.1106
IC CD4	CD5	CD6	CD7	1.6095	110.10	170.09	111.04	1.5055
IC CD7	CD5	*CD6	H6X	1.5055	111.04	-114.76	105.35	1.1116
IC H6X	CD5	*CD6	H6Y	1.1116	105.35	-122.63	110.38	1.1108
IC CD5	CD6	CD7	CD8	1.5117	111.04	-172.02	115.71	1.5289
IC CD8	CD6	*CD7	H7X	1.5289	115.71	-123.94	114.68	1.1110
IC H7X	CD6	*CD7	H7Y	1.1110	114.68	-126.78	107.85	1.1109
IC CD6	CD7	CD8	CD9	1.5055	115.71	-61.83	117.36	1.5186
IC CD9	CD7	*CD8	H8X	1.5186	117.36	-129.63	101.79	1.1109
IC H8X	CD7	*CD8	H8Y	1.1109	101.79	-111.91	105.86	1.1107
IC CD7	CD8	CD9	CD10	1.5289	117.36	179.97	120.32	1.3356
IC CD10	CD8	*CD9	H9X	1.3356	120.32	-177.34	116.78	1.1009
IC CD8	CD9	CD10	CD11	1.5186	120.32	-9.60	131.58	1.4710
IC CD11	CD9	*CD10	H10X	1.4710	131.58	-172.61	113.16	1.1005
IC CD9	CD10	CD11	CD12	1.3356	131.58	-124.79	115.05	1.5361





ATOM HB31	HAL2	0.09 !							
ATOM HB32	HAL2	0.09 !							
GROUP		!							
ATOM CA4	CTL1	0.17 !			HA4---CA4-----				
ATOM HA4	HAL1	0.09 !							
ATOM OA6	OSL	-0.49 !			OA6 OA7				
ATOM CA5	CL	0.90 !			\ //				
ATOM OA7	OBL	-0.63 !				CA5			
ATOM C12	CTL2	-0.22 !							
ATOM H2K	HAL2	0.09 !			H2K ---C12---H2L				
ATOM H2L	HAL2	0.09 !							
GROUP		!							
ATOM CA6	CTL2	0.08 !				HA61---CA6---HA62			
ATOM HA61	HAL2	0.09 !							
ATOM HA62	HAL2	0.09 !					OA8 OA9		
ATOM OA8	OSL	-0.49 !					\ //		
ATOM CA7	CL	0.90 !					CA7		
ATOM OA9	OBL	-0.63 !							
ATOM C22	CTL2	-0.22 !					H2L---C22---H2R		
ATOM H2R	HAL2	0.09 !							
ATOM H2L	HAL2	0.09 !							
GROUP		! tail 1							
ATOM C13	CTL2	-0.18 !							
ATOM H3K	HAL2	0.09 !			H3K ---C13---H3L				
ATOM H3L	HAL2	0.09 !							
GROUP		!							
ATOM C14	CTL2	-0.18 !							
ATOM H4K	HAL2	0.09 !			H4K ---C14---H4L				
ATOM H4L	HAL2	0.09 !							
GROUP		!							
ATOM C15	CTL2	-0.18 !							
ATOM H5K	HAL2	0.09 !			H5K ---C15---H5L				
ATOM H5L	HAL2	0.09 !							
GROUP		!							
ATOM C16	CTL2	-0.18 !							
ATOM H6K	HAL2	0.09 !			H6K ---C16---H6L				
ATOM H6L	HAL2	0.09 !							
GROUP		!							
ATOM C17	CTL2	-0.18 !							
ATOM H7K	HAL2	0.09 !			H7K ---C17---H7L				
ATOM H7L	HAL2	0.09 !							
GROUP		!							
ATOM C18	CTL2	-0.18 !							
ATOM H8K	HAL2	0.09 !			H8K ---C18---H8SL				
ATOM H8L	HAL2	0.09 !							
GROUP		!							
ATOM C19	CTL2	-0.18 !							
ATOM H9K	HAL2	0.09 !			H9K ---C19---H9SL				
ATOM H9L	HAL2	0.09 !							
GROUP		!							
ATOM C110	CTL2	-0.18 !							
ATOM H10K	HAL2	0.09 !			H10K---C110---H10L				
ATOM H10L	HAL2	0.09 !							
GROUP		!							
ATOM C111	CEL1	-0.15 !							
ATOM H11K	HEL1	0.15 !			H11K---C111				
GROUP		!			(CIS)				
ATOM C112	CEL1	-0.15 !							

ATOM H12K	HEL1	0.15	!		H12K---C112		
GROUP			!				
ATOM C113	CTL2	-0.18	!				
ATOM H13K	HAL2	0.09	!		H13K---C113--H13L		
ATOM H13L	HAL2	0.09	!				
GROUP			!				
ATOM C114	CTL2	-0.18	!				
ATOM H14K	HAL2	0.09	!		H14K---C114--H14L		
ATOM H14L	HAL2	0.09	!				
GROUP			!				
ATOM C115	CTL2	-0.18	!				
ATOM H15K	HAL2	0.09	!		H15K---C115--H15L		
ATOM H15L	HAL2	0.09	!				
GROUP			!				
ATOM C116	CTL2	-0.18	!				
ATOM H16K	HAL2	0.09	!		H16K---C116--H16L		
ATOM H16L	HAL2	0.09	!				
GROUP			!				
ATOM C117	CTL2	-0.18	!				
ATOM H17K	HAL2	0.09	!		H17K---C117--H17L		
ATOM H17L	HAL2	0.09	!				
GROUP			!				
ATOM C118	CTL3	-0.27	!				
ATOM H18K	HAL3	0.09	!		H18K---C118--H18L		
ATOM H18L	HAL3	0.09	!				
ATOM H18M	HAL3	0.09	!		H18M		
GROUP			!				
			!				
ATOM C23	CTL2	-0.18	!				
ATOM H3R	HAL2	0.09	!				H3R ---C23---H3S
ATOM H3S	HAL2	0.09	!				
GROUP			!				
ATOM C24	CTL2	-0.18	!				
ATOM H4R	HAL2	0.09	!				H4R ---C24---H4S
ATOM H4S	HAL2	0.09	!				
GROUP			!				
ATOM C25	CTL2	-0.18	!				
ATOM H5R	HAL2	0.09	!				H5R ---C25---H5S
ATOM H5S	HAL2	0.09	!				
GROUP			!				
ATOM C26	CTL2	-0.18	!				
ATOM H6X	HAL2	0.09	!				H6R ---C26---H6S
ATOM H6Y	HAL2	0.09	!				
GROUP			!				
ATOM C27	CTL2	-0.18	!				
ATOM H7R	HAL2	0.09	!				H7R ---C27---H7S
ATOM H7S	HAL2	0.09	!				
GROUP			!				
ATOM C28	CTL2	-0.18	!				
ATOM H8R	HAL2	0.09	!				H8R ---C28---H8S
ATOM H8S	HAL2	0.09	!				
GROUP			!				
ATOM C29	CTL2	-0.18	!				
ATOM H9R	HAL2	0.09	!				H9R ---C29---H9S
ATOM H9S	HAL2	0.09	!				
GROUP			!				
			!				
ATOM C210	CTL2	-0.18	!				
ATOM H10R	HAL2	0.09	!				H10R---C210---H10S
ATOM H10S	HAL2	0.09	!				
GROUP			!				
			!				
ATOM C211	CTL2	-0.15	!				
ATOM H11R	HEL1	0.15	!				H11R---C211
GROUP			!				(CIS)



ATOM H3Y	HAL2	0.09 !		
GROUP		!		
ATOM C34	CTL2	-0.18 !		
ATOM H4X	HAL2	0.09 !	H4Y ---C34---H4X	
ATOM H4Y	HAL2	0.09 !		
GROUP		!		
ATOM C35	CTL2	-0.18 !		
ATOM H5X	HAL2	0.09 !	H5X ---C35---H5Y	
ATOM H5Y	HAL2	0.09 !		
GROUP		!		
ATOM C36	CTL2	-0.18 !		
ATOM H6X	HAL2	0.09 !	H6X ---C36---H6Y	
ATOM H6Y	HAL2	0.09 !		
GROUP		!		
ATOM C37	CTL2	-0.18 !		
ATOM H7X	HAL2	0.09 !	H7X ---C37---H7Y	
ATOM H7Y	HAL2	0.09 !		
GROUP		!		
ATOM C38	CTL2	-0.18 !		
ATOM H8X	HAL2	0.09 !	H8X ---C38---H8Y	
ATOM H8Y	HAL2	0.09 !		
GROUP		!		
ATOM C39	CTL2	-0.18 !		
ATOM H9X	HAL2	0.09 !	H9X ---C39---H9SY	
ATOM H9Y	HAL2	0.09 !		
GROUP		!		
ATOM C310	CTL2	-0.18 !		
ATOM H10X	HAL2	0.09 !	H10X---C310---H10Y	
ATOM H10Y	HAL2	0.09 !		
GROUP		!		
ATOM C311	CEL1	-0.15 !		
ATOM H11X	HEL1	0.15 !	H11X---C311	
GROUP		!	(CIS)	
ATOM C312	CEL1	-0.15 !		
ATOM H12X	HEL1	0.15 !	H12X---C312	
GROUP		!		
ATOM C313	CTL2	-0.18 !		
ATOM H13X	HAL2	0.09 !	H13X---C313---H13Y	
ATOM H13Y	HAL2	0.09 !		
GROUP		!		
ATOM C314	CTL2	-0.18 !		
ATOM H14X	HAL2	0.09 !	H14X---C314---H14Y	
ATOM H14Y	HAL2	0.09 !		
GROUP		!		
ATOM C315	CTL2	-0.18 !		
ATOM H15X	HAL2	0.09 !	H15X---C315---H15Y	
ATOM H15Y	HAL2	0.09 !		
GROUP		!		
ATOM C316	CTL2	-0.18 !		
ATOM H16X	HAL2	0.09 !	H16X---C316---H16Y	
ATOM H16Y	HAL2	0.09 !		
GROUP		!		
ATOM C317	CTL2	-0.18 !		
ATOM H17X	HAL2	0.09 !	H17X---C317---H17Y	
ATOM H17Y	HAL2	0.09 !		
GROUP		!		
ATOM C318	CTL3	-0.27 !		
ATOM H18X	HAL3	0.09 !	H18X---C318---H18Y	
ATOM H18Y	HAL3	0.09 !		
ATOM H18Z	HAL3	0.09 !	H18Z	

GROUP			!	tail4		
ATOM C43	CTL2	-0.18	!			
ATOM H3Q	HAL2	0.09	!		H3Q	---C43---H3W
ATOM H3W	HAL2	0.09	!			
GROUP			!			
ATOM C44	CTL2	-0.18	!			
ATOM H4Q	HAL2	0.09	!		H4Q	---C44---H4W
ATOM H4W	HAL2	0.09	!			
GROUP			!			
ATOM C45	CTL2	-0.18	!			
ATOM H5Q	HAL2	0.09	!		H5Q	---C45---H5W
ATOM H5W	HAL2	0.09	!			
GROUP			!			
ATOM C46	CTL2	-0.18	!			
ATOM H6Q	HAL2	0.09	!		H6Q	---C46---H6W
ATOM H6Y	HAL2	0.09	!			
GROUP			!			
ATOM C47	CTL2	-0.18	!			
ATOM H7Q	HAL2	0.09	!		H7Q	---C47---H7W
ATOM H7W	HAL2	0.09	!			
GROUP			!			
ATOM C48	CTL2	-0.18	!			
ATOM H8Q	HAL2	0.09	!		H8Q	---C48---H8W
ATOM H8W	HAL2	0.09	!			
GROUP			!			
ATOM C49	CTL2	-0.18	!			
ATOM H9Q	HAL2	0.09	!		H9Q	---C49---H9W
ATOM H9W	HAL2	0.09	!			
GROUP			!			
ATOM C410	CTL2	-0.18	!			
ATOM H10Q	HAL2	0.09	!		H10Q	---C410---H10W
ATOM H10W	HAL2	0.09	!			
GROUP			!			
ATOM C411	CEL1	-0.15	!			
ATOM H11Q	HEL1	0.15	!		H11Q	---C411
GROUP			!			(CIS)
ATOM C412	CEL1	-0.18	!			
ATOM H12Q	HEL1	0.09	!		H12Q	---C412
GROUP			!			
ATOM C413	CTL2	-0.18	!			
ATOM H13Q	HAL2	0.09	!		H13Q	---C413---H13W
ATOM H13W	HAL2	0.09	!			
GROUP			!			
ATOM C414	CTL2	-0.18	!			
ATOM H14Q	HAL2	0.09	!		H14Q	---C414---H14W
ATOM H14W	HAL2	0.09	!			
GROUP			!			
ATOM C415	CTL2	-0.18	!			
ATOM H15Q	HAL2	0.09	!		H15Q	---C415---H15W
ATOM H15W	HAL2	0.09	!			
GROUP			!			
ATOM C416	CTL2	-0.18	!			
ATOM H16Q	HAL2	0.09	!		H16Q	---C416---H16W
ATOM H16W	HAL2	0.09	!			
GROUP			!			
ATOM C417	CTL2	-0.18	!			
ATOM H17Q	HAL2	0.09	!		H17Q	---C417---H17W
ATOM H17W	HAL2	0.09	!			
GROUP			!			
ATOM C418	CTL3	-0.27	!			
ATOM H18Q	HAL3	0.09	!		H18Q	---C418---H18W
ATOM H18W	HAL3	0.09	!			
ATOM H18G	HAL3	0.09	!			H18G

```

BOND C1 H1          C1 O1          O1 HO1          C1 CA2
BOND C1 CB2        CA2 HA21        CA2 HA22        CA2 OA2
BOND CB2 HB21      CB2 HB22        CB2 OB2         OA2 PA2
BOND PA2 OA3        PA2 OA4         PA2 OA5         OB2 PB2
BOND PB2 OB3        PB2 OB4         PB2 OB5         OA5 CA3
BOND CA3 HA31      CA3 HA32        CA3 CA4         CA4 HA4
BOND CA4 CA6        CA6 HA61        CA6 HA62        CA4 OA6
BOND CA6 OA8        OB5 CB3         CB3 HB31        CB3 HB32
BOND CB3 CB4        CB4 HB4         CB4 CB6         CB6 HB61
BOND CB6 HB62      CB4 OB6         CB6 OB8

! Chain Starting CA4
BOND OA6 CA5 CA5 C12
DOUBLE CA5 OA7
BOND C12 H2K        C12 H2L         C12 C13
BOND C13 H3K        C13 H3L         C13 C14
BOND C14 H4K        C14 H4L         C14 C15
BOND C15 H5K        C15 H5L         C15 C16
BOND C16 H6K        C16 H6L         C16 C17
BOND C17 H7K        C17 H7L         C17 C18
BOND C18 H8K        C18 H8L         C18 C19
BOND C19 H9K        C19 H9L         C19 C110
BOND C110 H10K      C110 H110L      C110 C111
BOND C111 H11K
DOUBLE C111 C112
BOND C112 H12K      C112 C113
BOND C113 H13K      C113 H13L        C113 C114
BOND C114 H14K      C114 H14L        C114 C115
BOND C115 H15K      C115 H15L        C115 C116
BOND C116 H16K      C116 H16L        C116 C117
BOND C117 H17K      C117 H17L        C117 C118
BOND C118 H18K      C118 H18L        C118 H18M

! Chain Starting CA6
BOND OA8 CA7 CA7 C22
DOUBLE CA7 OA9
BOND C22 H2R        C22 H2S         C22 C23
BOND C23 H3R        C23 H3S         C23 C24
BOND C24 H4R        C24 H4S         C24 C25
BOND C25 H5R        C25 H5S         C25 C26
BOND C26 H6R        C26 H6S         C26 C27
BOND C27 H7R        C27 H7S         C27 C28
BOND C28 H8R        C28 H8S         C28 C29
BOND C29 H9R        C29 H9S         C29 C210
BOND C210 H10R      C210 H10S       C210 C211
BOND C211 H11R
DOUBLE C211 C212
BOND C212 H12R      C212 C213
BOND C213 H13R      C213 H13S        C213 C214
BOND C214 H14R      C214 H14S        C214 C215
BOND C215 H15R      C215 H15S        C215 C216
BOND C216 H16R      C216 H16S        C216 C217
BOND C217 H17R      C217 H17S        C217 C218
BOND C218 H18R      C218 H18S        C218 H18T

! Chain Starting CB4
BOND OB6 CB5 CB5 C32
DOUBLE CB5 OB7
BOND C32 H2X        C32 H2Y         C32 C33
BOND C33 H3X        C33 H3Y         C33 C34
BOND C34 H4X        C34 H4Y         C34 C35
BOND C35 H5X        C35 H5Y         C35 C36
BOND C36 H6X        C36 H6Y         C36 C37
BOND C37 H7X        C37 H7Y         C37 C38
BOND C38 H8X        C38 H8Y         C38 C39

```

```

BOND C39 H9X C39 H9Y C39 C310
BOND C310 H10X C310 H110Y C310 C311
BOND C311 H11X
DOUBLE C311 C312
BOND C312 H12X C312 C313
BOND C313 H13X C313 H13Y C313 C314
BOND C314 H14X C314 H14Y C314 C315
BOND C315 H15X C315 H15Y C315 C316
BOND C316 H16X C316 H16Y C316 C317
BOND C317 H17X C317 H17Y C317 C318
BOND C318 H18X C318 H18Y C318 H18Z
! Chain Starting CB6
BOND OB8 CB7 CB7 C42
DOUBLE CB7 OB9
BOND C42 H2Q C42 H2W C42 C43
BOND C43 H3Q C43 H3W C43 C44
BOND C44 H4Q C44 H4W C44 C45
BOND C45 H5Q C45 H5W C45 C46
BOND C46 H6Q C46 H6W C46 C47
BOND C47 H7Q C47 H7W C47 C48
BOND C48 H8Q C48 H8W C48 C49
BOND C49 H9Q C49 H9W C49 C410
BOND C410 H10Q C410 H10W C410 C411
BOND C411 H11Q
DOUBLE C411 C412
BOND C412 H12Q C412 C413
BOND C413 H13Q C413 H13W C413 C414
BOND C414 H14Q C414 H14W C414 C415
BOND C415 H15Q C415 H15W C415 C416
BOND C416 H16Q C416 H16W C416 C417
BOND C417 H17Q C417 H17W C417 C418
BOND C418 H18Q C418 H18W C418 H18G

```

```

IMPR CA5 OA6 C12 OA7 CA7 OA8 C32 OA9
IMPR CB5 OB6 C52 OB7 CB7 OB8 C72 OB9

```

!PGs

```

RESI DVPG -1.00 ! 2,3-divaceny1-D-glycero-1-phosphatidylglycerol
! R1 - CH2
! |
! R2 - CH
! |
! CH2 - PO4 - CH2 - CH(OH) - CH2OH
!
! Polar Head and glycerol backbone
!!Derived from Mackerell top_all36_lipid.rf
!! by Stuart Rose 9/10/2013
!!RESI DOPG -1.00 ! 2,3-dioleoyl-D-glycero-1-phosphatidylglycerol
!!
!! R1 - CH2
!! |
!! R2 - CH
!! |
!! CH2 - PO4 - CH2 - CH(OH) - CH2OH
!!
!! Polar Head and glycerol backbone
GROUP !
ATOM C13 CTL2 0.05 !
ATOM H13A HAL2 0.09 ! H13A
ATOM H13B HAL2 0.09 ! |
ATOM OC3 OHL -0.65 ! |
ATOM HO3 HOL 0.42 ! H13B--C13---OC3--HO3

```

```

GROUP          !
ATOM C12  CTL1   0.14 !
ATOM H12A HAL1   0.09 !
ATOM OC2   OHL  -0.65 !
ATOM HO2   HOL   0.42 !
GROUP          !
ATOM C11  CTL2  -0.08 !
ATOM H11A HAL2   0.09 !
ATOM H11B HAL2   0.09 !
ATOM P     PL    1.50 !
ATOM O13   O2L  -0.78 !
ATOM O14   O2L  -0.78 !
ATOM O12   OSLP -0.57 !
ATOM O11   OSLP -0.57 !
ATOM C1    CTL2 -0.08 !
ATOM HA    HAL2  0.09 !
ATOM HB    HAL2  0.09 !
GROUP          !
ATOM C2    CTL1  0.17 !
ATOM HS    HAL1  0.09 !
ATOM O21   OSL  -0.49 !
ATOM C21   CL   0.90 !
ATOM O22   OBL  -0.63 !
ATOM C22   CTL2 -0.22 !
ATOM H2R   HAL2  0.09 !
ATOM H2S   HAL2  0.09 !
GROUP          !
ATOM C3    CTL2  0.08 !
ATOM HX    HAL2  0.09 !
ATOM HY    HAL2  0.09 !
ATOM O31   OSL  -0.49 !
ATOM C31   CL   0.90 !
ATOM O32   OBL  -0.63 !
ATOM C32   CTL2 -0.22 !
ATOM H2X   HAL2  0.09 !
ATOM H2Y   HAL2  0.09 !
GROUP          !
ATOM C23   CTL2 -0.18 !
ATOM H3R   HAL2  0.09 !
ATOM H3S   HAL2  0.09 !
GROUP          !
ATOM C24   CTL2 -0.18 !
ATOM H4R   HAL2  0.09 !
ATOM H4S   HAL2  0.09 !
GROUP          !
ATOM C25   CTL2 -0.18 !
ATOM H5R   HAL2  0.09 !
ATOM H5S   HAL2  0.09 !
GROUP          !
ATOM C26   CTL2 -0.18 !
ATOM H6R   HAL2  0.09 !
ATOM H6S   HAL2  0.09 !
GROUP          !
ATOM C27   CTL2 -0.18 !
ATOM H7R   HAL2  0.09 !
ATOM H7S   HAL2  0.09 !
GROUP          !
ATOM C28   CTL2 -0.18 !
ATOM H8R   HAL2  0.09 !
ATOM H8S   HAL2  0.09 !
GROUP          !
ATOM C29   CTL2 -0.18 !
ATOM H9R   HAL2  0.09 !
ATOM H9S   HAL2  0.09 !

```

|  
 |  
 |  
 H12A---C12---OC2---HO2  
 |  
 | alpha5  
 |  
 H11A---C11---H11B  
 | alpha4  
 |  
 (-) O13 O12  
 \ / alpha3  
 P (+)  
 / \ alpha2  
 (-) O14 O11  
 | alpha1  
 HA---C1---HB  
 | theta1  
 |  
 HS---C2-----  
 | beta1 |  
 O22 O21 theta3  
 \ / beta2 |  
 C21 |  
 | beta3 |  
 H2R---C22---H2S  
 |  
 | beta4 |  
 |  
 HX---C3---HY  
 | gamma1  
 O32 O31  
 \ / gamma2  
 C31 |  
 | gamma3  
 H2X---C32---H2Y  
 |  
 | gamma4  
 |  
 H3R ---C23---H3S  
 |  
 |  
 H4R ---C24---H4S  
 |  
 |  
 |  
 H5R ---C25---H5S  
 |  
 |  
 |  
 H6R ---C26---H6S  
 |  
 |  
 |  
 H7R ---C27---H7S  
 |  
 |  
 |  
 H8R ---C28---H8S  
 |  
 |  
 |  
 H9R ---C29---H9S  
 |



GROUP		!			
ATOM C210	CTL2	-0.18	!		
ATOM H10R	HAL2	0.09	!	H10R---C210--H10S	
ATOM H10S	HAL2	0.09	!		
GROUP		!			
ATOM C211	CTL2	-0.15	!		
ATOM H11R	HEL1	0.15	!	H11R---C211	
GROUP		!		(CIS)	
ATOM C212	CTL2	-0.15	!		
ATOM H12R	HEL1	0.15	!	H12R---C212	
GROUP		!			
ATOM C213	CTL2	-0.18	!		
ATOM H13R	HAL2	0.09	!	H13R---C213--H13S	
ATOM H13S	HAL2	0.09	!		
GROUP		!			
ATOM C214	CTL2	-0.18	!		
ATOM H14R	HAL2	0.09	!	H14R---C214--H14S	
ATOM H14S	HAL2	0.09	!		
GROUP		!			
ATOM C215	CTL2	-0.18	!		
ATOM H15R	HAL2	0.09	!	H15R---C215--H15S	
ATOM H15S	HAL2	0.09	!		
GROUP		!			
ATOM C216	CTL2	-0.18	!		
ATOM H16R	HAL2	0.09	!	H16R---C216--H16S	
ATOM H16S	HAL2	0.09	!		
GROUP		!			
ATOM C217	CTL2	-0.18	!		
ATOM H17R	HAL2	0.09	!	H17R---C217--H17S	
ATOM H17S	HAL2	0.09	!		
GROUP		!			
ATOM C218	CTL3	-0.27	!		
ATOM H18R	HAL3	0.09	!	H18R---C218--H18S	
ATOM H18S	HAL3	0.09	!		
ATOM H18T	HAL3	0.09	!	H18T	
GROUP		!			
ATOM C33	CTL2	-0.18	!		
ATOM H3X	HAL2	0.09	!		H3X ---C33---H3Y
ATOM H3Y	HAL2	0.09	!		
GROUP		!			
ATOM C34	CTL2	-0.18	!		
ATOM H4X	HAL2	0.09	!		H4X ---C34---H4Y
ATOM H4Y	HAL2	0.09	!		
GROUP		!			
ATOM C35	CTL2	-0.18	!		
ATOM H5X	HAL2	0.09	!		H5X ---C35---H5Y
ATOM H5Y	HAL2	0.09	!		
GROUP		!			
ATOM C36	CTL2	-0.18	!		
ATOM H6X	HAL2	0.09	!		H6X ---C36---H6Y
ATOM H6Y	HAL2	0.09	!		
GROUP		!			
ATOM C37	CTL2	-0.18	!		
ATOM H7X	HAL2	0.09	!		H7X ---C37---H7Y
ATOM H7Y	HAL2	0.09	!		
GROUP		!			
ATOM C38	CTL2	-0.18	!		
ATOM H8X	HAL2	0.09	!		H8X ---C38---H8Y
ATOM H8Y	HAL2	0.09	!		
GROUP		!			
ATOM C39	CTL2	-0.18	!		
ATOM H9X	HAL2	0.09	!		H9X ---C39---H9Y
ATOM H9Y	HAL2	0.09	!		
GROUP		!			

ATOM C310	CTL2	-0.18	!		
ATOM H10X	HAL2	0.09	!	H10X---C310--H10Y	
ATOM H10Y	HAL2	0.09	!		
GROUP			!		
ATOM C311	CTL2	-0.15	!		
ATOM H11X	HEL1	0.15	!	H11X---C311	
GROUP			!		
ATOM C312	CTL2	-0.15	!		
ATOM H12X	HEL1	0.15	!	H12X---C312	
GROUP			!		
ATOM C313	CTL2	-0.18	!		
ATOM H13X	HAL2	0.09	!	H13X---C313--H13Y	
ATOM H13Y	HAL2	0.09	!		
GROUP			!		
ATOM C314	CTL2	-0.18	!		
ATOM H14X	HAL2	0.09	!	H14X---C314--H14Y	
ATOM H14Y	HAL2	0.09	!		
GROUP			!		
ATOM C315	CTL2	-0.18	!		
ATOM H15X	HAL2	0.09	!	H15X---C315--H15Y	
ATOM H15Y	HAL2	0.09	!		
GROUP			!		
ATOM C316	CTL2	-0.18	!		
ATOM H16X	HAL2	0.09	!	H16X---C316--H16Y	
ATOM H16Y	HAL2	0.09	!		
GROUP			!		
ATOM C317	CTL2	-0.18	!		
ATOM H17X	HAL2	0.09	!	H17X---C317--H17Y	
ATOM H17Y	HAL2	0.09	!		
GROUP			!		
ATOM C318	CTL3	-0.27	!		
ATOM H18X	HAL3	0.09	!	H18X---C318--H18Y	
ATOM H18Y	HAL3	0.09	!		
ATOM H18Z	HAL3	0.09	!		H18Z

! Polar Head

BOND HO3	OC3	OC3	C13	C13	H13A	C13	H13B	C13	C12
BOND HO2	OC2	OC2	C12	C12	H12A	C12	C11		
BOND C11	H11A	C11	H11B	C11	O12	O11	C1		
BOND O12	P	P	O11	P	O13	P	O14		

! Glycerol Backbone

BOND C1	HA	C1	HB	C1	C2
BOND C2	HS	C2	C3	C2	O21
BOND C3	HX	C3	HY	C3	O31

! Chain from C2

BOND O21	C21				
BOND C21	C22				
DOUBLE C21	O22				
BOND C22	H2R	C22	H2S	C22	C23
BOND C23	H3R	C23	H3S	C23	C24
BOND C24	H4R	C24	H4S	C24	C25
BOND C25	H5R	C25	H5S	C25	C26
BOND C26	H6R	C26	H6S	C26	C27
BOND C27	H7R	C27	H7S	C27	C28
BOND C28	H8R	C28	H8S	C28	C29
BOND C29	H9R		C29 H9S		C29 C210
BOND C210	H10R	C210	H10S		C210 C211
BOND C211	H11R				
DOUBLE C211	C212				
BOND C212	H12R	C212	C213		
BOND C213	H13R	C213	H13S	C213	C214
BOND C214	H14R	C214	H14S	C214	C215
BOND C215	H15R	C215	H15S	C215	C216
BOND C216	H16R	C216	H16S	C216	C217

```

BOND C217 H17R      C217 H17S      C217 C218
BOND C218 H18R      C218 H18S      C218 H18T
! Chain From C3
BOND O31 C31
BOND C31 C32
DOUBLE C31 O32
BOND C32 H2X      C32 H2Y      C32 C33
BOND C33 H3X      C33 H3Y      C33 C34
BOND C34 H4X      C34 H4Y      C34 C35
BOND C35 H5X      C35 H5Y      C35 C36
BOND C36 H6X      C36 H6Y      C36 C37
BOND C37 H7X      C37 H7Y      C37 C38
BOND C38 H8X      C38 H8Y      C38 C39
BOND C39 H9X      C39 H9Y      C39 C310
BOND C310 H10X     C310 H11Y     C310 C311
BOND C311 H11X
DOUBLE C311 C312
BOND C312 H12X     C312 C313
BOND C313 H13X     C313 H13Y     C313 C314
BOND C314 H14X     C314 H14Y     C314 C315
BOND C315 H15X     C315 H15Y     C315 C316
BOND C316 H16X     C316 H16Y     C316 C317
BOND C317 H17X     C317 H17Y     C317 C318
BOND C318 H18X     C318 H18Y     C318 H18Z

```

```

IMPR C21 O21 C22 O22      C31 O31 C32 O32

```

IC C13	C12	C11	O12	1.5583	113.89	93.01	113.50	1.4295
IC OC3	C13	C12	C11	1.4375	112.31	69.20	113.89	1.5573
IC OC3	C12	*C13	H13A	1.4375	112.31	119.90	108.06	1.1118
IC OC3	C12	*C13	H13B	1.4375	112.31	-123.06	109.89	1.1097
IC C12	C13	OC3	HO3	1.5583	112.31	-141.84	106.96	0.9777
IC C11	C13	*C12	OC2	1.5573	113.89	-121.65	107.64	1.4259
IC OC2	C13	*C12	H12A	1.4259	107.64	-117.84	109.30	1.1131
IC C13	C12	OC2	HO2	1.5583	107.64	38.09	100.52	0.9671
IC O12	C12	*C11	H11A	1.4295	113.50	-126.35	109.70	1.1125
IC H11A	C12	*C11	H11B	1.1125	109.70	-115.65	107.71	1.1131
IC C12	C11	O12	P	1.5573	113.50	-72.69	124.80	1.5783
IC C11	O12	P	O11	1.4295	124.80	-30.02	102.66	1.5825
IC O11	O12	*P	O13	1.5825	102.66	113.88	109.00	1.4783
IC O11	O12	*P	O14	1.5825	102.66	-115.27	109.77	1.4781
IC O12	P	O11	C1	1.5783	102.66	-80.21	120.83	1.4246
IC P	O11	C1	C2	1.5825	120.83	177.68	108.67	1.5488
IC C2	O11	*C1	HA	1.5488	108.67	-120.91	111.25	1.1145
IC HA	O11	*C1	HB	1.1145	111.25	-120.47	110.06	1.1152
IC O11	C1	C2	C3	1.4246	108.67	45.70	110.42	1.5580
IC C3	C1	*C2	O21	1.5580	110.42	120.25	110.13	1.4420
IC C3	C1	*C2	HS	1.5580	110.42	-116.94	108.10	1.1164
IC C1	C2	O21	C21	1.5488	110.13	74.82	114.08	1.3218
IC C2	O21	C21	C22	1.4420	114.08	-171.58	108.87	1.5297
IC C22	O21	*C21	O22	1.5297	108.87	-179.18	126.27	1.2166
IC O21	C21	C22	C23	1.3218	108.87	167.60	112.03	1.5460
IC C23	C21	*C22	H2R	1.5460	112.03	-121.40	108.25	1.1088
IC H2R	C21	*C22	H2S	1.1088	108.25	-117.05	107.34	1.1068
IC C1	C2	C3	O31	1.5488	110.42	-172.10	112.95	1.4472
IC O31	C2	*C3	HX	1.4472	112.95	-119.90	106.80	1.1123
IC HX	C2	*C3	HY	1.1123	106.80	-114.66	109.95	1.1147
IC C2	C3	O31	C31	1.5580	112.95	84.38	114.39	1.3267
IC C3	O31	C31	C32	1.4472	114.39	176.82	109.50	1.5275
IC C32	O31	*C31	O32	1.5275	109.50	-179.44	126.11	1.2173
IC O31	C31	C32	C33	1.3267	109.50	-66.76	112.63	1.5535
IC C33	C31	*C32	H2X	1.5535	112.63	121.43	107.50	1.1085
IC H2X	C31	*C32	H2Y	1.1085	107.50	116.64	107.32	1.1097
IC C21	C22	C23	C24	1.5289	112.21	175.76	112.39	1.5338

IC C24	C22	*C23	H3R	1.5338	112.39	-120.69	109.57	1.1147
IC H3R	C22	*C23	H3S	1.1147	109.57	-117.65	109.64	1.1142
IC C22	C23	C24	C25	1.5449	112.39	-179.39	112.35	1.5346
IC C25	C23	*C24	H4R	1.5346	112.35	-121.52	109.41	1.1131
IC H4R	C23	*C24	H4S	1.1131	109.41	-117.57	108.97	1.1134
IC C23	C24	C25	C26	1.5338	112.35	176.31	112.80	1.5344
IC C26	C24	*C25	H5R	1.5344	112.80	-121.01	108.95	1.1135
IC H5R	C24	*C25	H5S	1.1135	108.95	-117.24	109.16	1.1132
IC C24	C25	C26	C27	1.5346	112.80	-179.44	112.48	1.5356
IC C27	C25	*C26	H6R	1.5356	112.48	-121.49	109.32	1.1129
IC H6R	C25	*C26	H6S	1.1129	109.32	-117.47	108.94	1.1132
IC C25	C26	C27	C28	1.5344	112.48	176.92	112.46	1.5398
IC C28	C26	*C27	H7R	1.5398	112.46	-121.38	108.40	1.1139
IC H7R	C26	*C27	H7S	1.1139	108.40	-116.93	108.77	1.1139
IC C26	C27	C28	C29	1.5356	112.46	-178.53	111.43	1.5097
IC C29	C27	*C28	H8R	1.5097	111.43	-123.58	107.80	1.1132
IC H8R	C27	*C28	H8S	1.1132	107.80	-115.43	108.37	1.1128
IC C27	C28	C29	C210	1.5344	112.48	176.92	112.46	1.5398
IC C210	C28	*C29	H9R	1.5398	112.46	-121.38	108.40	1.1139
IC H9R	C28	*C29	H9S	1.1139	108.40	-116.93	108.77	1.1139
IC C28	C29	C210	C211	1.5356	112.46	-178.53	111.43	1.5097
IC C211	C29	*C210	H10R	1.5097	111.43	-123.58	107.80	1.1132
IC H10R	C29	*C210	H9S	1.1132	107.80	-115.43	108.37	1.1128
IC C29	C210	C211	C212	1.5398	111.43	-126.96	126.62	1.3465
IC C212	C210	*C211	H11R	1.3465	126.62	178.41	114.65	1.1012
IC C210	C211	C212	C213	1.5097	126.62	-1.69	126.32	1.5088
IC C213	C211	*C212	H12R	1.5088	126.32	-179.55	118.79	1.1012
IC C211	C212	C213	C214	1.5392	112.29	179.81	112.68	1.5345
IC C214	C212	*C213	H13R	1.5345	112.68	-121.26	109.04	1.1132
IC H13R	C212	*C213	H13S	1.1132	109.04	-117.39	109.10	1.1131
IC C212	C213	C214	C215	1.5354	112.68	179.80	112.59	1.5347
IC C215	C213	*C214	H14R	1.5347	112.59	-121.29	109.09	1.1132
IC H14R	C213	*C214	H14S	1.1132	109.09	-117.37	109.11	1.1133
IC C213	C214	C215	C216	1.5345	112.59	-179.58	112.63	1.5347
IC C216	C214	*C215	H15R	1.5347	112.63	-121.36	109.09	1.1132
IC H15R	C214	*C215	H15S	1.1132	109.09	-117.38	109.07	1.1132
IC C214	C215	C216	C217	1.5347	112.63	179.65	112.69	1.5339
IC C217	C215	*C216	H16R	1.5339	112.69	-121.27	109.11	1.1132
IC H16R	C215	*C216	H16S	1.1132	109.11	-117.36	109.14	1.1132
IC C215	C216	C217	C218	1.5347	112.69	-179.93	113.30	1.5309
IC C218	C216	*C217	H17R	1.5309	113.30	-121.70	108.75	1.1140
IC H17R	C216	*C217	H17S	1.1140	108.75	-116.65	108.73	1.1141
IC C216	C217	C218	H18R	1.5339	113.30	-59.98	110.46	1.1113
IC H18R	C217	*C218	H18S	1.1113	110.46	119.84	110.45	1.1114
IC H18R	C217	*C218	H18T	1.1113	110.46	-120.09	110.62	1.1112
IC C31	C32	C33	C34	1.5288	113.05	179.24	111.73	1.5343
IC C34	C32	*C33	H3X	1.5343	111.73	-120.85	109.62	1.1140
IC H3X	C32	*C33	H3Y	1.1140	109.62	-117.95	109.78	1.1144
IC C32	C33	C34	C35	1.5447	111.73	-176.74	112.91	1.5345
IC C35	C33	*C34	H4X	1.5345	112.91	-121.67	109.15	1.1134
IC H4X	C33	*C34	H4Y	1.1134	109.15	-117.32	108.98	1.1134
IC C33	C34	C35	C36	1.5343	112.91	178.63	112.42	1.5349
IC C36	C34	*C35	H5X	1.5349	112.42	-120.99	108.94	1.1133
IC H5X	C34	*C35	H5Y	1.1133	108.94	-117.41	109.31	1.1131
IC C34	C35	C36	C37	1.5345	112.42	-176.73	112.80	1.5356
IC C37	C35	*C36	H6X	1.5356	112.80	-121.69	109.16	1.1130
IC H6X	C35	*C36	H6Y	1.1130	109.16	-117.32	108.94	1.1133
IC C35	C36	C37	C38	1.5349	112.80	178.92	112.27	1.5402
IC C38	C36	*C37	H7X	1.5402	112.27	-121.37	108.23	1.1139
IC H7X	C36	*C37	H7Y	1.1139	108.23	-117.01	109.05	1.1137
IC C36	C37	C38	C39	1.5356	112.27	-174.92	111.69	1.5099
IC C39	C37	*C38	H8X	1.5099	111.69	-124.14	107.77	1.1124
IC H8X	C37	*C38	H8Y	1.1124	107.77	-115.13	108.30	1.1128
IC C37	C38	C39	C310	1.5349	112.80	178.92	112.27	1.5402

IC C310	C38	*C39	H9X	1.5402	112.27	-121.37	108.23	1.1139
IC H9X	C38	*C39	H9Y	1.1139	108.23	-117.01	109.05	1.1137
IC C38	C39	C310	C311	1.5356	112.27	-174.92	111.69	1.5099
IC C311	C39	*C310	H10X	1.5099	111.69	-124.14	107.77	1.1124
IC H10X	C39	*C310	H10Y	1.1124	107.77	-115.13	108.30	1.1128
IC C39	C310	C311	C312	1.5402	111.69	-121.39	127.35	1.3470
IC C312	C310	*C311	H11X	1.3470	127.35	179.11	114.24	1.1012
IC C310	C311	C312	C313	1.5099	127.35	-0.69	127.25	1.5096
IC C313	C311	*C312	H12X	1.5096	127.25	179.82	118.43	1.1012
IC C311	C312	C313	C314	1.3470	127.25	106.03	111.65	1.5393
IC C314	C312	*C313	H13X	1.5393	111.65	-121.49	112.10	1.1123
IC H13X	C312	*C313	H13Y	1.1123	112.10	-117.95	109.83	1.1127
IC C312	C313	C314	C315	1.5096	111.65	179.63	112.41	1.5355
IC C315	C313	*C314	H14X	1.5355	112.41	-121.09	109.75	1.1135
IC H14X	C313	*C314	H14Y	1.1135	109.75	-118.07	109.46	1.1143
IC C313	C314	C315	C316	1.5347	112.66	-179.12	112.61	1.5348
IC C316	C314	*C315	H15X	1.5348	112.61	-121.34	109.09	1.1132
IC H15X	C314	*C315	H15Y	1.1132	109.09	-117.41	109.09	1.1132
IC C314	C315	C316	C317	1.5347	112.61	179.83	112.71	1.5340
IC C317	C315	*C316	H16X	1.5340	112.71	-121.28	109.10	1.1132
IC H16X	C315	*C316	H16Y	1.1132	109.10	-117.35	109.13	1.1133
IC C315	C316	C317	C318	1.5348	112.71	-179.67	113.30	1.5309
IC C318	C316	*C317	H17X	1.5309	113.30	-121.68	108.77	1.1141
IC H17X	C316	*C317	H17Y	1.1141	108.77	-116.68	108.76	1.1141
IC C316	C317	C318	H18X	1.5340	113.30	-59.94	110.46	1.1113
IC H18X	C317	*C318	H18Y	1.1113	110.46	119.86	110.45	1.1113
IC H18Y	C317	*C318	H18Z	1.1113	110.46	-120.06	110.61	1.1112

RESI VSPG -1.00 ! 1-Vaccinyl 2-stereoyl-D-glycero-1-phosphatidylglycerol

```

!
! R1 - CH2
!   |
! R2 - CH
!   |
!   CH2 - PO4 - CH2 - CH(OH) - CH2OH
!
! Polar Head and glycerol backbone
!!Derived from Mackerell top_all36_lipid.rf
!! by Stuart Rose 9/10/2013

```

!!RESI DOPG -1.00 ! 2,3-dioleoyl-D-glycero-1-phosphatidylglycerol

```

!!
!! R1 - CH2
!!   |
!! R2 - CH
!!   |
!!   CH2 - PO4 - CH2 - CH(OH) - CH2OH
!!
!! Polar Head and glycerol backbone
GROUP !
ATOM C13 CTL2 0.05 !
ATOM H13A HAL2 0.09 ! H13A
ATOM H13B HAL2 0.09 ! |
ATOM OC3 OHL -0.65 ! |
ATOM HO3 HOL 0.42 ! H13B--C13---OC3--HO3
GROUP ! |
ATOM C12 CTL1 0.14 ! |
ATOM H12A HAL1 0.09 ! |
ATOM OC2 OHL -0.65 ! H12A--C12---OC2--HO2
ATOM HO2 HOL 0.42 ! |
GROUP ! | alpha5
ATOM C11 CTL2 -0.08 ! |
ATOM H11A HAL2 0.09 ! H11A--C11---H11B
ATOM H11B HAL2 0.09 ! | alpha4

```

ATOM P	PL	1.50 !	(-) O13 O12		
ATOM O13	O2L	-0.78 !	\ /	alpha3	
ATOM O14	O2L	-0.78 !	P (+)		
ATOM O12	OSLP	-0.57 !	/ \	alpha2	
ATOM O11	OSLP	-0.57 !	(-) O14 O11		
ATOM C1	CTL2	-0.08 !		alpha1	
ATOM HA	HAL2	0.09 !	HA---C1---HB		
ATOM HB	HAL2	0.09 !		theta1	
GROUP		!			
ATOM C2	CTL1	0.17 !	HS---C2-----		
ATOM HS	HAL1	0.09 !		beta1	
ATOM O21	OSL	-0.49 !	O22 O21	theta3	
ATOM C21	CL	0.90 !	\ \ /	beta2	
ATOM O22	OBL	-0.63 !	C21		
ATOM C22	CTL2	-0.22 !		beta3	
ATOM H2R	HAL2	0.09 !	H2R---C22---H2S		
ATOM H2S	HAL2	0.09 !			
GROUP		!		beta4	
ATOM C3	CTL2	0.08 !			
ATOM HX	HAL2	0.09 !		HX---C3---HY	
ATOM HY	HAL2	0.09 !			gamma1
ATOM O31	OSL	-0.49 !		O32 O31	
ATOM C31	CL	0.90 !		\ \ /	gamma2
ATOM O32	OBL	-0.63 !		C31	
ATOM C32	CTL2	-0.22 !			gamma3
ATOM H2X	HAL2	0.09 !		H2X---C32---H2Y	
ATOM H2Y	HAL2	0.09 !			gamma4
GROUP		!			
ATOM C23	CTL2	-0.18 !			
ATOM H3R	HAL2	0.09 !	H3R ---C23---H3S		
ATOM H3S	HAL2	0.09 !			
GROUP		!			
ATOM C24	CTL2	-0.18 !			
ATOM H4R	HAL2	0.09 !	H4R ---C24---H4S		
ATOM H4S	HAL2	0.09 !			
GROUP		!			
ATOM C25	CTL2	-0.18 !			
ATOM H5R	HAL2	0.09 !	H5R ---C25---H5S		
ATOM H5S	HAL2	0.09 !			
GROUP		!			
ATOM C26	CTL2	-0.18 !			
ATOM H6R	HAL2	0.09 !	H6R ---C26---H6S		
ATOM H6S	HAL2	0.09 !			
GROUP		!			
ATOM C27	CTL2	-0.18 !			
ATOM H7R	HAL2	0.09 !	H7R ---C27---H7S		
ATOM H7S	HAL2	0.09 !			
GROUP		!			
ATOM C28	CTL2	-0.18 !			
ATOM H8R	HAL2	0.09 !	H8R ---C28---H8S		
ATOM H8S	HAL2	0.09 !			
GROUP		!			
ATOM C29	CTL2	-0.18 !			
ATOM H9R	HAL2	0.09 !	H9R ---C29---H9S		
ATOM H9S	HAL2	0.09 !			
GROUP		!			
ATOM C210	CTL2	-0.18 !			
ATOM H10R	HAL2	0.09 !	H10R---C210--H10S		
ATOM H10S	HAL2	0.09 !			
GROUP		!			
ATOM C211	CEL1	-0.15 !			
ATOM H11R	HEL1	0.15 !	H11R---C211		
GROUP		!	(CIS)		
ATOM C212	CEL1	-0.15 !			

ATOM H12R	HEL1	0.15	!	H12R---C212		
GROUP			!			
ATOM C213	CTL2	-0.18	!			
ATOM H13R	HAL2	0.09	!	H13R---C213--H13S		
ATOM H13S	HAL2	0.09	!			
GROUP			!			
ATOM C214	CTL2	-0.18	!			
ATOM H14R	HAL2	0.09	!	H14R---C214--H14S		
ATOM H14S	HAL2	0.09	!			
GROUP			!			
ATOM C215	CTL2	-0.18	!			
ATOM H15R	HAL2	0.09	!	H15R---C215--H15S		
ATOM H15S	HAL2	0.09	!			
GROUP			!			
ATOM C216	CTL2	-0.18	!			
ATOM H16R	HAL2	0.09	!	H16R---C216--H16S		
ATOM H16S	HAL2	0.09	!			
GROUP			!			
ATOM C217	CTL2	-0.18	!			
ATOM H17R	HAL2	0.09	!	H17R---C217--H17S		
ATOM H17S	HAL2	0.09	!			
GROUP			!			
ATOM C218	CTL3	-0.27	!			
ATOM H18R	HAL3	0.09	!	H18R---C218--H18S		
ATOM H18S	HAL3	0.09	!			
ATOM H18T	HAL3	0.09	!	H18T		
GROUP			!			
ATOM C33	CTL2	-0.18	!			
ATOM H3X	HAL2	0.09	!		H3X ---C33---H3Y	
ATOM H3Y	HAL2	0.09	!			
GROUP			!			
ATOM C34	CTL2	-0.18	!			
ATOM H4X	HAL2	0.09	!		H4X ---C34---H4Y	
ATOM H4Y	HAL2	0.09	!			
GROUP			!			
ATOM C35	CTL2	-0.18	!			
ATOM H5X	HAL2	0.09	!		H5X ---C35---H5Y	
ATOM H5Y	HAL2	0.09	!			
GROUP			!			
ATOM C36	CTL2	-0.18	!			
ATOM H6X	HAL2	0.09	!		H6X ---C36---H6Y	
ATOM H6Y	HAL2	0.09	!			
GROUP			!			
ATOM C37	CTL2	-0.18	!			
ATOM H7X	HAL2	0.09	!		H7X ---C37---H7Y	
ATOM H7Y	HAL2	0.09	!			
GROUP			!			
ATOM C38	CTL2	-0.18	!			
ATOM H8X	HAL2	0.09	!		H8X ---C38---H8Y	
ATOM H8Y	HAL2	0.09	!			
GROUP			!			
ATOM C39	CTL2	-0.18	!			
ATOM H9X	HAL2	0.09	!		H9X ---C39---H9Y	
ATOM H9Y	HAL2	0.09	!			
GROUP			!			
ATOM C310	CTL2	-0.18	!			
ATOM H10X	HAL2	0.09	!		H10X---C310--H10Y	
ATOM H10Y	HAL2	0.09	!			
GROUP			!			
ATOM C311	CTL2	-0.18	!			
ATOM H11X	HAL2	0.09	!		H11X---C311--H11Y	
ATOM H11Y	HAL2	0.09	!			
GROUP			!			
ATOM C312	CTL2	-0.18	!			

ATOM H12X HAL2	0.09 !	H12X---C312--H12Y
ATOM H12Y HAL2	0.09 !	
GROUP	!	
ATOM C313 CTL2	-0.18 !	
ATOM H13X HAL2	0.09 !	H13X---C313--H13Y
ATOM H13Y HAL2	0.09 !	
GROUP	!	
ATOM C314 CTL2	-0.18 !	
ATOM H14X HAL2	0.09 !	H14X---C314--H14Y
ATOM H14Y HAL2	0.09 !	
GROUP	!	
ATOM C315 CTL2	-0.18 !	
ATOM H15X HAL2	0.09 !	H15X---C315--H15Y
ATOM H15Y HAL2	0.09 !	
GROUP	!	
ATOM C316 CTL2	-0.18 !	
ATOM H16X HAL2	0.09 !	H16X---C316--H16Y
ATOM H16Y HAL2	0.09 !	
GROUP	!	
ATOM C317 CTL2	-0.18 !	
ATOM H17X HAL2	0.09 !	H17X---C317--H17Y
ATOM H17Y HAL2	0.09 !	
GROUP	!	
ATOM C318 CTL3	-0.27 !	
ATOM H18X HAL3	0.09 !	H18X---C318--H18Y
ATOM H18Y HAL3	0.09 !	
ATOM H18Z HAL3	0.09 !	H18Z

! Polar Head

BOND HO3 OC3	OC3 C13	C13 H13A	C13 H13B	C13 C12
BOND HO2 OC2	OC2 C12	C12 H12A	C12 C11	
BOND C11 H11A	C11 H11B	C11 O12	O11 C1	
BOND O12 P	P O11	P O13	P O14	

! Glycerol Backbone

BOND C1 HA	C1 HB	C1 C2
BOND C2 HS	C2 C3	C2 O21
BOND C3 HX	C3 HY	C3 O31

! Chain from C2

BOND O21 C21		
BOND C21 C22		
DOUBLE C21 O22		
BOND C22 H2R	C22 H2S	C22 C23
BOND C23 H3R	C23 H3S	C23 C24
BOND C24 H4R	C24 H4S	C24 C25
BOND C25 H5R	C25 H5S	C25 C26
BOND C26 H6R	C26 H6S	C26 C27
BOND C27 H7R	C27 H7S	C27 C28
BOND C28 H8R	C28 H8S	C28 C29
BOND C29 H9R	C29 H9S	C29 C210
BOND C210 H10R	C210 H10S	C210 C211
BOND C211 H11R		
DOUBLE C211 C212		
BOND C212 H12R	C212 C213	
BOND C213 H13R	C213 H13S	C213 C214
BOND C214 H14R	C214 H14S	C214 C215
BOND C215 H15R	C215 H15S	C215 C216
BOND C216 H16R	C216 H16S	C216 C217
BOND C217 H17R	C217 H17S	C217 C218
BOND C218 H18R	C218 H18S	C218 H18T

! Chain From C3

BOND O31 C31		
BOND C31 C32		
DOUBLE C31 O32		
BOND C32 H2X	C32 H2Y	C32 C33



BOND	C33	H3X	C33	H3Y	C33	C34
BOND	C34	H4X	C34	H4Y	C34	C35
BOND	C35	H5X	C35	H5Y	C35	C36
BOND	C36	H6X	C36	H6Y	C36	C37
BOND	C37	H7X	C37	H7Y	C37	C38
BOND	C38	H8X	C38	H8Y	C38	C39
BOND	C39	H9X	C39	H9Y	C39	C310
BOND	C310	H10X	C310	H10Y	C310	C311
BOND	C311	H11X	C311	H11Y	C311	C312
BOND	C312	H12X	C312	H12Y	C312	C313
BOND	C313	H13X	C313	H13Y	C313	C314
BOND	C314	H14X	C314	H14Y	C314	C315
BOND	C315	H15X	C315	H15Y	C315	C316
BOND	C316	H16X	C316	H16Y	C316	C317
BOND	C317	H17X	C317	H17Y	C317	C318
BOND	C318	H18X	C318	H18Y	C318	H18Z

IMPR C21 O21 C22 O22 C31 O31 C32 O32

IC	C13	C12	C11	O12	1.5583	113.89	93.01	113.50	1.4295
IC	OC3	C13	C12	C11	1.4375	112.31	69.20	113.89	1.5573
IC	OC3	C12	*C13	H13A	1.4375	112.31	119.90	108.06	1.1118
IC	OC3	C12	*C13	H13B	1.4375	112.31	-123.06	109.89	1.1097
IC	C12	C13	OC3	HO3	1.5583	112.31	-141.84	106.96	0.9777
IC	C11	C13	*C12	OC2	1.5573	113.89	-121.65	107.64	1.4259
IC	OC2	C13	*C12	H12A	1.4259	107.64	-117.84	109.30	1.1131
IC	C13	C12	OC2	HO2	1.5583	107.64	38.09	100.52	0.9671
IC	O12	C12	*C11	H11A	1.4295	113.50	-126.35	109.70	1.1125
IC	H11A	C12	*C11	H11B	1.1125	109.70	-115.65	107.71	1.1131
IC	C12	C11	O12	P	1.5573	113.50	-72.69	124.80	1.5783
IC	C11	O12	P	O11	1.4295	124.80	-30.02	102.66	1.5825
IC	O11	O12	*P	O13	1.5825	102.66	113.88	109.00	1.4783
IC	O11	O12	*P	O14	1.5825	102.66	-115.27	109.77	1.4781
IC	O12	P	O11	C1	1.5783	102.66	-80.21	120.83	1.4246
IC	P	O11	C1	C2	1.5825	120.83	177.68	108.67	1.5488
IC	C2	O11	*C1	HA	1.5488	108.67	-120.91	111.25	1.1145
IC	HA	O11	*C1	HB	1.1145	111.25	-120.47	110.06	1.1152
IC	O11	C1	C2	C3	1.4246	108.67	45.70	110.42	1.5580
IC	C3	C1	*C2	O21	1.5580	110.42	120.25	110.13	1.4420
IC	C3	C1	*C2	HS	1.5580	110.42	-116.94	108.10	1.1164
IC	C1	C2	O21	C21	1.5488	110.13	74.82	114.08	1.3218
IC	C2	O21	C21	C22	1.4420	114.08	-171.58	108.87	1.5297
IC	C22	O21	*C21	O22	1.5297	108.87	-179.18	126.27	1.2166
IC	O21	C21	C22	C23	1.3218	108.87	167.60	112.03	1.5460
IC	C23	C21	*C22	H2R	1.5460	112.03	-121.40	108.25	1.1088
IC	H2R	C21	*C22	H2S	1.1088	108.25	-117.05	107.34	1.1068
IC	C1	C2	C3	O31	1.5488	110.42	-172.10	112.95	1.4472
IC	O31	C2	*C3	HX	1.4472	112.95	-119.90	106.80	1.1123
IC	HX	C2	*C3	HY	1.1123	106.80	-114.66	109.95	1.1147
IC	C2	C3	O31	C31	1.5580	112.95	84.38	114.39	1.3267
IC	C3	O31	C31	C32	1.4472	114.39	176.82	109.50	1.5275
IC	C32	O31	*C31	O32	1.5275	109.50	-179.44	126.11	1.2173
IC	O31	C31	C32	C33	1.3267	109.50	-66.76	112.63	1.5535
IC	C33	C31	*C32	H2X	1.5535	112.63	121.43	107.50	1.1085
IC	H2X	C31	*C32	H2Y	1.1085	107.50	116.64	107.32	1.1097
IC	C21	C22	C23	C24	1.5289	112.21	175.76	112.39	1.5338
IC	C24	C22	*C23	H3R	1.5338	112.39	-120.69	109.57	1.1147
IC	H3R	C22	*C23	H3S	1.1147	109.57	-117.65	109.64	1.1142
IC	C22	C23	C24	C25	1.5449	112.39	-179.39	112.35	1.5346
IC	C25	C23	*C24	H4R	1.5346	112.35	-121.52	109.41	1.1131
IC	H4R	C23	*C24	H4S	1.1131	109.41	-117.57	108.97	1.1134
IC	C23	C24	C25	C26	1.5338	112.35	176.31	112.80	1.5344
IC	C26	C24	*C25	H5R	1.5344	112.80	-121.01	108.95	1.1135
IC	H5R	C24	*C25	H5S	1.1135	108.95	-117.24	109.16	1.1132

IC C24	C25	C26	C27	1.5346	112.80	-179.44	112.48	1.5356	
IC C27	C25	*C26	H6R	1.5356	112.48	-121.49	109.32	1.1129	
IC H6R	C25	*C26	H6S	1.1129	109.32	-117.47	108.94	1.1132	
IC C25	C26	C27	C28	1.5344	112.48	176.92	112.46	1.5398	
IC C28	C26	*C27	H7R	1.5398	112.46	-121.38	108.40	1.1139	
IC H7R	C26	*C27	H7S	1.1139	108.40	-116.93	108.77	1.1139	
IC C26	C27	C28	C29	1.5356	112.46	-178.53	111.43	1.5097	
IC C29	C27	*C28	H8R	1.5097	111.43	-123.58	107.80	1.1132	
IC H8R	C27	*C28	H8S	1.1132	107.80	-115.43	108.37	1.1128	
IC C27	C28	C29	C210	1.5344	112.48	176.92	112.46	1.5398	
IC C210	C28	*C29	H9R	1.5398	112.46	-121.38	108.40	1.1139	
IC H9R	C28	*C29	H9S		1.1139	108.40	-116.93	108.77	1.1139
IC C28	C29	C210	C211	1.5356	112.46	-178.53	111.43	1.5097	
IC C211	C29	*C210	H10R	1.5097	111.43	-123.58	107.80	1.1132	
IC H10R	C29	*C210	H9S		1.1132	107.80	-115.43	108.37	1.1128
IC C29	C210	C211	C212	1.5398	111.43	-126.96	126.62	1.3465	
IC C212	C210	*C211	H11R	1.3465	126.62	178.41	114.65	1.1012	
IC C210	C211	C212	C213	1.5097	126.62	-1.69	126.32	1.5088	
IC C213	C211	*C212	H12R	1.5088	126.32	-179.55	118.79	1.1012	
IC C211	C212	C213	C214	1.5392	112.29	179.81	112.68	1.5345	
IC C214	C212	*C213	H13R	1.5345	112.68	-121.26	109.04	1.1132	
IC H13R	C212	*C213	H13S	1.1132	109.04	-117.39	109.10	1.1131	
IC C212	C213	C214	C215	1.5354	112.68	179.80	112.59	1.5347	
IC C215	C213	*C214	H14R	1.5347	112.59	-121.29	109.09	1.1132	
IC H14R	C213	*C214	H14S	1.1132	109.09	-117.37	109.11	1.1133	
IC C213	C214	C215	C216	1.5345	112.59	-179.58	112.63	1.5347	
IC C216	C214	*C215	H15R	1.5347	112.63	-121.36	109.09	1.1132	
IC H15R	C214	*C215	H15S	1.1132	109.09	-117.38	109.07	1.1132	
IC C214	C215	C216	C217	1.5347	112.63	179.65	112.69	1.5339	
IC C217	C215	*C216	H16R	1.5339	112.69	-121.27	109.11	1.1132	
IC H16R	C215	*C216	H16S	1.1132	109.11	-117.36	109.14	1.1132	
IC C215	C216	C217	C218	1.5347	112.69	-179.93	113.30	1.5309	
IC C218	C216	*C217	H17R	1.5309	113.30	-121.70	108.75	1.1140	
IC H17R	C216	*C217	H17S	1.1140	108.75	-116.65	108.73	1.1141	
IC C216	C217	C218	H18R	1.5339	113.30	-59.98	110.46	1.1113	
IC H18R	C217	*C218	H18S	1.1113	110.46	119.84	110.45	1.1114	
IC H18R	C217	*C218	H18T	1.1113	110.46	-120.09	110.62	1.1112	
IC C31	C32	C33	C34	1.5288	113.05	179.24	111.73	1.5343	
IC C34	C32	*C33	H3X	1.5343	111.73	-120.85	109.62	1.1140	
IC H3X	C32	*C33	H3Y	1.1140	109.62	-117.95	109.78	1.1144	
IC C32	C33	C34	C35	1.5447	111.73	-176.74	112.91	1.5345	
IC C35	C33	*C34	H4X	1.5345	112.91	-121.67	109.15	1.1134	
IC H4X	C33	*C34	H4Y	1.1134	109.15	-117.32	108.98	1.1134	
IC C33	C34	C35	C36	1.5343	112.91	178.63	112.42	1.5349	
IC C36	C34	*C35	H5X	1.5349	112.42	-120.99	108.94	1.1133	
IC H5X	C34	*C35	H5Y	1.1133	108.94	-117.41	109.31	1.1131	
IC C34	C35	C36	C37	1.5345	112.42	-176.73	112.80	1.5356	
IC C37	C35	*C36	H6X	1.5356	112.80	-121.69	109.16	1.1130	
IC H6X	C35	*C36	H6Y	1.1130	109.16	-117.32	108.94	1.1133	
IC C35	C36	C37	C38	1.5349	112.80	178.92	112.27	1.5402	
IC C38	C36	*C37	H7X	1.5402	112.27	-121.37	108.23	1.1139	
IC H7X	C36	*C37	H7Y	1.1139	108.23	-117.01	109.05	1.1137	
IC C36	C37	C38	C39	1.5356	112.27	-174.92	111.69	1.5099	
IC C39	C37	*C38	H8X	1.5099	111.69	-124.14	107.77	1.1124	
IC H8X	C37	*C38	H8Y	1.1124	107.77	-115.13	108.30	1.1128	
IC C37	C38	C39	C310	1.5349	112.80	178.92	112.27	1.5402	
IC C310	C38	*C39	H9X	1.5402	112.27	-121.37	108.23	1.1139	
IC H9X	C38	*C39	H9Y	1.1139	108.23	-117.01	109.05	1.1137	
IC C38	C39	C310	C311	1.5356	112.27	-174.92	111.69	1.5099	
IC C311	C39	*C310	H10X	1.5099	111.69	-124.14	107.77	1.1124	
IC H10X	C39	*C310	H10Y	1.1124	107.77	-115.13	108.30	1.1128	
IC C39	C310	C311	C312	1.5402	111.69	-121.39	127.35	1.3470	
IC C312	C310	*C311	H11X	1.3470	127.35	179.11	114.24	1.1012	
IC C310	C311	C312	C313	1.5099	127.35	-0.69	127.25	1.5096	

IC C313	C311	*C312	H12X	1.5096	127.25	179.82	118.43	1.1012
IC C311	C312	C313	C314	1.3470	127.25	106.03	111.65	1.5393
IC C314	C312	*C313	H13X	1.5393	111.65	-121.49	112.10	1.1123
IC H13X	C312	*C313	H13Y	1.1123	112.10	-117.95	109.83	1.1127
IC C312	C313	C314	C315	1.5096	111.65	179.63	112.41	1.5355
IC C315	C313	*C314	H14X	1.5355	112.41	-121.09	109.75	1.1135
IC H14X	C313	*C314	H14Y	1.1135	109.75	-118.07	109.46	1.1143
IC C313	C314	C315	C316	1.5347	112.66	-179.12	112.61	1.5348
IC C316	C314	*C315	H15X	1.5348	112.61	-121.34	109.09	1.1132
IC H15X	C314	*C315	H15Y	1.1132	109.09	-117.41	109.09	1.1132
IC C314	C315	C316	C317	1.5347	112.61	179.83	112.71	1.5340
IC C317	C315	*C316	H16X	1.5340	112.71	-121.28	109.10	1.1132
IC H16X	C315	*C316	H16Y	1.1132	109.10	-117.35	109.13	1.1133
IC C315	C316	C317	C318	1.5348	112.71	-179.67	113.30	1.5309
IC C318	C316	*C317	H17X	1.5309	113.30	-121.68	108.77	1.1141
IC H17X	C316	*C317	H17Y	1.1141	108.77	-116.68	108.76	1.1141
IC C316	C317	C318	H18X	1.5340	113.30	-59.94	110.46	1.1113
IC H18X	C317	*C318	H18Y	1.1113	110.46	119.86	110.45	1.1113
IC H18X	C317	*C318	H18Z	1.1113	110.46	-120.06	110.61	1.1112

!PEs

```
RESI DVPE          0.00 ! 2,3-divacenoyl-D-glycero-1-phosphatidylethanolamine
!
! R1 - CH2
! |
! (angles and atom names from Sundaralingam)
! R2 - CH
! |
! CH2 - PO4 - CH2 - CH2 - NH3
!
! Polar Head and glycerol backbone
```

!!Derived from Mackerell top\_all36\_lipid.rf

!! by Stuart Rose 9/10/2013

```
!!RESI DOPE          0.00 ! 2,3-dioleoyl-D-glycero-1-phosphatidylethanolamine
!!
!! R1 - CH2
!! |
!! (angles and atom names from Sundaralingam)
!! R2 - CH
!! |
!! CH2 - PO4 - CH2 - CH2 - NH3
!!
!! Polar Head and glycerol backbone
```

```
GROUP              !
ATOM N      NH3L   -0.30 !           HN2
ATOM HN1    HCL    0.33 !           |
ATOM HN2    HCL    0.33 ! (+) HN1---N---HN3
ATOM HN3    HCL    0.33 !           |
ATOM C12    CTL2   0.13 !           |
ATOM H12A   HAL2   0.09 !           H12A--C12---H12B
ATOM H12B   HAL2   0.09 !           |
GROUP              !           |           alpha5
ATOM C11    CTL2  -0.08 !           |
ATOM H11A   HAL2   0.09 !           H11A--C11---H11B
ATOM H11B   HAL2   0.09 !           |           alpha4
ATOM P      PL     1.50 ! (-) O13 O12
ATOM O13    O2L   -0.78 !           \ /           alpha3
ATOM O14    O2L   -0.78 !           P (+)
ATOM O11    OSLP  -0.57 !           / \           alpha2
ATOM O12    OSLP  -0.57 ! (-) O14 O11
ATOM C1     CTL2  -0.08 !           |           alpha1
```

ATOM HA	HAL2	0.09 !	HA---C1---HB		
ATOM HB	HAL2	0.09 !		theta1	
GROUP		!			
ATOM C2	CTL1	0.17 !	HS---C2- - - - -		
ATOM HS	HAL1	0.09 !		beta1	
ATOM O21	OSL	-0.49 !	O22 O21	theta3	
ATOM C21	CL	0.90 !	\\ /	beta2	
ATOM O22	OBL	-0.63 !	C21		
ATOM C22	CTL2	-0.22 !		beta3	
ATOM H2R	HAL2	0.09 !	H2R---C22---H2S		
ATOM H2S	HAL2	0.09 !			
GROUP		!		beta4	
ATOM C3	CTL2	0.08 !			
ATOM HX	HAL2	0.09 !		HX---C3---HY	
ATOM HY	HAL2	0.09 !			gamma1
ATOM O31	OSL	-0.49 !		O32 O31	
ATOM C31	CL	0.90 !		\\ /	gamma2
ATOM O32	OBL	-0.63 !		C31	
ATOM C32	CTL2	-0.22 !			gamma3
ATOM H2X	HAL2	0.09 !		H2X---C32---H2Y	
ATOM H2Y	HAL2	0.09 !			
GROUP		!			gamma4
ATOM C23	CTL2	-0.18 !			
ATOM H3R	HAL2	0.09 !	H3R ---C23---H3S		
ATOM H3S	HAL2	0.09 !			
GROUP		!			
ATOM C24	CTL2	-0.18 !			
ATOM H4R	HAL2	0.09 !	H4R ---C24---H4S		
ATOM H4S	HAL2	0.09 !			
GROUP		!			
ATOM C25	CTL2	-0.18 !			
ATOM H5R	HAL2	0.09 !	H5R ---C25---H5S		
ATOM H5S	HAL2	0.09 !			
GROUP		!			
ATOM C26	CTL2	-0.18 !			
ATOM H6R	HAL2	0.09 !	H6R ---C26---H6S		
ATOM H6S	HAL2	0.09 !			
GROUP		!			
ATOM C27	CTL2	-0.18 !			
ATOM H7R	HAL2	0.09 !	H7R ---C27---H7S		
ATOM H7S	HAL2	0.09 !			
GROUP		!			
ATOM C28	CTL2	-0.18 !			
ATOM H8R	HAL2	0.09 !	H8R ---C28---H8S		
ATOM H8S	HAL2	0.09 !			
GROUP		!			
ATOM C29	CTL2	-0.18 !			
ATOM H9R	HAL2	0.09 !	H9R ---C29---H9S		
ATOM H9S	HAL2	0.09 !			
GROUP		!			
ATOM C210	CTL2	-0.18 !			
ATOM H10R	HAL2	0.09 !	H10R---C210--H10S		
ATOM H10S	HAL2	0.09 !			
GROUP		!			
ATOM C211	CEL1	-0.15 !			
ATOM H11R	HEL1	0.15 !	H11R---C211		
GROUP		!		(CIS)	
ATOM C212	CEL1	-0.15 !			
ATOM H12R	HEL1	0.15 !	H12R---C212		
GROUP		!			
ATOM C213	CTL2	-0.18 !			
ATOM H13R	HAL2	0.09 !	H13R---C213--H13S		
ATOM H13S	HAL2	0.09 !			
GROUP		!			

ATOM C214	CTL2	-0.18	!		
ATOM H14R	HAL2	0.09	!	H14R---C214--H14S	
ATOM H14S	HAL2	0.09	!		
GROUP			!		
ATOM C215	CTL2	-0.18	!		
ATOM H15R	HAL2	0.09	!	H15R---C215--H15S	
ATOM H15S	HAL2	0.09	!		
GROUP			!		
ATOM C216	CTL2	-0.18	!		
ATOM H16R	HAL2	0.09	!	H16R---C216--H16S	
ATOM H16S	HAL2	0.09	!		
GROUP			!		
ATOM C217	CTL2	-0.18	!		
ATOM H17R	HAL2	0.09	!	H17R---C217--H17S	
ATOM H17S	HAL2	0.09	!		
GROUP			!		
ATOM C218	CTL3	-0.27	!		
ATOM H18R	HAL3	0.09	!	H18R---C218--H18S	
ATOM H18S	HAL3	0.09	!		
ATOM H18T	HAL3	0.09	!	H18T	
GROUP			!		
ATOM C33	CTL2	-0.18	!		H3X ---C33---H3Y
ATOM H3X	HAL2	0.09	!		
ATOM H3Y	HAL2	0.09	!		
GROUP			!		
ATOM C34	CTL2	-0.18	!		H4X ---C34---H4Y
ATOM H4X	HAL2	0.09	!		
ATOM H4Y	HAL2	0.09	!		
GROUP			!		
ATOM C35	CTL2	-0.18	!		H5X ---C35---H5Y
ATOM H5X	HAL2	0.09	!		
ATOM H5Y	HAL2	0.09	!		
GROUP			!		
ATOM C36	CTL2	-0.18	!		H6X ---C36---H6Y
ATOM H6X	HAL2	0.09	!		
ATOM H6Y	HAL2	0.09	!		
GROUP			!		
ATOM C37	CTL2	-0.18	!		H7X ---C37---H7Y
ATOM H7X	HAL2	0.09	!		
ATOM H7Y	HAL2	0.09	!		
GROUP			!		
ATOM C38	CTL2	-0.18	!		H8X ---C38---H8Y
ATOM H8X	HAL2	0.09	!		
ATOM H8Y	HAL2	0.09	!		
GROUP			!		
ATOM C39	CTL2	-0.18	!		H9X ---C39---H9Y
ATOM H9X	HAL2	0.09	!		
ATOM H9Y	HAL2	0.09	!		
GROUP			!		
ATOM C310	CTL2	-0.18	!		H10X---C310---H10Y
ATOM H10X	HAL2	0.09	!		
ATOM H10Y	HAL2	0.09	!		
GROUP			!		
ATOM C311	CEL1	-0.15	!		H11X---C311
ATOM H11X	HEL1	0.15	!		(CIS)
GROUP			!		
ATOM C312	CEL1	-0.15	!		H12X---C312
ATOM H12X	HEL1	0.15	!		
GROUP			!		
ATOM C313	CTL2	-0.18	!		H13X---C313--H13Y
ATOM H13X	HAL2	0.09	!		
ATOM H13Y	HAL2	0.09	!		
GROUP			!		
ATOM C314	CTL2	-0.18	!		

ATOM H14X	HAL2	0.09	!	H14X---	C314--	H14Y
ATOM H14Y	HAL2	0.09	!			
GROUP			!			
ATOM C315	CTL2	-0.18	!			
ATOM H15X	HAL2	0.09	!	H15X---	C315--	H15Y
ATOM H15Y	HAL2	0.09	!			
GROUP			!			
ATOM C316	CTL2	-0.18	!			
ATOM H16X	HAL2	0.09	!	H16X---	C316--	H16Y
ATOM H16Y	HAL2	0.09	!			
GROUP			!			
ATOM C317	CTL2	-0.18	!			
ATOM H17X	HAL2	0.09	!	H17X---	C317--	H17Y
ATOM H17Y	HAL2	0.09	!			
GROUP			!			
ATOM C318	CTL3	-0.27	!			
ATOM H18X	HAL3	0.09	!	H18X---	C318--	H18Y
ATOM H18Y	HAL3	0.09	!			
ATOM H18Z	HAL3	0.09	!			H18Z

! Polar Head

BOND N	HN1	N	HN2	N	HN3	N	C12
BOND C12	H12A	C12	H12B	C12	C11		
BOND C11	H11A	C11	H11B	C11	O12		
BOND O12	P	P	O11	P	O13	P	O14

! Glycerol Backbone

BOND C1	HA	C1	HB	C1	C2	C1	O11
BOND C2	HS	C2	C3	C2	O21		
BOND C3	HX	C3	HY	C3	O31		

! Chain from C2

BOND O21	C21						
BOND C21	C22						
DOUBLE C21	O22						
BOND C22	H2R	C22	H2S	C22	C23		
BOND C23	H3R	C23	H3S	C23	C24		
BOND C24	H4R	C24	H4S	C24	C25		
BOND C25	H5R	C25	H5S	C25	C26		
BOND C26	H6R	C26	H6S	C26	C27		
BOND C27	H7R	C27	H7S	C27	C28		
BOND C28	H8R	C28	H8S	C28	C29		
BOND C29	H9R	C29	H9S	C29	C210		
BOND C210	H10R	C210	H10S	C210	C211		
BOND C211	H11R						
DOUBLE C211	C212						
BOND C212	H12R	C212	C213				
BOND C213	H13R	C213	H13S	C213	C214		
BOND C214	H14R	C214	H14S	C214	C215		
BOND C215	H15R	C215	H15S	C215	C216		
BOND C216	H16R	C216	H16S	C216	C217		
BOND C217	H17R	C217	H17S	C217	C218		
BOND C218	H18R	C218	H18S	C218	H18T		

! Chain From C3

BOND O31	C31						
BOND C31	C32						
DOUBLE C31	O32						
BOND C32	H2X	C32	H2Y	C32	C33		
BOND C33	H3X	C33	H3Y	C33	C34		
BOND C34	H4X	C34	H4Y	C34	C35		
BOND C35	H5X	C35	H5Y	C35	C36		
BOND C36	H6X	C36	H6Y	C36	C37		
BOND C37	H7X	C37	H7Y	C37	C38		
BOND C38	H8X	C38	H8Y	C38	C39		
BOND C39	H9X	C39	H9Y	C39	C310		
BOND C310	H10X	C310	H10Y	C310	C311		

BOND	C311	H11X						
DOUBLE	C311	C312						
BOND	C312	H12X	C312	C313				
BOND	C313	H13X	C313	H13Y	C313	C314		
BOND	C314	H14X	C314	H14Y	C314	C315		
BOND	C315	H15X	C315	H15Y	C315	C316		
BOND	C316	H16X	C316	H16Y	C316	C317		
BOND	C317	H17X	C317	H17Y	C317	C318		
BOND	C318	H18X	C318	H18Y	C318	H18Z		

IMPR C21 O21 C22 O22 C31 O31 C32 O32

IC N	C12	C11	O12	1.5110	111.97	65.84	112.46	1.4308
IC HN1	C12	*N	HN2	1.0342	114.60	119.70	105.60	1.0654
IC HN1	C12	*N	HN3	1.0342	114.60	-127.78	110.56	1.0397
IC HN1	N	C12	C11	1.0342	114.60	-177.91	111.97	1.5465
IC C11	N	*C12	H12A	1.5465	111.97	-121.58	107.97	1.1086
IC H12A	N	*C12	H12B	1.1086	107.97	-118.25	107.67	1.1104
IC O12	C12	*C11	H11A	1.4308	112.46	-126.31	111.01	1.1167
IC H11A	C12	*C11	H11B	1.1167	111.01	-115.41	107.63	1.1146
IC C12	C11	O12	P	1.5465	112.46	-80.62	120.62	1.5839
IC C11	O12	P	O11	1.4308	120.62	-156.78	104.60	1.5751
IC O11	O12	*P	O13	1.5751	104.60	-117.47	103.31	1.4823
IC O11	O12	*P	O14	1.5751	104.60	120.67	107.16	1.4736
IC O12	P	O11	C1	1.5839	104.60	-58.82	120.34	1.4318
IC P	O11	C1	C2	1.5751	120.34	-92.48	111.72	1.5536
IC C2	O11	*C1	HA	1.5536	111.72	-119.08	108.93	1.1133
IC HA	O11	*C1	HB	1.1133	108.93	-117.83	112.18	1.1155
IC O11	C1	C2	C3	1.4318	111.72	162.49	110.59	1.5553
IC C3	C1	*C2	O21	1.5553	110.59	120.51	108.20	1.4410
IC C3	C1	*C2	HS	1.5553	110.59	-117.47	107.37	1.1169
IC C1	C2	O21	C21	1.5536	108.20	145.45	115.07	1.3229
IC C2	O21	C21	C22	1.4410	115.07	175.60	109.17	1.5330
IC C22	O21	*C21	O22	1.5330	109.17	179.92	126.38	1.2173
IC O21	C21	C22	C23	1.3229	109.17	-134.07	111.55	1.5472
IC C23	C21	*C22	H2R	1.5472	111.55	-119.81	106.70	1.1095
IC H2R	C21	*C22	H2S	1.1095	106.70	-117.59	109.58	1.1081
IC C1	C2	C3	O31	1.5536	110.59	178.88	111.62	1.4432
IC O31	C2	*C3	HX	1.4432	111.62	-121.40	107.66	1.1142
IC HX	C2	*C3	HY	1.1142	107.66	-116.77	107.26	1.1152
IC C2	C3	O31	C31	1.5553	111.62	174.54	113.52	1.3270
IC C3	O31	C31	C32	1.4432	113.52	178.76	109.19	1.5276
IC C32	O31	*C31	O32	1.5276	109.19	-179.68	125.26	1.2176
IC O31	C31	C32	C33	1.3270	109.19	-153.26	112.50	1.5449
IC C33	C31	*C32	H2X	1.5449	112.50	120.40	107.84	1.1092
IC H2X	C31	*C32	H2Y	1.1092	107.84	117.16	108.28	1.1081
IC C21	C22	C23	C24	1.5289	112.21	175.76	112.39	1.5338
IC C24	C22	*C23	H3R	1.5338	112.39	-120.69	109.57	1.1147
IC H3R	C22	*C23	H3S	1.1147	109.57	-117.65	109.64	1.1142
IC C22	C23	C24	C25	1.5449	112.39	-179.39	112.35	1.5346
IC C25	C23	*C24	H4R	1.5346	112.35	-121.52	109.41	1.1131
IC H4R	C23	*C24	H4S	1.1131	109.41	-117.57	108.97	1.1134
IC C23	C24	C25	C26	1.5338	112.35	176.31	112.80	1.5344
IC C26	C24	*C25	H5R	1.5344	112.80	-121.01	108.95	1.1135
IC H5R	C24	*C25	H5S	1.1135	108.95	-117.24	109.16	1.1132
IC C24	C25	C26	C27	1.5346	112.80	-179.44	112.48	1.5356
IC C27	C25	*C26	H6R	1.5356	112.48	-121.49	109.32	1.1129
IC H6R	C25	*C26	H6S	1.1129	109.32	-117.47	108.94	1.1132
IC C25	C26	C27	C28	1.5344	112.48	176.92	112.46	1.5398
IC C28	C26	*C27	H7R	1.5398	112.46	-121.38	108.40	1.1139
IC H7R	C26	*C27	H7S	1.1139	108.40	-116.93	108.77	1.1139
IC C26	C27	C28	C29	1.5346	112.80	-179.44	112.48	1.5356
IC C29	C27	*C28	H8R	1.5356	112.48	-121.49	109.32	1.1129
IC H8R	C27	*C28	H8S	1.1129	109.32	-117.47	108.94	1.1132

IC C27	C28	C29	C210	1.5344	112.48	176.92	112.46	1.5398
IC C210	C28	*C29	H9R	1.5398	112.46	-121.38	108.40	1.1139
IC H9R	C28	*C29	H9S	1.1139	108.40	-116.93	108.77	1.1139
IC C28	C29	C210	C211	1.5356	112.46	-178.53	111.43	1.5097
IC C211	C29	*C210	H10R	1.5097	111.43	-123.58	107.80	1.1132
IC H10R	C29	*C210	H10S	1.1132	107.80	-115.43	108.37	1.1128
IC C29	C210	C211	C212	1.5398	111.43	-126.96	126.62	1.3465
IC C212	C210	*C211	H11R	1.3465	126.62	178.41	114.65	1.1012
IC C210	C211	C212	C213	1.5097	126.62	-1.69	126.32	1.5088
IC C213	C211	*C212	H12R	1.5088	126.32	-179.55	118.79	1.1012
IC C211	C212	C213	C214	1.3465	126.32	93.02	112.15	1.5392
IC C214	C212	*C213	H13R	1.5392	112.15	-121.30	111.28	1.1133
IC H13R	C212	*C213	H13S	1.1133	111.28	-117.50	110.00	1.1126
IC C212	C213	C214	C215	1.5088	112.15	-178.81	112.29	1.5354
IC C215	C213	*C214	H14R	1.5354	112.29	-121.34	109.78	1.1133
IC H14R	C213	*C214	H14S	1.1133	109.78	-118.01	109.42	1.1144
IC C213	C214	C215	C216	1.5345	112.59	-179.58	112.63	1.5347
IC C216	C214	*C215	H15R	1.5347	112.63	-121.36	109.09	1.1132
IC H15R	C214	*C215	H15S	1.1132	109.09	-117.38	109.07	1.1132
IC C214	C215	C216	C217	1.5347	112.63	179.65	112.69	1.5339
IC C217	C215	*C216	H16R	1.5339	112.69	-121.27	109.11	1.1132
IC H16R	C215	*C216	H16S	1.1132	109.11	-117.36	109.14	1.1132
IC C215	C216	C217	C218	1.5347	112.69	-179.93	113.30	1.5309
IC C218	C216	*C217	H17R	1.5309	113.30	-121.70	108.75	1.1140
IC H17R	C216	*C217	H17S	1.1140	108.75	-116.65	108.73	1.1141
IC C216	C217	C218	H18R	1.5339	113.30	-59.98	110.46	1.1113
IC H18R	C217	*C218	H18S	1.1113	110.46	119.84	110.45	1.1114
IC H18R	C217	*C218	H18T	1.1113	110.46	-120.09	110.62	1.1112
IC C31	C32	C33	C34	1.5288	113.05	179.24	111.73	1.5343
IC C34	C32	*C33	H3X	1.5343	111.73	-120.85	109.62	1.1140
IC H3X	C32	*C33	H3Y	1.1140	109.62	-117.95	109.78	1.1144
IC C32	C33	C34	C35	1.5447	111.73	-176.74	112.91	1.5345
IC C35	C33	*C34	H4X	1.5345	112.91	-121.67	109.15	1.1134
IC H4X	C33	*C34	H4Y	1.1134	109.15	-117.32	108.98	1.1134
IC C33	C34	C35	C36	1.5343	112.91	178.63	112.42	1.5349
IC C36	C34	*C35	H5X	1.5349	112.42	-120.99	108.94	1.1133
IC H5X	C34	*C35	H5Y	1.1133	108.94	-117.41	109.31	1.1131
IC C34	C35	C36	C37	1.5345	112.42	-176.73	112.80	1.5356
IC C37	C35	*C36	H6X	1.5356	112.80	-121.69	109.16	1.1130
IC H6X	C35	*C36	H6Y	1.1130	109.16	-117.32	108.94	1.1133
IC C35	C36	C37	C38	1.5343	112.91	178.63	112.42	1.5349
IC C38	C36	*C37	H7X	1.5349	112.42	-120.99	108.94	1.1133
IC H7X	C36	*C37	H7Y	1.1133	108.94	-117.41	109.31	1.1131
IC C36	C37	C38	C39	1.5345	112.42	-176.73	112.80	1.5356
IC C39	C37	*C38	H8X	1.5356	112.80	-121.69	109.16	1.1130
IC H8X	C37	*C38	H8Y	1.1130	109.16	-117.32	108.94	1.1133
IC C37	C38	C39	C310	1.5349	112.80	178.92	112.27	1.5402
IC C310	C38	*C39	H9X	1.5402	112.27	-121.37	108.23	1.1139
IC H9X	C38	*C39	H9Y	1.1139	108.23	-117.01	109.05	1.1137
IC C38	C39	C310	C311	1.5356	112.27	-174.92	111.69	1.5099
IC C311	C39	*C310	H10X	1.5099	111.69	-124.14	107.77	1.1124
IC H10X	C39	*C310	H10Y	1.1124	107.77	-115.13	108.30	1.1128
IC C39	C310	C311	C312	1.5402	111.69	-121.39	127.35	1.3470
IC C312	C310	*C311	H11X	1.3470	127.35	179.11	114.24	1.1012
IC C310	C311	C312	C313	1.5099	127.35	0.00	127.25	1.5096
IC C313	C311	*C312	H12X	1.5096	127.25	179.82	118.43	1.1012
IC C311	C312	C313	C314	1.3470	127.25	106.03	111.65	1.5393
IC C314	C312	*C313	H13X	1.5393	111.65	-121.49	112.10	1.1123
IC H13X	C312	*C313	H13Y	1.1123	112.10	-117.95	109.83	1.1127
IC C312	C313	C314	C315	1.5096	111.65	179.63	112.41	1.5355
IC C315	C313	*C314	H14X	1.5355	112.41	-121.09	109.75	1.1135
IC H14X	C313	*C314	H14Y	1.1135	109.75	-118.07	109.46	1.1143
IC C313	C314	C315	C316	1.5347	112.66	-179.12	112.61	1.5348
IC C316	C314	*C315	H15X	1.5348	112.61	-121.34	109.09	1.1132



```

IC H15X  C314  *C315  H15Y      1.1132  109.09 -117.41  109.09  1.1132
IC C314  C315  C316   C317      1.5347  112.61  179.83  112.71  1.5340
IC C317  C315  *C316  H16X      1.5340  112.71 -121.28  109.10  1.1132
IC H16X  C315  *C316  H16Y      1.1132  109.10 -117.35  109.13  1.1133
IC C315  C316  C317   C318      1.5348  112.71 -179.67  113.30  1.5309
IC C318  C316  *C317  H17X      1.5309  113.30 -121.68  108.77  1.1141
IC H17X  C316  *C317  H17Y      1.1141  108.77 -116.68  108.76  1.1141
IC C316  C317  C318   H18X      1.5340  113.30 -59.94  110.46  1.1113
IC H18X  C317  *C318  H18Y      1.1113  110.46  119.86  110.45  1.1113
IC H18X  C317  *C318  H18Z      1.1113  110.46 -120.06  110.61  1.1112

```

!PEs

```

RESI VSPE      0.00 ! ? 2,3-vacenyl- steroeyl D-glycero-1-phosphatidylethanolamine
! VSPE stands for 18:0/18:1 configuration
!:: removed C311 - C312 double bond but did not do detailed rearrangement of IC
! R1 - CH2
!   |
!   (angles and atom names from Sundaralingam)
! R2 - CH
!   |
!   CH2 - PO4 - CH2 - CH2 - NH3
!
! Polar Head and glycerol backbone

```

!!Derived from Mackerell top\_all36\_lipid.rf

!! by Stuart Rose 9/10/2013

```

!!RESI DOPE      0.00 ! 2,3-dioleoyl-D-glycero-1-phosphatidylethanolamine
!!
!! R1 - CH2
!!   |
!!   (angles and atom names from Sundaralingam)
!! R2 - CH
!!   |
!!   CH2 - PO4 - CH2 - CH2 - NH3
!!
!! Polar Head and glycerol backbone

```

```

GROUP          !
ATOM N         NH3L -0.30 !           HN2
ATOM HN1      HCL   0.33 !           |
ATOM HN2      HCL   0.33 ! (+) HN1---N---HN3
ATOM HN3      HCL   0.33 !           |
ATOM C12      CTL2  0.13 !           |
ATOM H12A     HAL2  0.09 !           H12A--C12---H12B
ATOM H12B     HAL2  0.09 !           |
GROUP          !           |           alpha5
ATOM C11      CTL2 -0.08 !           |
ATOM H11A     HAL2  0.09 !           H11A--C11---H11B
ATOM H11B     HAL2  0.09 !           |           alpha4
ATOM P        PL    1.50 ! (-) O13 O12
ATOM O13      O2L  -0.78 !           \ /           alpha3
ATOM O14      O2L  -0.78 !           P (+)
ATOM O11      OSLP -0.57 !           / \           alpha2
ATOM O12      OSLP -0.57 ! (-) O14 O11
ATOM C1        CTL2 -0.08 !           |           alpha1
ATOM HA       HAL2  0.09 !           HA---C1---HB
ATOM HB       HAL2  0.09 !           |           theta1
GROUP          !           |
ATOM C2       CTL1  0.17 !           HS---C2- - - - -
ATOM HS       HAL1  0.09 !           | beta1           |
ATOM O21      OSL  -0.49 !           O22 O21           theta3
ATOM C21      CL   0.90 !           \ \ / beta2           |
ATOM O22      OBL  -0.63 !           C21
ATOM C22      CTL2 -0.22 !           | beta3           |
ATOM H2R      HAL2  0.09 !           H2R---C22---H2S

```

ATOM H2S	HAL2	0.09	!			
GROUP			!		beta4	
ATOM C3	CTL2	0.08	!			
ATOM HX	HAL2	0.09	!			HX---C3---HY
ATOM HY	HAL2	0.09	!			gamma1
ATOM O31	OSL	-0.49	!			O32 O31
ATOM C31	CL	0.90	!			\\ / gamma2
ATOM O32	OBL	-0.63	!			C31
ATOM C32	CTL2	-0.22	!			gamma3
ATOM H2X	HAL2	0.09	!			H2X---C32---H2Y
ATOM H2Y	HAL2	0.09	!			
GROUP			!			gamma4
ATOM C23	CTL2	-0.18	!			
ATOM H3R	HAL2	0.09	!	H3R	---C23---	H3S
ATOM H3S	HAL2	0.09	!			
GROUP			!			
ATOM C24	CTL2	-0.18	!			
ATOM H4R	HAL2	0.09	!	H4R	---C24---	H4S
ATOM H4S	HAL2	0.09	!			
GROUP			!			
ATOM C25	CTL2	-0.18	!			
ATOM H5R	HAL2	0.09	!	H5R	---C25---	H5S
ATOM H5S	HAL2	0.09	!			
GROUP			!			
ATOM C26	CTL2	-0.18	!			
ATOM H6R	HAL2	0.09	!	H6R	---C26---	H6S
ATOM H6S	HAL2	0.09	!			
GROUP			!			
ATOM C27	CTL2	-0.18	!			
ATOM H7R	HAL2	0.09	!	H7R	---C27---	H7S
ATOM H7S	HAL2	0.09	!			
GROUP			!			
ATOM C28	CTL2	-0.18	!			
ATOM H8R	HAL2	0.09	!	H8R	---C28---	H8S
ATOM H8S	HAL2	0.09	!			
GROUP			!			
ATOM C29	CTL2	-0.18	!			
ATOM H9R	HAL2	0.09	!	H9R	---C29---	H9S
ATOM H9S	HAL2	0.09	!			
GROUP			!			
ATOM C210	CTL2	-0.18	!			
ATOM H10R	HAL2	0.09	!	H10R	---C210---	H10S
ATOM H10S	HAL2	0.09	!			
GROUP			!			
ATOM C211	CEL1	-0.15	!			
ATOM H11R	HEL1	0.15	!	H11R	---C211	
GROUP			!		(CIS)	
ATOM C212	CEL1	-0.15	!			
ATOM H12R	HEL1	0.15	!	H12R	---C212	
GROUP			!			
ATOM C213	CTL2	-0.18	!			
ATOM H13R	HAL2	0.09	!	H13R	---C213---	H13S
ATOM H13S	HAL2	0.09	!			
GROUP			!			
ATOM C214	CTL2	-0.18	!			
ATOM H14R	HAL2	0.09	!	H14R	---C214---	H14S
ATOM H14S	HAL2	0.09	!			
GROUP			!			
ATOM C215	CTL2	-0.18	!			
ATOM H15R	HAL2	0.09	!	H15R	---C215---	H15S
ATOM H15S	HAL2	0.09	!			
GROUP			!			
ATOM C216	CTL2	-0.18	!			
ATOM H16R	HAL2	0.09	!	H16R	---C216---	H16S

ATOM H16S	HAL2	0.09	!		
GROUP			!		
ATOM C217	CTL2	-0.18	!		
ATOM H17R	HAL2	0.09	!	H17R---C217--H17S	
ATOM H17S	HAL2	0.09	!		
GROUP			!		
ATOM C218	CTL3	-0.27	!		
ATOM H18R	HAL3	0.09	!	H18R---C218--H18S	
ATOM H18S	HAL3	0.09	!		
ATOM H18T	HAL3	0.09	!	H18T	
GROUP			!		
ATOM C33	CTL2	-0.18	!		
ATOM H3X	HAL2	0.09	!	H3X ---C33---H3Y	
ATOM H3Y	HAL2	0.09	!		
GROUP			!		
ATOM C34	CTL2	-0.18	!		
ATOM H4X	HAL2	0.09	!	H4X ---C34---H4Y	
ATOM H4Y	HAL2	0.09	!		
GROUP			!		
ATOM C35	CTL2	-0.18	!		
ATOM H5X	HAL2	0.09	!	H5X ---C35---H5Y	
ATOM H5Y	HAL2	0.09	!		
GROUP			!		
ATOM C36	CTL2	-0.18	!		
ATOM H6X	HAL2	0.09	!	H6X ---C36---H6Y	
ATOM H6Y	HAL2	0.09	!		
GROUP			!		
ATOM C37	CTL2	-0.18	!		
ATOM H7X	HAL2	0.09	!	H7X ---C37---H7Y	
ATOM H7Y	HAL2	0.09	!		
GROUP			!		
ATOM C38	CTL2	-0.18	!		
ATOM H8X	HAL2	0.09	!	H8X ---C38---H8Y	
ATOM H8Y	HAL2	0.09	!		
GROUP			!		
ATOM C39	CTL2	-0.18	!		
ATOM H9X	HAL2	0.09	!	H9X ---C39---H9Y	
ATOM H9Y	HAL2	0.09	!		
GROUP			!		
ATOM C310	CTL2	-0.18	!		
ATOM H10X	HAL2	0.09	!	H10X---C310--H10Y	
ATOM H10Y	HAL2	0.09	!		
GROUP			!		
ATOM C311	CTL2	-0.18	!		
ATOM H11X	HAL2	0.09	!	H11X---C311--H11Y	
ATOM H11Y	HAL2	0.09	!		
GROUP			!		
ATOM C312	CTL2	-0.18	!		
ATOM H12X	HAL2	0.09	!	H12X---C312--H12Y	
ATOM H12Y	HAL2	0.09	!		
GROUP			!		
ATOM C313	CTL2	-0.18	!		
ATOM H13X	HAL2	0.09	!	H13X---C313--H13Y	
ATOM H13Y	HAL2	0.09	!		
GROUP			!		
ATOM C314	CTL2	-0.18	!		
ATOM H14X	HAL2	0.09	!	H14X---C314--H14Y	
ATOM H14Y	HAL2	0.09	!		
GROUP			!		
ATOM C315	CTL2	-0.18	!		
ATOM H15X	HAL2	0.09	!	H15X---C315--H15Y	
ATOM H15Y	HAL2	0.09	!		
GROUP			!		



BOND		C318 H18X		C318 H18Y		C318 H18Z					
IMPR	C21	O21	C22	O22	C31	O31	C32	O32			
IC	N		C12	C11	O12		1.5110	111.97	65.84	112.46	1.4308
IC	HN1		C12	*N	HN2		1.0342	114.60	119.70	105.60	1.0654
IC	HN1		C12	*N	HN3		1.0342	114.60	-127.78	110.56	1.0397
IC	HN1		N	C12	C11		1.0342	114.60	-177.91	111.97	1.5465
IC	C11		N	*C12	H12A		1.5465	111.97	-121.58	107.97	1.1086
IC	H12A		N	*C12	H12B		1.1086	107.97	-118.25	107.67	1.1104
IC	O12		C12	*C11	H11A		1.4308	112.46	-126.31	111.01	1.1167
IC	H11A		C12	*C11	H11B		1.1167	111.01	-115.41	107.63	1.1146
IC	C12		C11	O12	P		1.5465	112.46	-80.62	120.62	1.5839
IC	C11		O12	P	O11		1.4308	120.62	-156.78	104.60	1.5751
IC	O11		O12	*P	O13		1.5751	104.60	-117.47	103.31	1.4823
IC	O11		O12	*P	O14		1.5751	104.60	120.67	107.16	1.4736
IC	O12		P	O11	C1		1.5839	104.60	-58.82	120.34	1.4318
IC	P		O11	C1	C2		1.5751	120.34	-92.48	111.72	1.5536
IC	C2		O11	*C1	HA		1.5536	111.72	-119.08	108.93	1.1133
IC	HA		O11	*C1	HB		1.1133	108.93	-117.83	112.18	1.1155
IC	O11		C1	C2	C3		1.4318	111.72	162.49	110.59	1.5553
IC	C3		C1	*C2	O21		1.5553	110.59	120.51	108.20	1.4410
IC	C3		C1	*C2	HS		1.5553	110.59	-117.47	107.37	1.1169
IC	C1		C2	O21	C21		1.5536	108.20	145.45	115.07	1.3229
IC	C2		O21	C21	C22		1.4410	115.07	175.60	109.17	1.5330
IC	C22		O21	*C21	O22		1.5330	109.17	179.92	126.38	1.2173
IC	O21		C21	C22	C23		1.3229	109.17	-134.07	111.55	1.5472
IC	C23		C21	*C22	H2R		1.5472	111.55	-119.81	106.70	1.1095
IC	H2R		C21	*C22	H2S		1.1095	106.70	-117.59	109.58	1.1081
IC	C1		C2	C3	O31		1.5536	110.59	178.88	111.62	1.4432
IC	O31		C2	*C3	HX		1.4432	111.62	-121.40	107.66	1.1142
IC	HX		C2	*C3	HY		1.1142	107.66	-116.77	107.26	1.1152
IC	C2		C3	O31	C31		1.5553	111.62	174.54	113.52	1.3270
IC	C3		O31	C31	C32		1.4432	113.52	178.76	109.19	1.5276
IC	C32		O31	*C31	O32		1.5276	109.19	-179.68	125.26	1.2176
IC	O31		C31	C32	C33		1.3270	109.19	-153.26	112.50	1.5449
IC	C33		C31	*C32	H2X		1.5449	112.50	120.40	107.84	1.1092
IC	H2X		C31	*C32	H2Y		1.1092	107.84	117.16	108.28	1.1081
IC	C21		C22	C23	C24		1.5289	112.21	175.76	112.39	1.5338
IC	C24		C22	*C23	H3R		1.5338	112.39	-120.69	109.57	1.1147
IC	H3R		C22	*C23	H3S		1.1147	109.57	-117.65	109.64	1.1142
IC	C22		C23	C24	C25		1.5449	112.39	-179.39	112.35	1.5346
IC	C25		C23	*C24	H4R		1.5346	112.35	-121.52	109.41	1.1131
IC	H4R		C23	*C24	H4S		1.1131	109.41	-117.57	108.97	1.1134
IC	C23		C24	C25	C26		1.5338	112.35	176.31	112.80	1.5344
IC	C26		C24	*C25	H5R		1.5344	112.80	-121.01	108.95	1.1135
IC	H5R		C24	*C25	H5S		1.1135	108.95	-117.24	109.16	1.1132
IC	C24		C25	C26	C27		1.5346	112.80	-179.44	112.48	1.5356
IC	C27		C25	*C26	H6R		1.5356	112.48	-121.49	109.32	1.1129
IC	H6R		C25	*C26	H6S		1.1129	109.32	-117.47	108.94	1.1132
IC	C25		C26	C27	C28		1.5344	112.48	176.92	112.46	1.5398
IC	C28		C26	*C27	H7R		1.5398	112.46	-121.38	108.40	1.1139
IC	H7R		C26	*C27	H7S		1.1139	108.40	-116.93	108.77	1.1139
IC	C26		C27	C28	C29		1.5346	112.80	-179.44	112.48	1.5356
IC	C29		C27	*C28	H8R		1.5356	112.48	-121.49	109.32	1.1129
IC	H8R		C27	*C28	H8S		1.1129	109.32	-117.47	108.94	1.1132
IC	C27		C28	C29	C210		1.5344	112.48	176.92	112.46	1.5398
IC	C210		C28	*C29	H9R		1.5398	112.46	-121.38	108.40	1.1139
IC	H9R		C28	*C29	H9S		1.1139	108.40	-116.93	108.77	1.1139
IC	C28		C29	C210	C211		1.5356	112.46	-178.53	111.43	1.5097
IC	C211		C29	*C210	H10R		1.5097	111.43	-123.58	107.80	1.1132
IC	H10R		C29	*C210	H10S		1.1132	107.80	-115.43	108.37	1.1128
IC	C29		C210	C211	C212		1.5398	111.43	-126.96	126.62	1.3465
IC	C212		C210	*C211	H11R		1.3465	126.62	178.41	114.65	1.1012

IC C210	C211	C212	C213	1.5097	126.62	-1.69	126.32	1.5088
IC C213	C211	*C212	H12R	1.5088	126.32	-179.55	118.79	1.1012
IC C211	C212	C213	C214	1.3465	126.32	93.02	112.15	1.5392
IC C214	C212	*C213	H13R	1.5392	112.15	-121.30	111.28	1.1133
IC H13R	C212	*C213	H13S	1.1133	111.28	-117.50	110.00	1.1126
IC C212	C213	C214	C215	1.5088	112.15	-178.81	112.29	1.5354
IC C215	C213	*C214	H14R	1.5354	112.29	-121.34	109.78	1.1133
IC H14R	C213	*C214	H14S	1.1133	109.78	-118.01	109.42	1.1144
IC C213	C214	C215	C216	1.5345	112.59	-179.58	112.63	1.5347
IC C216	C214	*C215	H15R	1.5347	112.63	-121.36	109.09	1.1132
IC H15R	C214	*C215	H15S	1.1132	109.09	-117.38	109.07	1.1132
IC C214	C215	C216	C217	1.5347	112.63	179.65	112.69	1.5339
IC C217	C215	*C216	H16R	1.5339	112.69	-121.27	109.11	1.1132
IC H16R	C215	*C216	H16S	1.1132	109.11	-117.36	109.14	1.1132
IC C215	C216	C217	C218	1.5347	112.69	-179.93	113.30	1.5309
IC C218	C216	*C217	H17R	1.5309	113.30	-121.70	108.75	1.1140
IC H17R	C216	*C217	H17S	1.1140	108.75	-116.65	108.73	1.1141
IC C216	C217	C218	H18R	1.5339	113.30	-59.98	110.46	1.1113
IC H18R	C217	*C218	H18S	1.1113	110.46	119.84	110.45	1.1114
IC H18R	C217	*C218	H18T	1.1113	110.46	-120.09	110.62	1.1112
IC C31	C32	C33	C34	1.5288	113.05	179.24	111.73	1.5343
IC C34	C32	*C33	H3X	1.5343	111.73	-120.85	109.62	1.1140
IC H3X	C32	*C33	H3Y	1.1140	109.62	-117.95	109.78	1.1144
IC C32	C33	C34	C35	1.5447	111.73	-176.74	112.91	1.5345
IC C35	C33	*C34	H4X	1.5345	112.91	-121.67	109.15	1.1134
IC H4X	C33	*C34	H4Y	1.1134	109.15	-117.32	108.98	1.1134
IC C33	C34	C35	C36	1.5343	112.91	178.63	112.42	1.5349
IC C36	C34	*C35	H5X	1.5349	112.42	-120.99	108.94	1.1133
IC H5X	C34	*C35	H5Y	1.1133	108.94	-117.41	109.31	1.1131
IC C34	C35	C36	C37	1.5345	112.42	-176.73	112.80	1.5356
IC C37	C35	*C36	H6X	1.5356	112.80	-121.69	109.16	1.1130
IC H6X	C35	*C36	H6Y	1.1130	109.16	-117.32	108.94	1.1133
IC C35	C36	C37	C38	1.5343	112.91	178.63	112.42	1.5349
IC C38	C36	*C37	H7X	1.5349	112.42	-120.99	108.94	1.1133
IC H7X	C36	*C37	H7Y	1.1133	108.94	-117.41	109.31	1.1131
IC C36	C37	C38	C39	1.5345	112.42	-176.73	112.80	1.5356
IC C39	C37	*C38	H8X	1.5356	112.80	-121.69	109.16	1.1130
IC H8X	C37	*C38	H8Y	1.1130	109.16	-117.32	108.94	1.1133
IC C37	C38	C39	C310	1.5349	112.80	178.92	112.27	1.5402
IC C310	C38	*C39	H9X	1.5402	112.27	-121.37	108.23	1.1139
IC H9X	C38	*C39	H9Y	1.1139	108.23	-117.01	109.05	1.1137
IC C38	C39	C310	C311	1.5356	112.27	-174.92	111.69	1.5099
IC C311	C39	*C310	H10X	1.5099	111.69	-124.14	107.77	1.1124
IC H10X		C39	*C310 H10Y	1.1124	107.77	-115.13	108.30	1.1128
IC C39	C310	C311	C312	1.5402	111.69	-121.39	127.35	1.3470
IC C312	C310	*C311	H11X	1.3470	127.35	179.11	114.24	1.1012
IC H11X	C310	*C311	H9Y	1.1139	108.23	-117.01	109.05	1.1137
5/17/2015	need to check around	C311	C312					
IC C310	C311	C312	C313	1.5099	127.35	0.00	127.25	1.5096
IC C313	C311	*C312	H12X	1.5096	127.25	179.82	118.43	1.1012
IC H12X		C311	*C312 H10Y	1.1124	107.77	-115.13	108.30	1.1128
IC C311	C312	C313	C314	1.3470	127.25	106.03	111.65	1.5393
IC C314	C312	*C313	H13X	1.5393	111.65	-121.49	112.10	1.1123
IC H13X	C312	*C313	H13Y	1.1123	112.10	-117.95	109.83	1.1127
IC C312	C313	C314	C315	1.5096	111.65	179.63	112.41	1.5355
IC C315	C313	*C314	H14X	1.5355	112.41	-121.09	109.75	1.1135
IC H14X	C313	*C314	H14Y	1.1135	109.75	-118.07	109.46	1.1143
IC C313	C314	C315	C316	1.5347	112.66	-179.12	112.61	1.5348
IC C316	C314	*C315	H15X	1.5348	112.61	-121.34	109.09	1.1132
IC H15X	C314	*C315	H15Y	1.1132	109.09	-117.41	109.09	1.1132
IC C314	C315	C316	C317	1.5347	112.61	179.83	112.71	1.5340
IC C317	C315	*C316	H16X	1.5340	112.71	-121.28	109.10	1.1132
IC H16X	C315	*C316	H16Y	1.1132	109.10	-117.35	109.13	1.1133
IC C315	C316	C317	C318	1.5348	112.71	-179.67	113.30	1.5309

IC C318	C316	*C317	H17X	1.5309	113.30	-121.68	108.77	1.1141
IC H17X	C316	*C317	H17Y	1.1141	108.77	-116.68	108.76	1.1141
IC C316	C317	C318	H18X	1.5340	113.30	-59.94	110.46	1.1113
IC H18X	C317	*C318	H18Y	1.1113	110.46	119.86	110.45	1.1113
IC H18X	C317	*C318	H18Z	1.1113	110.46	-120.06	110.61	1.1112

```
RESI SQDG -1.00 !
!
!
!
!
!
```

! Adaped from:

```
! RESI SAPI -1.00 ! Phosphatidylinositol
!
! Stearoyl - CH2 Uses RESI INI1 - cyclic myi-inositol,
! |
! Arachidonyl - CH RESI SAPC
! | (-)
! CH2 - PO4 - inositol
!
```

GROUP

ATOM S	SG301	1.35	!	O7
ATOM O7	OG2P1	-0.716	!	
ATOM O8	OG2P1	-0.716	!	O8---S---O9
ATOM O9	OG2P1	-0.716	!	
GROU		!		
ATOM C1	CC3162	0.340	!	
ATOM H1	HCA1	0.090	!	H61---C6---H62
ATOM O1	OC311	-0.650	!	
ATOM C5	CC3163	0.075	!	H5-C5---O5
ATOM H5	HCA1	0.074	!	H4 / \ H1
ATOM O5	OC3C61	-0.457	!	\ / HO3 \ /
GROU		!		C4   C1
ATOM C2	CC3161	-0.008	!	/ \ O3 H2 / \
ATOM H2	HCA1	0.075	!	HO4-O4 \     / O6
ATOM O2	OC311	-0.681	!	C3---C2
ATOM HO2	HCP1	0.439	!	O2-HO2
GROU		!		H3
ATOM C3	CC3161	0.357	!	
ATOM H3	HCA1	0.012	!	
ATOM O3	OC311	-0.712	!	
ATOM HO3	HCP1	0.413	!	
GROU		!		
ATOM C4	CC3161	0.340	!	
ATOM H4	HCA1	0.000	!	
ATOM O4	OC311	-0.718	!	-----
ATOM HO4	HCP1	0.440	!	
GROU		!		
ATOM C6	CC321	-0.288	!	
ATOM H61	HCA2	0.064	!	
ATOM H62	HCA2	0.064	!	
GROU		!		
ATOM C44	CTL2	0.305	!	alpha1
ATOM HA	HAL2	0.005	!	H44A---C44---H44B
ATOM HB	HAL2	0.005	!	theta1
GROU		!		
ATOM C45	CTL1	0.214	!	H45---C45-----
ATOM H45	HAL1	0.036	!	beta1
ATOM O47	OSL	-0.531	!	O49 O47 theta3
ATOM C7	CL	0.927	!	\ / beta2

ATOM O49	OBL	-0.625 !		C7	
ATOM C8	CTL2	-0.376 !			beta3
ATOM H8R	HAL2	0.131 !	H8R---	C8---	H8S
ATOM H8S	HAL2	0.131 !			
GROUP		!			beta4
ATOM C46	CTL2	0.146 !			
ATOM H46X	HAL2	0.056 !			H46X--C46--H46Y
ATOM H46Y	HAL2	0.056 !			
ATOM O48	OSL	-0.406 !			O32 O31
ATOM C23	CL	0.913 !			\\ /
ATOM O10	OBL	-0.644 !			C23
ATOM C24	CTL2	-0.409 !			
ATOM H24X	HAL2	0.145 !			1H24X---C24---H24Y
ATOM H24Y	HAL2	0.145 !			
GROUP		!			gamma4
ATOM C23	CTL2	-0.18 !			
ATOM H3R	HAL2	0.09 !	H9R ---	C9---	H9S
ATOM H3S	HAL2	0.09 !			
GROUP		!			
ATOM C24	CTL2	-0.18 !			
ATOM H4R	HAL2	0.09 !	HR ---	C24---	H4S
ATOM H4S	HAL2	0.09 !			
GROUP		!			
ATOM C25	CEL1	-0.15 !			
ATOM H5R	HEL1	0.15 !	H5R ---	C25	
GROUP		!			!! (CIS)
ATOM C26	CEL1	-0.15 !			!!
ATOM H6R	HEL1	0.15 !	H6R ---	C26	
GROUP		!			
ATOM C27	CTL2	-0.18 !			
ATOM H7R	HAL2	0.09 !	H7R ---	C27---	H7S
ATOM H7S	HAL2	0.09 !			
GROUP		!			
ATOM C28	CEL1	-0.15 !			
ATOM H8R	HEL1	0.15 !	H8R ---	C28	
GROUP		!			!! (CIS)
ATOM C29	CEL1	-0.15 !			!!
ATOM H9R	HEL1	0.15 !	H9R ---	C29	
GROUP		!			
ATOM C210	CTL2	-0.18 !			
ATOM H10R	HAL2	0.09 !	H10R---	C210--	H10S
ATOM H10S	HAL2	0.09 !			
GROUP		!			
ATOM C211	CEL1	-0.15 !			
ATOM H11R	HEL1	0.15 !	H11R---	C211	
GROUP		!			!! (CIS)
ATOM C212	CEL1	-0.15 !			!!
ATOM H12R	HEL1	0.15 !	H12R---	C212	
GROUP		!			
ATOM C213	CTL2	-0.18 !			
ATOM H13R	HAL2	0.09 !	H13R---	C213--	H13S
ATOM H13S	HAL2	0.09 !			
GROUP		!			
ATOM C214	CEL1	-0.15 !			
ATOM H14R	HEL1	0.15 !	H14R---	C214	
GROUP		!			!! (CIS)
ATOM C215	CEL1	-0.15 !			!!
ATOM H15R	HEL1	0.15 !	H15R---	C215	
GROUP		!			
ATOM C216	CTL2	-0.18 !			
ATOM H16R	HAL2	0.09 !	H16R---	C216--	H16S
ATOM H16S	HAL2	0.09 !			
GROUP		!			
ATOM C217	CTL2	-0.18 !			



ATOM H17R	HAL2	0.09	!	H17R---C217--H17S	
ATOM H17S	HAL2	0.09	!		
GROUP			!		
ATOM C218	CTL2	-0.27	!		
ATOM H18R	HAL2	0.09	!	H18R---C218--H18S	
ATOM H18S	HAL2	0.09	!		
GROUP			!		
ATOM C219	CTL2	-0.18	!		
ATOM H19R	HAL2	0.09	!	H19R---C219--H19S	
ATOM H19S	HAL2	0.09	!		
GROUP			!		
ATOM C220	CTL3	-0.18	!		
ATOM H20R	HAL3	0.09	!	H20R---C220--H20S	
ATOM H20S	HAL3	0.09	!		
ATOM H20T	HAL3	0.09	!	H20T	
GROUP			!		
ATOM C33	CTL2	-0.18	!		
ATOM H3X	HAL2	0.09	!	H3X ---C33---H3Y	
ATOM H3Y	HAL2	0.09	!		
GROUP			!		
ATOM C34	CTL2	-0.18	!		
ATOM H4X	HAL2	0.09	!	H4X ---C34---H4Y	
ATOM H4Y	HAL2	0.09	!		
GROUP			!		
ATOM C35	CTL2	-0.18	!		
ATOM H5X	HAL2	0.09	!	H5X ---C35---H5Y	
ATOM H5Y	HAL2	0.09	!		
GROUP			!		
ATOM C36	CTL2	-0.18	!		
ATOM H6X	HAL2	0.09	!	H6X ---C36---H6Y	
ATOM H6Y	HAL2	0.09	!		
GROUP			!		
ATOM C37	CTL2	-0.18	!		
ATOM H7X	HAL2	0.09	!	H7X ---C37---H7Y	
ATOM H7Y	HAL2	0.09	!		
GROUP			!		
ATOM C38	CTL2	-0.18	!		
ATOM H8X	HAL2	0.09	!	H8X ---C38---H8Y	
ATOM H8Y	HAL2	0.09	!		
GROUP			!		
ATOM C39	CTL2	-0.18	!		
ATOM H9X	HAL2	0.09	!	H9X ---C39---H9Y	
ATOM H9Y	HAL2	0.09	!		
GROUP			!		
ATOM C310	CTL2	-0.18	!		
ATOM H10X	HAL2	0.09	!	H10X---C310--H10Y	
ATOM H10Y	HAL2	0.09	!		
GROUP			!		
ATOM C311	CTL2	-0.18	!		
ATOM H11X	HAL2	0.09	!	H11X---C311--H11Y	
ATOM H11Y	HAL2	0.09	!		
GROUP			!		
ATOM C312	CTL2	-0.18	!		
ATOM H12X	HAL2	0.09	!	H12X---C312--H12Y	
ATOM H12Y	HAL2	0.09	!		
GROUP			!		
ATOM C313	CTL2	-0.18	!		
ATOM H13X	HAL2	0.09	!	H13X---C313--H13Y	
ATOM H13Y	HAL2	0.09	!		
GROUP			!		
ATOM C314	CTL2	-0.18	!		
ATOM H14X	HAL2	0.09	!	H14X---C314--H14Y	
ATOM H14Y	HAL2	0.09	!		
GROUP			!		



```

BOND C216 H16R      C216 H16S      C216 C217
BOND C217 H17R      C217 H17S      C217 C218
BOND C218 H18R      C218 H18S      C218 C219
BOND C219 H19R      C219 H19S      C219 C220
BOND C220 H20R      C220 H20S      C220 H20T
! Chain From C3
BOND O31 C31
BOND C31 C32
DOUBLE C31 O32
BOND C32 H2X      C32 H2Y      C32 C33
BOND C33 H3X      C33 H3Y      C33 C34
BOND C34 H4X      C34 H4Y      C34 C35
BOND C35 H5X      C35 H5Y      C35 C36
BOND C36 H6X      C36 H6Y      C36 C37
BOND C37 H7X      C37 H7Y      C37 C38
BOND C38 H8X      C38 H8Y      C38 C39
BOND C39 H9X      C39 H9Y      C39 C310
BOND C310 H10X     C310 H10Y     C310 C311
BOND C311 H11X     C311 H11Y     C311 C312
BOND C312 H12X     C312 H12Y     C312 C313
BOND C313 H13X     C313 H13Y     C313 C314
BOND C314 H14X     C314 H14Y     C314 C315
BOND C315 H15X     C315 H15Y     C315 C316
BOND C316 H16X     C316 H16Y     C316 C317
BOND C317 H17X     C317 H17Y     C317 C318
BOND C318 H18X     C318 H18Y     C318 H18Z

```

```

IMPR C21 O21 C22 O22      C31 O31 C32 O32

```

```

ACCEPTOR O1 S
ACCEPTOR O2 S
ACCEPTOR O3 S

```

```

!      I      J      K      L      R(IK)      T(IKJ)      PHI      T(JKL)      R(KL)
! Sulfonate
ACCEPTOR O1 S
ACCEPTOR O2 S
ACCEPTOR O3 S
IC C2 C1 S O1 0.0 0.00 180.00 0.0 0.0
IC C1 O1 *S O2 0.0 0.00 120.00 0.0 0.0
IC C1 O1 *S O3 0.0 0.00 -120.00 0.0 0.0
IC S C2 *C1 H11 0.0 0.00 120.00 0.0 0.0
IC S C2 *C1 H12 0.0 0.00 -120.00 0.0 0.0
IC S C1 C2 C3 0.0 0.00 180.00 0.0 0.0

```

```

! Inositol Head Group
IC C11 C12 C13 C14 1.5530 107.31 -59.93 109.11 1.5612
IC C12 C13 C14 C15 1.4341 109.11 59.27 114.44 1.4654
IC C13 C12 C11 O12 1.4341 107.31 -175.79 117.69 1.4086
IC C13 C14 C15 C16 1.5612 114.44 -55.48 109.80 1.5350
IC C14 C15 C16 C11 1.4654 109.80 55.05 107.18 1.5598
IC C12 C13 C14 O4 1.4341 109.11 -177.27 106.06 1.4595
IC C13 C14 C15 O5 1.5612 114.44 171.27 114.28 1.4386
IC C12 C13 C14 H4 1.4341 109.11 -64.25 106.39 1.1684
IC O12 C12 *C11 H1 1.4086 117.69 -121.05 110.98 1.1834
IC O12 C11 C12 O2 1.4086 117.69 51.01 111.79 1.4490
IC O12 C11 C12 H2 1.4086 117.69 -61.28 98.22 1.1105
IC C13 C14 C15 H5 1.5612 114.44 52.34 110.34 1.0922
IC O2 C11 *C12 C13 1.4490 111.79 133.20 107.31 1.4341
IC O3 C14 *C13 H3 1.4537 110.99 114.31 113.73 1.1394
IC O3 C12 *C13 C14 1.4537 105.59 119.36 109.11 1.5612
IC O4 C13 *C14 C15 1.4595 106.06 -123.46 114.44 1.4654
IC C16 C14 *C15 O5 1.5350 109.80 -133.25 114.28 1.4386

```

IC C14	C15	O5	HO5	1.4654	114.28	-73.20	108.55	0.9726	
IC C14	C15	C16	O6	1.4654	109.80	-179.24	110.87	1.4043	
IC C16	C11	O12	P	1.5530	117.69	300.00	114.27	0.9451	! gauche
IC C11	C12	O2	HO2	1.5530	111.79	-31.80	115.65	0.9404	
IC C12	C13	O3	HO3	1.4341	105.59	37.19	107.10	0.9920	
IC C13	C14	O4	HO4	1.5612	106.06	35.00	105.15	0.9686	
IC C15	C16	O6	HO6	1.5350	110.87	51.35	112.65	0.9879	
IC C14	C15	C16	H6	1.4654	109.80	-58.40	111.34	1.0796	
! Phosphate Linker									
IC C11	O12	P	O11	1.3655	121.23	153.36	102.74	1.5058	
IC O11	O12	*P	O13	1.5867	101.18	-114.47	107.73	1.4832	
IC O11	O12	*P	O14	1.5867	101.18	116.82	109.30	1.4741	
IC O12	P	O11	C1	1.5958	101.18	180.00	122.31	1.4271	! trans
IC P	O11	C1	C2	1.5867	122.31	180.00	111.45	1.5517	! trans
IC C2	O11	*C1	HA	1.5517	111.45	117.99	107.86	1.1119	
IC HA	O11	*C1	HB	1.1119	107.86	116.85	112.59	1.1137	
IC O11	C1	C2	O21	1.4271	111.45	-175.58	109.40	1.4420	
! Backbone									
IC O21	C1	*C2	C3	1.4420	109.40	-121.10	110.56	1.5561	
IC C3	C1	*C2	HS	1.5561	110.56	-116.88	109.10	1.1148	
IC C1	C2	O21	C21	1.5517	109.40	75.31	115.18	1.3240	
IC C2	O21	C21	C22	1.4420	115.18	-167.64	109.38	1.5349	
IC C22	O21	*C21	O22	1.5349	109.38	177.97	125.87	1.2208	
IC O21	C21	C22	C23	1.3240	109.38	-106.88	114.46	1.5510	
IC C23	C21	*C22	H2R	1.5510	114.46	120.85	107.59	1.1114	
IC H2R	C21	*C22	H2S	1.1114	107.59	115.88	108.08	1.1076	
IC C1	C2	C3	O31	1.5517	110.56	-174.46	111.33	1.4462	
IC O31	C2	*C3	HX	1.4462	111.33	-122.32	107.11	1.1154	
IC HX	C2	*C3	HY	1.1154	107.11	-116.45	107.97	1.1151	
IC C2	C3	O31	C31	1.5561	111.33	-170.38	113.09	1.3331	
IC C3	O31	C31	C32	1.4462	113.09	-178.75	108.33	1.5405	
IC C32	O31	*C31	O32	1.5405	108.33	-179.57	125.60	1.2151	
IC O31	C31	C32	C33	1.3331	108.33	-179.15	116.85	1.6060	
IC C33	C31	*C32	H2X	1.6060	116.85	-121.70	105.08	1.1113	
IC H2X	C31	*C32	H2Y	1.1113	105.08	-115.26	107.43	1.1071	
! Acyl Chain 1									
IC C21	C22	C23	C24	1.5329	113.78	180.00	112.27	1.5435	
IC C24	C22	*C23	H3R	1.5435	112.27	-122.24	109.63	1.1133	
IC C24	C22	*C23	H3S	1.5435	112.27	120.06	108.89	1.1154	
IC C22	C23	C24	C25	1.5483	112.27	180.00	115.67	1.5107	
IC C25	C23	*C24	H4R	1.5107	115.67	-121.06	107.11	1.1144	
IC C25	C23	*C24	H4S	1.5107	115.67	124.06	108.43	1.1128	
IC C23	C24	C25	C26	1.5435	115.67	180.00	125.97	1.3453	
IC C26	C24	*C25	H5R	1.3453	125.97	-176.85	115.39	1.1011	
IC C24	C25	C26	C27	1.5107	125.97	0.00	125.28	1.5097	!cis db
IC C27	C25	*C26	H6R	1.5097	125.28	178.19	119.65	1.1004	
IC C25	C26	C27	C28	1.3453	125.28	120.00	121.35	1.5192	
IC C28	C26	*C27	H7R	1.5192	121.35	-124.15	108.68	1.1135	
IC C28	C26	*C27	H7S	1.5192	121.35	123.34	106.97	1.1121	
IC C26	C27	C28	C29	1.5097	121.35	120.00	132.80	1.3549	
IC C29	C27	*C28	H8R	1.3549	132.80	-178.43	111.35	1.1010	
IC C27	C28	C29	C210	1.5192	132.80	0.00	130.38	1.5115	!cis db
IC C210	C28	*C29	H9R	1.5115	130.38	178.53	117.07	1.1014	
IC C28	C29	C210	C211	1.3549	130.38	120.00	111.80	1.5083	
IC C211	C29	*C210	H10R	1.5192	121.35	-124.15	108.68	1.1135	
IC C211	C29	*C210	H10S	1.5192	121.35	123.34	106.97	1.1128	
IC C29	C210	C211	C212	1.5115	111.80	120.00	124.32	1.3436	
IC C212	C210	*C211	H11R	1.3436	125.97	-176.85	115.39	1.1011	
IC C210	C211	C212	C213	1.5083	124.32	0.00	125.45	1.5067	!cis db
IC C213	C211	*C212	H12R	1.5097	125.28	178.19	119.65	1.1004	
IC C211	C212	C213	C214	1.3436	125.45	120.00	111.57	1.5090	
IC C214	C212	*C213	H13R	1.5192	121.35	-124.15	108.68	1.1135	
IC C214	C212	*C213	H13S	1.5192	121.35	123.34	106.97	1.1128	
IC C212	C213	C214	C215	1.5067	111.57	120.00	126.10	1.3471	

IC	C215	C213	*C214	H14R	1.3453	125.97	-176.85	115.39	1.1011	
IC	C213	C214	C215	C216	1.5090	126.10	0.00	125.86	1.5091	!cis db
IC	C216	C214	*C215	H15R	1.5097	125.28	178.19	119.65	1.1004	
IC	C214	C215	C216	C217	1.3471	125.86	180.00	113.25	1.5428	
IC	C217	C215	*C216	H16R	1.5192	121.35	-124.15	108.68	1.1135	
IC	C217	C215	*C216	H16S	1.5192	121.35	123.34	106.97	1.1128	
IC	C215	C216	C217	C218	1.5091	113.25	180.00	115.19	1.5395	
IC	C218	C216	*C217	H17R	1.5192	121.35	-124.15	108.68	1.1135	
IC	C218	C216	*C217	H17S	1.5192	121.35	123.34	106.97	1.1128	
IC	C216	C217	C218	C219	1.5428	115.19	180.00	113.95	1.5345	
IC	C219	C217	*C218	H18R	1.5192	121.35	-124.15	108.68	1.1135	
IC	C219	C217	*C218	H18S	1.5192	121.35	123.34	106.97	1.1128	
IC	C217	C218	C219	C220	1.5395	113.95	180.00	112.95	1.5309	
IC	C220	C218	*C219	H19R	1.5192	121.35	-124.15	108.68	1.1135	
IC	C220	C218	*C219	H19S	1.5192	121.35	123.34	106.97	1.1128	
IC	C218	C219	C220	H20T	1.5345	112.95	180.00	110.39	1.1115	
IC	H20T	C219	*C220	H20R	1.5192	121.35	-124.15	108.68	1.1135	
IC	H20T	C219	*C220	H20S	1.5192	121.35	123.34	106.97	1.1128	
! Acyl Chain 2										
IC	C31	C32	C33	C34	1.5405	116.85	180.00	126.13	1.5951	
IC	C34	C32	*C33	H3X	1.5410	113.36	-119.96	111.74	1.1148	
IC	C34	C32	*C33	H3Y	1.5192	121.35	123.34	106.97	1.1128	
IC	C32	C33	C34	C35	1.6060	126.13	180.00	113.36	1.5410	
IC	C35	C33	*C34	H4X	1.5396	113.52	-123.43	110.53	1.1101	
IC	C35	C33	*C34	H4Y	1.5192	121.35	123.34	106.97	1.1128	
IC	C33	C34	C35	C36	1.5951	113.36	180.00	113.52	1.5396	
IC	C36	C34	*C35	H5X	1.5396	113.52	-123.43	110.53	1.1101	
IC	C36	C34	*C35	H5Y	1.5192	121.35	123.34	106.97	1.1128	
IC	C34	C35	C36	C37	1.5410	113.52	180.00	114.47	1.5397	
IC	C37	C35	*C36	H6X	1.5396	113.52	-123.43	110.53	1.1101	
IC	C37	C35	*C36	H6Y	1.5192	121.35	123.34	106.97	1.1128	
IC	C35	C36	C37	C38	1.5396	114.47	180.00	113.41	1.5386	
IC	C38	C36	*C37	H7X	1.5396	113.52	-123.43	110.53	1.1101	
IC	C38	C36	*C37	H7Y	1.5192	121.35	123.34	106.97	1.1128	
IC	C36	C37	C38	C39	1.5397	113.41	180.00	113.71	1.5382	
IC	C39	C37	*C38	H8X	1.5396	113.52	-123.43	110.53	1.1101	
IC	C39	C37	*C38	H8Y	1.5192	121.35	123.34	106.97	1.1128	
IC	C37	C38	C39	C310	1.5386	113.71	180.00	113.75	1.5392	
IC	C310	C38	*C39	H9X	1.5396	113.52	-123.43	110.53	1.1101	
IC	C310	C38	*C39	H9Y	1.5192	121.35	123.34	106.97	1.1128	
IC	C38	C39	C310	C311	1.5382	113.75	180.00	114.19	1.5353	
IC	C311	C39	*C310	H10X	1.5396	113.52	-123.43	110.53	1.1101	
IC	C311	C39	*C310	H10Y	1.5192	121.35	123.34	106.97	1.1128	
IC	C39	C310	C311	C312	1.5392	114.19	180.00	112.28	1.5347	
IC	C312	C310	*C311	H11X	1.5396	113.52	-123.43	110.53	1.1101	
IC	C312	C310	*C311	H11Y	1.5192	121.35	123.34	106.97	1.1128	
IC	C310	C311	C312	C313	1.5353	112.28	180.00	113.98	1.5367	
IC	C313	C311	*C312	H12X	1.5396	113.52	-123.43	110.53	1.1101	
IC	C313	C311	*C312	H12Y	1.5192	121.35	123.34	106.97	1.1128	
IC	C311	C312	C313	C314	1.5347	113.98	180.00	113.72	1.5377	
IC	C314	C312	*C313	H13X	1.5396	113.52	-123.43	110.53	1.1101	
IC	C314	C312	*C313	H13Y	1.5192	121.35	123.34	106.97	1.1128	
IC	C312	C313	C314	C315	1.5367	113.72	180.00	113.85	1.5357	
IC	C315	C313	*C314	H14X	1.5396	113.52	-123.43	110.53	1.1101	
IC	C315	C313	*C314	H14Y	1.5192	121.35	123.34	106.97	1.1128	
IC	C313	C314	C315	C316	1.5377	113.85	180.00	111.81	1.5374	
IC	C316	C314	*C315	H15X	1.5396	113.52	-123.43	110.53	1.1101	
IC	C316	C314	*C315	H15Y	1.5192	121.35	123.34	106.97	1.1128	
IC	C314	C315	C316	C317	1.5357	111.81	180.00	114.29	1.5985	
IC	C317	C315	*C316	H16X	1.5396	113.52	-123.43	110.53	1.1101	
IC	C317	C315	*C316	H16Y	1.5192	121.35	123.34	106.97	1.1128	
IC	C315	C316	C317	C318	1.5374	114.29	180.00	130.92	1.5745	
IC	C318	C316	*C317	H17X	1.5396	113.52	-123.43	110.53	1.1101	
IC	C318	C316	*C317	H17Y	1.5192	121.35	123.34	106.97	1.1128	

IC	C316	C317	C318	H18X	1.5985	130.92	180.00	110.90	1.1113
IC	H18X	C317	*C318	H18Y	1.5396	113.52	-123.43	110.53	1.1101
IC	H18X	C317	*C318	H18Z	1.5192	121.35	123.34	106.97	1.1128

# Appendix B. Ubiquinones (UQ10 – UQ, UQH2, and neutral semiquinone)

File: <ubiquinone.inp>

```

!This is a reduced topology file, suitable for building Ubiquinone and derivatives.
!Uses lipid nomenclature to build isoprene tails, which can get built up from isoprenoid
units.
MASS 1 H 1.00800 H ! polar H
MASS 136 HL 1.008000 H ! polar H (equivalent to protein H)
MASS 137 HCL 1.008000 H ! charged H for PE (equivalent to protein HC)
MASS 138 HOL 1.008000 H ! Nucleic acid phosphate hydroxyl proton
MASS 139 HAL1 1.008000 H ! alphatic proton
MASS 140 HAL2 1.008000 H ! alphatic proton
MASS 141 HAL3 1.008000 H ! alphatic proton
MASS 142 HEL1 1.008000 H ! for alkene; RHC=CR
MASS 143 HEL2 1.008000 H ! for alkene; H2C=CR. Currently unused.
MASS 144 HBL 1.008000 H ! POPS SER backbone H
MASS 145 CL 12.011000 C ! carbonyl C (acetic acid/methyl acetate)
MASS 146 CTL1 12.011000 C ! sp3 carbon with 1 H (-CH1-)
MASS 147 CTL2 12.011000 C ! carbon of methylene group (-CH2-)
MASS 148 CTL3 12.011000 C ! carbon of methyl group (-CH3)
MASS 149 CTL5 12.011000 C ! carbon of methyl group (-CH3) for tetramethylammonium
MASS 150 CEL1 12.011000 C ! for alkene; RHC=CR
MASS 151 CEL2 12.011000 C ! for alkene; H2C=CR. Currently unused.
MASS 201 HAN 1.00800 H ! nonpolar H
MASS 202 CN 12.01100 C ! polar C
MASS 203 CTN 12.01100 C ! tetrahedral C
MASS 225 CUQ1 12.01100 C ! for quinones
MASS 226 CUQ2 12.01100 C ! for quinones
MASS 227 CUQ3 12.01100 C ! for quinones
MASS 228 CUQ4 12.01100 C ! for quinones
MASS 229 OUQ1 15.99900 O ! for quinones
MASS 230 OUQ2 15.99900 O ! for quinones
!When QA and QB are populated by different quinones, they need distinct types to keep the
parameters consistent.
MASS 201 HAN2 1.00800 H ! nonpolar H
MASS 202 CN2 12.01100 C ! polar C
MASS 203 CTN2 12.01100 C ! tetrahedral C
MASS 225 CUQ5 12.01100 C ! for quinones
MASS 226 CUQ6 12.01100 C ! for quinones
MASS 227 CUQ7 12.01100 C ! for quinones
MASS 228 CUQ8 12.01100 C ! for quinones
MASS 229 OUQ3 15.99900 O ! for quinones
MASS 230 OUQ4 15.99900 O ! for quinones
MASS 240 CNQ1 12.01100 C ! for naphthoquinone
MASS 241 CNQ2 12.01100 C ! for naphthoquinone
MASS 242 HP 1.00800 H ! aromatic hydrogen

RESI NAPQ 0.00000 !Naphthoquinone (vitamin K)

GROUP ! ubiquinone ring

ATOM C1 CUQ3 -0.317 !
ATOM C2 CUQ1 0.586 !
ATOM O2 OUQ1 -0.456 !
ATOM C3 CUQ2 0.055 !
ATOM C12 CNQ1 -0.336 !
ATOM C4 CUQ2 0.055 !
ATOM C9 CNQ1 -0.336 !
ATOM C5 CUQ1 0.586 !
ATOM O5 OUQ1 -0.456 !
ATOM C6 CUQ4 0.014 !
ATOM C1M CTN -0.120 !
ATOM C11 CNQ2 -0.045 !
ATOM C10 CNQ2 -0.045 !
ATOM H1 HAN 0.09 !
ATOM H2 HAN 0.09 !
ATOM H3 HAN 0.09 !
ATOM H4 HAN 0.14 !

```

```

ATOM H5  HAN  0.14  !
ATOM H6  HAN  0.14  !
ATOM H7  HAN  0.14  !
!ATOM H8  HAN  0.09  !
!ATOM H9  HAN  0.09  !
!
!      isoprenic tail stub !
!
ATOM C7  CTN  -0.175 !
ATOM C8  CN   -0.27  !
ATOM H10 HAN  0.09  !
ATOM H11 HAN  0.09  !
ATOM H12 HAN  0.09  !
ATOM H13 HAN  0.09  !
ATOM H14 HAN  0.09  !

!      bonds for ubiquinone ring
BOND C1 C2  C2 C3  C3 C4  C4 C5
BOND C5 C6  C6 C1
BOND C2 O2  C3 O3  C4 O4  C5 O5
BOND O4 C4M C4M H7  C4M H8  C4M H9
BOND O3 C3M C3M H4  C3M H5  C3M H6
BOND C1 C1M C1M H1  C1M H2  C1M H3
!Isoprene tail stub
BOND C6 C7  C7 H10  C7 H11  C7 C8  C8 H12  C8 H13 C8 H14
AUTOGENERATE ANGLES DIHEDRALS

```

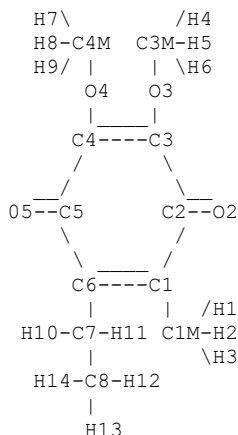
```
RESI UBIQ      0.00000 !UBIQUINONE 6 FOR SPHAER FEHER, M SIDE
```

```
GROUP ! ubiquinone ring
```

```

ATOM C1  CUQ3  -0.317  !
ATOM C2  CUQ1  0.586   !
ATOM O2  OUQ1  -0.456  !
ATOM C3  CUQ2  0.055   !
ATOM C4  CUQ2  0.055   !
ATOM O4  OUQ2  -0.336  !
ATOM C5  CUQ1  0.586   !
ATOM O5  OUQ1  -0.456  !
ATOM C6  CUQ4  0.014   !
ATOM C1M CTN   -0.120  !
ATOM C3M CTN   -0.045  !
ATOM C4M CTN   -0.045  !
ATOM H1  HAN    0.09   !
ATOM H2  HAN    0.09   !
ATOM H3  HAN    0.09   !
ATOM H4  HAN    0.09   !
ATOM H5  HAN    0.09   !
ATOM H6  HAN    0.09   !
ATOM H7  HAN    0.09   !
ATOM H8  HAN    0.09   !
ATOM H9  HAN    0.09   !

```



```
!      isoprenic tail stub !
```

```

ATOM C7  CTN  -0.175 !
ATOM C8  CN   -0.27  !
ATOM H10 HAN  0.09  !
ATOM H11 HAN  0.09  !
ATOM H12 HAN  0.09  !
ATOM H13 HAN  0.09  !
ATOM H14 HAN  0.09  !

```

```

!      bonds for ubiquinone ring
BOND C1 C2  C2 C3  C3 C4  C4 C5
BOND C5 C6  C6 C1
BOND C2 O2  C3 O3  C4 O4  C5 O5
BOND O4 C4M C4M H7  C4M H8  C4M H9
BOND O3 C3M C3M H4  C3M H5  C3M H6
BOND C1 C1M C1M H1  C1M H2  C1M H3
!Isoprene tail stub

```



BOND C6 C7 C7 H10 C7 H11 C7 C8 C8 H12 C8 H13 C8 H14  
 AUTOGENERATE ANGLES DIHEDRALS

RESI 3MEO 0.00000 !3-methoxy Ubiquinone

GROUP ! ubiquinone ring

ATOM C1	CUQ3	-0.059	!	
ATOM C2	CUQ1	0.462	!	H7\ /H4
ATOM O2	OUQ1	-0.439	!	H8-C4M C3M-H5
ATOM C3	CUQ2	0.037	!	H9/     \H6
ATOM O3	OUQ2	-0.247	!	O3
ATOM C4	CUQ2	-0.012	!	
!ATOM O4	OUQ2	-0.20	!	C4-----C3
ATOM C5	CUQ1	0.395	!	/ \
ATOM O5	OUQ1	-0.447	!	05--C5 C2--O2
ATOM C6	CUQ4	0.034	!	/ \
ATOM C1M	CTN	-0.231	!	C6-----C1
ATOM C3M	CTN	-0.060	!	/H1
ATOM C4M	CTN	-0.266	!	H10-C7-H11 C1M-H2
ATOM H1	HAN	0.09	!	\H3
ATOM H2	HAN	0.09	!	H14-C8-H12
ATOM H3	HAN	0.09	!	
ATOM H4	HAN	0.09	!	H13
ATOM H5	HAN	0.09	!	
ATOM H6	HAN	0.09	!	
ATOM H7	HAN	0.09	!	
ATOM H8	HAN	0.09	!	
ATOM H9	HAN	0.09	!	

! isoprenic tail stub !

ATOM C7	CTN	-0.157	!
ATOM C8	CN	-0.27	!
ATOM H10	HAN	0.09	!
ATOM H11	HAN	0.09	!
ATOM H12	HAN	0.09	!
ATOM H13	HAN	0.09	!
ATOM H14	HAN	0.09	!

! bonds for ubiquinone ring

BOND C1 C2	C2 C3	C3 C4	C4 C5
BOND C5 C6	C6 C1		
BOND C2 O2	C3 O3	C4 C4M	C5 O5
BOND C4M H7	C4M H8	C4M H9	
BOND O3 C3M	C3M H4	C3M H5	C3M H6
BOND C1 C1M	C1M H1	C1M H2	C1M H3
!Isoprene tail stub			
BOND C6 C7	C7 H10	C7 H11	C7 C8 C8 H12 C8 H13 C8 H14
AUTOGENERATE ANGLES DIHEDRALS			

RESI 2MEO 0.00000 !2-methoxy Ubiquinone

GROUP ! ubiquinone ring

ATOM C1	CUQ3	0.029	!	
ATOM C2	CUQ1	0.480	!	H7\ /H4
ATOM O2	OUQ1	-0.459	!	H8-C4M C3M-H5
ATOM C3	CUQ2	-0.056	!	H9/     \H6
!ATOM O3	OUQ2	-0.20	!	O4
ATOM C4	CUQ2	-0.001	!	
ATOM O4	OUQ2	-0.286	!	C4-----C3
ATOM C5	CUQ1	0.486	!	/ \
ATOM O5	OUQ1	-0.368	!	05--C5 C2--O2
ATOM C6	CUQ4	-0.148	!	/ \
ATOM C1M	CTN	-0.226	!	C6-----C1
ATOM C3M	CTN	-0.256	!	/H1
ATOM C4M	CTN	-0.014	!	H10-C7-H11 C1M-H2
ATOM H1	HAN	0.09	!	\H3
ATOM H2	HAN	0.09	!	
ATOM H3	HAN	0.09	!	

```

ATOM H4  HAN    0.09  !           H14-C8-H12
ATOM H5  HAN    0.09  !           |
ATOM H6  HAN    0.09  !           H13
ATOM H7  HAN    0.09  !
ATOM H8  HAN    0.09  !
ATOM H9  HAN    0.09  !
!
!       isoprenic tail stub !
!
ATOM C7  CTN   -0.171 !
ATOM C8  CN    -0.27  !
ATOM H10 HAN    0.09  !
ATOM H11 HAN    0.09  !
ATOM H12 HAN    0.09  !
ATOM H13 HAN    0.09  !
ATOM H14 HAN    0.09  !

!       bonds for ubiquinone ring
BOND C1 C2    C2 C3    C3 C4    C4 C5
BOND C5 C6    C6 C1
BOND C2 O2    C3 C3M   C4 O4    C5 O5
BOND O4 C4M   C4M H7   C4M H8   C4M H9
BOND C3M H4   C3M H5   C3M H6
BOND C1 C1M   C1M H1   C1M H2   C1M H3
!Isoprene tail stub
BOND C6 C7    C7 H10   C7 H11   C7 C8    C8 H12   C8 H13 C8 H14
AUTOGENERATE ANGLES DIHEDRALS

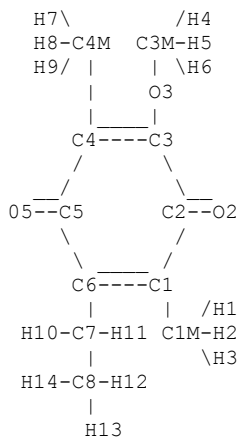
RESI 3MOM      0.00000 !3-methoxy Ubiquinone with mixed-appropriate naming.

GROUP ! ubiquinone ring

ATOM C1  CUQ7  -0.059  !
ATOM C2  CUQ5   0.462  !
ATOM O2  OUQ3  -0.439  !
ATOM C3  CUQ6   0.037  !
ATOM O3  OUQ4  -0.247  !
ATOM C4  CUQ6  -0.012  !
!ATOM O4  OUQ4  -0.20  !
ATOM C5  CUQ5   0.395  !
ATOM O5  OUQ3  -0.447  !
ATOM C6  CUQ8   0.034  !
ATOM C1M CTN2  -0.231  !
ATOM C3M CTN2  -0.060  !
ATOM C4M CTN2  -0.266  !
ATOM H1  HAN2   0.09  !
ATOM H2  HAN2   0.09  !
ATOM H3  HAN2   0.09  !
ATOM H4  HAN2   0.09  !
ATOM H5  HAN2   0.09  !
ATOM H6  HAN2   0.09  !
ATOM H7  HAN2   0.09  !
ATOM H8  HAN2   0.09  !
ATOM H9  HAN2   0.09  !
!
!       isoprenic tail stub !
!
ATOM C7  CTN2  -0.157  !
ATOM C8  CN2   -0.27  !
ATOM H10 HAN2   0.09  !
ATOM H11 HAN2   0.09  !
ATOM H12 HAN2   0.09  !
ATOM H13 HAN2   0.09  !
ATOM H14 HAN2   0.09  !

!       bonds for ubiquinone ring
BOND C1 C2    C2 C3    C3 C4    C4 C5
BOND C5 C6    C6 C1
BOND C2 O2    C3 O3    C4 C4M   C5 O5
BOND C4M H7   C4M H8   C4M H9
BOND O3 C3M   C3M H4   C3M H5   C3M H6

```



```

BOND C1 C1M C1M H1 C1M H2 C1M H3
!Isoprene tail stub
BOND C6 C7 C7 H10 C7 H11 C7 C8 C8 H12 C8 H13 C8 H14
AUTOGENERATE ANGLES DIHEDRALS

```

```
RESI 2MOM 0.00000 !2-methoxy Ubiquinone with mixed-appropriate naming.
```

```
GROUP ! ubiquinone ring
```

ATOM C1	CUQ7	0.029	!	
ATOM C2	CUQ5	0.480	!	H7\ /H4
ATOM O2	OUQ3	-0.459	!	H8-C4M C3M-H5
ATOM C3	CUQ6	-0.056	!	H9/     \H6
!ATOM O3	OUQ4	-0.20	!	O4
ATOM C4	CUQ6	-0.001	!	
ATOM O4	OUQ4	-0.286	!	C4-----C3
ATOM C5	CUQ5	0.486	!	/ \
ATOM O5	OUQ3	-0.368	!	05--C5 C2--O2
ATOM C6	CUQ8	-0.148	!	/ \
ATOM C1M	CTN2	-0.226	!	
ATOM C3M	CTN2	-0.256	!	C6-----C1
ATOM C4M	CTN2	-0.014	!	/H1
ATOM H1	HAN2	0.09	!	H10-C7-H11 C1M-H2
ATOM H2	HAN2	0.09	!	\H3
ATOM H3	HAN2	0.09	!	H14-C8-H12
ATOM H4	HAN2	0.09	!	
ATOM H5	HAN2	0.09	!	H13
ATOM H6	HAN2	0.09	!	
ATOM H7	HAN2	0.09	!	
ATOM H8	HAN2	0.09	!	
ATOM H9	HAN2	0.09	!	

! isoprenic tail stub !

ATOM C7	CTN2	-0.171	!
ATOM C8	CN2	-0.27	!
ATOM H10	HAN2	0.09	!
ATOM H11	HAN2	0.09	!
ATOM H12	HAN2	0.09	!
ATOM H13	HAN2	0.09	!
ATOM H14	HAN2	0.09	!

```
! bonds for ubiquinone ring
```

```

BOND C1 C2 C2 C3 C3 C4 C4 C5
BOND C5 C6 C6 C1
BOND C2 O2 C3 C3M C4 O4 C5 O5
BOND O4 C4M C4M H7 C4M H8 C4M H9
BOND C3M H4 C3M H5 C3M H6
BOND C1 C1M C1M H1 C1M H2 C1M H3
!Isoprene tail stub
BOND C6 C7 C7 H10 C7 H11 C7 C8 C8 H12 C8 H13 C8 H14
AUTOGENERATE ANGLES DIHEDRALS

```

```
RESI Q0 0.00000 !2,3-Dimethoxy-5-dimethyl-1,4-benzoquinone
```

```
GROUP ! ubiquinone ring
```

ATOM C1	CUQ3	-0.317	!	
ATOM C2	CUQ1	0.586	!	H7\ /H4
ATOM O2	OUQ1	-0.456	!	H8-C4M C3M-H5
ATOM C3	CUQ2	0.055	!	H9/     \H6
ATOM O3	OUQ2	-0.336	!	O4 O3
ATOM C4	CUQ2	0.055	!	
ATOM O4	OUQ2	-0.336	!	C4-----C3
ATOM C5	CUQ1	0.586	!	/ \
ATOM O5	OUQ1	-0.456	!	05--C5 C2--O2
ATOM C6	CUQ4	0.014	!	/ \
ATOM C1M	CTN	-0.120	!	
ATOM C3M	CTN	-0.045	!	C6-----C1
ATOM C4M	CTN	-0.045	!	

```

ATOM H1  HAN    0.09  !           |   | /H1
ATOM H2  HAN    0.09  !         H10  C1M-H2
ATOM H3  HAN    0.09  !           \H3
ATOM H4  HAN    0.09  !
ATOM H5  HAN    0.09  !
ATOM H6  HAN    0.09  !
ATOM H7  HAN    0.09  !
ATOM H8  HAN    0.09  !
ATOM H9  HAN    0.09  !
!isoprene tail stub stub.
ATOM H10 HAN    0.085 !

! bonds for ubiquinone ring
BOND C1 C2  C2 C3  C3 C4  C4 C5
BOND C5 C6  C6 C1
BOND C2 O2  C3 O3  C4 O4  C5 O5
BOND O4 C4M C4M H7  C4M H8  C4M H9
BOND O3 C3M C3M H4  C3M H5  C3M H6
BOND C1 C1M C1M H1  C1M H2  C1M H3
!Isoprene tail stub
BOND C6 H10
AUTOGENERATE ANGLES DIHEDRALS

RESI Q0M      0.00000 !2,3-Dimethoxy-5,6-dimethyl-1,4-benzoquinone

GROUP ! ubiquinone ring

ATOM C1  CUQ3  -0.317  !
ATOM C2  CUQ1  0.586   !           H7\           /H4
ATOM O2  OUQ1  -0.456  !         H8-C4M  C3M-H5
ATOM C3  CUQ2  0.055   !         H9/   |   | \H6
ATOM O3  OUQ2  -0.336  !           O4   O3
ATOM C4  CUQ2  0.055   !           |-----|
ATOM O4  OUQ2  -0.336  !         C4-----C3
ATOM C5  CUQ1  0.586   !           /-----\
ATOM O5  OUQ1  -0.456  !         O5--C5       C2--O2
ATOM C6  CUQ4  0.014   !           \-----/
ATOM C1M CTN  -0.120  !           C6-----C1
ATOM C3M CTN  -0.045  !           |           | /H1
ATOM C4M CTN  -0.045  !         H10-C7-H11 C1M-H2
ATOM H1  HAN    0.09  !           |           \H3
ATOM H2  HAN    0.09  !
ATOM H3  HAN    0.09  !
ATOM H4  HAN    0.09  !
ATOM H5  HAN    0.09  !
ATOM H6  HAN    0.09  !
ATOM H7  HAN    0.09  !
ATOM H8  HAN    0.09  !
ATOM H9  HAN    0.09  !
ATOM H9  HAN    0.09  !
!
! isoprenic tail stub !
!
ATOM C7  CTN  -0.265  ! -0.175 - 0.09
ATOM H10 HAN    0.09  !
ATOM H11 HAN    0.09  !
ATOM H12 HAN    0.09  !

! bonds for ubiquinone ring
BOND C1 C2  C2 C3  C3 C4  C4 C5
BOND C5 C6  C6 C1
BOND C2 O2  C3 O3  C4 O4  C5 O5
BOND O4 C4M C4M H7  C4M H8  C4M H9
BOND O3 C3M C3M H4  C3M H5  C3M H6
BOND C1 C1M C1M H1  C1M H2  C1M H3
!Isoprene tail stub
BOND C6 C7  C7 H10  C7 H11  C7 H12
AUTOGENERATE ANGLES DIHEDRALS

RESI ISOP 0.0000 !Isoprene unit.
GROUP !
ATOM C1  CTL2 -0.18  !           H8
ATOM H1  HAL2  0.09  !           \
           H3           C5---H9

```

```

ATOM H2   HAL2   0.09   !           \      /      \
GROUP     !           C2==C3   H7
ATOM C2   CEL1  -0.15   !           /      \
ATOM H3   HEL1   0.15   !   H1-C1-H2   C4-H(4-6)
GROUP     !
ATOM C3   CEL1   0.00   !Also try CG2D1 from cgenff. Basically the same.
GROUP
ATOM C4   CTL3  -0.27
ATOM H4   HAL3   0.09
ATOM H5   HAL3   0.09
ATOM H6   HAL3   0.09
GROUP
ATOM C5   CTL3  -0.27
ATOM H7   HAL3   0.09
ATOM H8   HAL3   0.09
ATOM H9   HAL3   0.09
BOND C1  C2  C2  C3  C3  C4  C3  C5
BOND C1  H1  C1  H2  C2  H3
BOND C4  H4  C4  H5  C4  H6
BOND C5  H7  C5  H8  C5  H9

```

! I don't like these impropers. However the parameters you guys have used for these rings contains them. Odds are we can just supply zeros for the parameters we use, or comment these out.

```

!IMPR C2 H3 C1 C3
!IMPR C3 C2 C4 C5
AUTOGENERATE ANGLES DIHEDRALS

```

```

RESI SMA      0.11   ! Stigmatellin

```

```

GROUP !

```

```

! methoxy groups           !   H4\                /H9
ATOM C5M CG331 -0.0740 !   H6-C5M           C7M-H10
ATOM H4  HGA3  0.0820 !   H5/ |             | \H8
ATOM H5  HGA3  0.0820 !       O5  H7       O7
ATOM H6  HGA3  0.0820 !       |         |
ATOM C7M CG331 -0.0360 !       |         C6---C7
ATOM H8  HGA3  0.0830 !       | //         \\
ATOM H9  HGA3  0.0830 !       -----C5         C8-O8-H44
ATOM H10 HGA3  0.0830 !           \         /
ATOM O5  OG301 -0.1590 !           C4A-----C8A
ATOM O7  OG301 -0.2820 !           /         \
! top ring                 !   04--C4           O1
ATOM C5  CG2R61 0.0940 !           \         /
ATOM C6  CG2R61 -0.2580 !           C3-----C2
ATOM H7  HGR61  0.1740 !   H1\ /             |
ATOM C8  CG2R61 0.2220 !   H3-C3M H12-C9-H11
ATOM O8  OG311 -0.6230 !   H2/ |
ATOM H44 HGP1   0.4470 !           H14-C10-H13
ATOM C4A CG2R61 -0.1090 !           H30\      |
ATOM C8A CG2R61 0.0420 !           H31-C22-C11-H15
! bottom ring             !   H29/ |             /H32
ATOM O1  OG3R60 -0.08000 !           |             H16-C12-O12-C23-H34
ATOM C2  CG2D10 -0.0170 !           |             \H33
ATOM C3  CG2R62 -0.0430 !           |             /H36
! methyl group           !   H17-C13-C24-H37
ATOM C3M CG331 -0.1860 !           |             \H35
ATOM H1  HGA3  0.0750 !           H38\      |
ATOM H2  HGA3  0.0750 !           H40-C25-O14-C14-H18
ATOM H3  HGA3  0.0750 !           H39/      |
ATOM C4  CG2R63 0.4880 !           |             H19-C15
ATOM O4  OG2D4  -0.5420 !           |             \\
!tail                 !           C16-H21
ATOM C9  CG321  -0.0860 !           /
ATOM H11 HGA2  0.0800 !           |             H22-C17
ATOM H12 HGA2  0.0800 !           |             \\
ATOM C10 CG321 -0.1030 !           |             C18-H23
ATOM H13 HGA2  0.0860 !           |
ATOM H14 HGA2  0.0860 !           |             C19
ATOM C11 CG311  0.0650 !           // \      /H41

```

ATOM	C12	CG311	-0.0390	!	H25-C20	C26-H43
ATOM	C13	CG311	0.0230	!		\H42
ATOM	C14	CG311	-0.0200	!		C21
ATOM	C15	CG2DC1	-0.2420	!	H26/ \H27	
ATOM	C16	CG2DC1	-0.0960	!	H28	
ATOM	C17	CG2DC2	-0.0440			
ATOM	C18	CG2DC2	-0.3240			
ATOM	C19	CG2DC1	0.0820			
ATOM	C20	CG2DC1	-0.0114			
ATOM	C21	CG331	-0.2660			
ATOM	C22	CG331	-0.5000			
ATOM	C23	CG331	0.0540			
ATOM	C24	CG331	-0.2330			
ATOM	C25	CG331	0.0020			
ATOM	C26	CG331	-0.0760			
ATOM	O12	OG301	-0.3970			
ATOM	O14	OG301	-0.3010			
ATOM	H15	HGA1	0.0790			
ATOM	H16	HGA1	0.1600			
ATOM	H17	HGA1	0.0840			
ATOM	H18	HGA1	0.1750			
ATOM	H19	HGA4	0.1370			
ATOM	H29	HGA3	0.1330			
ATOM	H30	HGA3	0.1330			
ATOM	H31	HGA3	0.1330			
ATOM	H32	HGA3	0.0440			
ATOM	H33	HGA3	0.0440			
ATOM	H34	HGA3	0.0440			
ATOM	H35	HGA3	0.0640			
ATOM	H36	HGA3	0.0640			
ATOM	H37	HGA3	0.0640			
ATOM	H38	HGA3	0.0490			
ATOM	H39	HGA3	0.0490			
ATOM	H40	HGA3	0.0490			
ATOM	H21	HGA4	0.1500			
ATOM	H22	HGA4	0.1240			
ATOM	H23	HGA4	0.1420			
ATOM	H41	HGA3	0.0380			
ATOM	H42	HGA3	0.0380			
ATOM	H43	HGA3	0.0380			
ATOM	H25	HGA4	0.1070			
ATOM	H26	HGA3	0.0910			
ATOM	H27	HGA3	0.0910			
ATOM	H28	HGA3	0.0910			

BOND	C2	C3	C2	O1	C2	C9	C3	C4
BOND	C3	C3M	C3M	H1	C3M	H2	C3M	H3
BOND	C4	C4A	C4	O4	C4A	C8A	C4A	C5
BOND	C5	C6	C5	O5	C5M	O5		
BOND	C5M	H4	C5M	H5	C5M	H6	C6	C7
BOND	C6	H7	C7	C8	C7	O7	C7M	O7
BOND	C7M	H8	C7M	H9	C7M	H10	C8	O8
BOND	C8	C8A	O8	H44	C8A	O1		
BOND	C9	H11	C9	H12	C9	C10	C10	H13
BOND	C10	H14	C10	C11				
BOND	C11	C22	C11	C12	C11	H15	C12	O12
BOND	C12	C13	C12	H16	C13	C24	C13	C14
BOND	C13	H17	C14	O14	C14	C15	C14	H18
BOND	C15	C16	C15	H19	C16	C17	C16	H21
BOND	C17	C18	C17	H22	C18	C19	C18	H23
BOND	C19	C20	C19	C26	C20	C21	C20	H25
BOND	C21	H26	C21	H27	C21	H28	C22	H29
BOND	C22	H30	C22	H31	C23	O12	C23	H32
BOND	C23	H33	C23	H34	C24	H35	C24	H36
BOND	C24	H37	C25	O14	C25	H38	C25	H40
BOND	C25	H39	C26	H41	C26	H43	C26	H42

AUTOGENERATE ANGLES DIHEDRALS

```
PRES UILK 0.0000 !Ubiquinone-isoprene link Ubiquinone(1), Isoprene (2)
DELETE ATOM 1C8
DELETE ATOM 1H12
DELETE ATOM 1H13
DELETE ATOM 1H14
DELETE ATOM 2C1
DELETE ATOM 2H1
DELETE ATOM 2H2
BOND 1C7 2C2
AUTO ANGL DIHE
```

```
PRES IILK 0.0000 !Isoprene-isoprene link
DELETE ATOM 1H9
ATOM 1C5 CTL2 -0.18
ATOM 1H7 HAL2 0.09
ATOM 1H8 HAL2 0.09
BOND 1C5 2C1
AUTO ANGL DIHE
```

## Appendix C. Script for calculation of Diffusion for Membrane Lipids

```
# Membrane diffusion
# Author: Stuart Rose
# Date: 4/7/2017
#
# Notes: needs to be run in run file for configuration. Need to load last
xscfile
#           in
#           Run proc MSDcalc after changing restart extened configuration
files *.xsc
#           in Doft
#
#
# lipidnames: DVPC DVPE DVPG TOCL2 VSPC VSPE VSPG

proc ::MSDcalc {} {

    set A [atomselect top "segname MEMB"]
    set lipidnames [lsort -unique [$A get resname]]
    # set lipidnames "VSPG"
    foreach k $lipidnames {
        # Exclude interior lipids
        if {$k == "VSPG"} {
            set seltext "resname VSPG and not resid 610 611"
            set headtext "C1 C11 C12 C13 OC2 OC3 O11 O12 O13 O14 P"
        } else {
            set seltext "resname $k"
        }
    }
    if {$k == "DVPC"} {
        set headtext "C1 C11 C12 C13 C14 N O11 O12 O13 O14 P"
    }
    if {$k == "DVPE"} {
        set headtext "C1 C11 C12 N O11 O12 O13 O14 P"
    }
    if {$k == "DVPG"} {
        set headtext "C1 C11 C12 C13 OC2 OC3 O11 O12 O13 O14 P1"
    }
    if {$k == "TOCL2"} {
        set headtext "C1 C2 C3 C11 C31 OG12 OP11 OP12 OP13 OP31
OP32 OP34 P1 P3 "
    }
    if {$k == "VSPC"} {
        set headtext "C1 C11 C12 C13 C14 N O11 O12 O13 O14 P"
    }
    if {$k == "VSPE"} {
        set headtext "C1 C11 C12 N O11 O12 O13 O14 P"
    }
    }
    set sel [atomselect top $seltext]
    set lipids [lsort -unique [$sel get residue]]

    Doft $k $headtext $headtext "prod_conf1_2_run_8" $lipids
    $sel delete
# close bracket for "foreach k $lipidnames"
}
```



```

#close bracket for proc ::MSDcalc
}

proc ::get_xy { xscfile } {
    set fd [open $xscfile r]
    gets $fd
    gets $fd
    gets $fd line
    puts "$line"
    set x_coord [lindex $line 1]
    set y_coord [lindex $line 5]
    close $fd
    return "$x_coord $y_coord"
}

proc ::Doft { name headtext1 headtext2 f_xsc_in lipids } {

    set nf [molinfo top get numframes]

    set N [llength $lipids]
    puts "there are $N lipids and lipids are: $lipids"

    set xy [get_xy ./f_xsc_in.restart.xsc]

    set outfile1 [open ./output/Doft_$name w]
    set outfile2 [open ./output/Sum_$name w]
    puts $outfile1 "t $name:$N"
    puts $outfile2 "t $name:$N"

    foreach j $lipids {
        for {set k 1} {$k <= $nf} {incr k} {
            set simdata1($k.r) "0"
        }
        set seltext1 "residue $j and name $headtext1"
        set seltext2 "residue $j and name $headtext2"

        # atom selection sel0 is the reference
        set sel0 [atomselect top "$seltext1"]
        $sel0 frame 0

        set lipidname [lsort -unique [$sel0 get resname]]
        set outfile [open ./output/${lipidname}_$j w]
        puts $outfile "t ${lipidname}_$j"

        set sel1 [atomselect top "$seltext1"]
        $sel1 frame 0

        set sel2 [atomselect top "$seltext2"]
        $sel2 frame 0

        set com0 [measure center $sel0 weight mass]
        set com1 $com0
        set com2 $com0

        set sum 0
        set adjx 0
    }
}

```

```

set adjy 0

for {set i 1} {$i < 286} {incr i} {
    $sel2 frame $i
    set com2 [measure center $sel2 weight mass]

    set jump [expr {[lindex $com2 0] - [lindex $com1 0]}]

    if {[expr {$jump < -50}]} {set adjx [expr {$adjx == 0 ? 1 :
0}}}
    if {[expr {$jump > 50}]} {set adjx [expr {$adjx == 0 ? -1 :
0}}}

    set jump [expr [lindex $com2 1] - [lindex $com1 1]]

    if { $jump < -100 }      {set adjy [expr {$adjy == 0 ? 1 :
0}}}
    if { $jump > 100 } {
        set adjy [expr {$adjy == 0 ? -1 : 0} ]
    }

    set com1 $com2
    set com2 "[expr {[lindex $com2 0]+[expr {$adjx * [lindex
$xy 0]}]}] [expr {[lindex $com2 1]+[expr {$adjy * [lindex $xy 1]}]}]
[lindex $com2 2]"

    if {$adjy == 1 } {puts "${lipidname}_$j: com1: $com1, com2:
$com2"}

    # measure distance from start and accumulate for total dist
from start (dr)
    set simdata($i.r) [expr { $i > 1 ? [expr {[veclength
[vecsub $com0 $com2]]}] : 0}]

    set simdata1($i.r) [expr {$simdata1($i.r) + [expr
$simdata($i.r) * $simdata($i.r)]]

    set j [expr 2*$i]
}

# this is 1 fs timestep frames
for {set i 286} {$i < $nf} {incr i} {
    set j [expr 1 + $j]

    $sel2 frame $i

    set com2 [measure center $sel2 weight mass]

    set jump [expr {[lindex $com2 0] - [lindex $com1 0]}]

    if {[expr {$jump < -100}]} {puts "second jump"}
    if {[expr {$jump < -100}]} {set adjx [expr {$adjx == 0 ? 1
: 0}]}

    if { $jump > 100 } { set adjx [expr {$adjx == 0 ? -1 : 0}]}

    set jump [expr {[lindex $com2 1] - [lindex $com1 1]}]
    if { $jump < -100 } {set adjy [expr {$adjy == 0 ? 1 : 0}]}
    if { $jump > 100 } {set adjy [expr {$adjy == 0 ? -1 : 0}]}
}

```

```

        set com1 $com2
        set com2 "[expr {[lindex $com2 0]+[expr {$adjx * [lindex
$xy 0]}}] ][expr {[lindex $com2 1]+[expr {$adjy * [lindex $xy 1]}}] ][
[lindex $com2 2]"

# measure distance from start and accumulate for total dist
from start (dr)
        set simdata($i.r) [expr { $i > 1 ? [expr {[veclength
[vecsub $com0 $com2]]}] : 0}]
        puts $outfile "[expr $j] $simdata($i.r)"

        set simdata1($i.r) [expr {$simdata1($i.r) + [expr
$simdata($i.r) * $simdata($i.r)]]
    }
    close $outfile
# close bracket for each of j $lipids
}

for {set i 1} {$i < 286} {incr i} {
    set j [expr 2*$i]
    set bottom [expr {$j * $N * 4}]
    puts $outfile2 "$i $simdata1($i.r)"

    set simdata2($j.r) [expr {$simdata1($i.r)/($bottom)}]
    puts $outfile1 "$j $simdata2($j.r)"
}

for {set i 286} {$i < $nf} {incr i} {

    set j [expr 1 + $j]
    set bottom [expr {$j * $N * 4}]
    puts $outfile2 "$i $simdata1($i.r)"
    set simdata2($j.r) [expr {$simdata1($i.r)/($bottom)}]
    puts $outfile1 "$j $simdata2($j.r)"
}

close $outfile1
close $outfile2

$sel0 delete
$sel1 delete
$sel2 delete
}

```